Report to

NATIONAL SCIENCE FOUNDATION
Washington, D.C.
Grant No. ENV77-15333

EARTHQUAKE RESISTANT STRUCTURAL WALLS -
COUPLED WALL TESTS

by

K. N. Shiu
J. D. Aristizabal-Ochoa
G. B. Barney
A. E. Fiorato
W. G. Corley

Submitted by
CONSTRUCTION TECHNOLOGY LABORATORIES
A Division of Portland Cement Association
5420 Old Orchard Road
Skokie, Illinois 60077

July 1981

50272-101

REPORT DOCUMENTATION PAGE	1. REPORT NO. NSF/CEE-81034	2.	3. Recipient's Accession No. PB82 131954

4. Title and Subtitle	5. Report Date
Earthquake Resistant Structural Walls - Coupled Wall Tests	July 1981
	6. U328053

7. Author(s) W.G. Corley, PI, K.N. Shiu, J.D. Aristizabal-Ochoa, G.B. Barney,*	8. Performing Organization Rept. No.

9. Performing Organization Name and Address	10. Project/Task/Work Unit No.
Portland Cement Association Construction Technology Laboratories 5420 Old Orchard Road Skokie, IL 60077	11. Contract(C) or Grant(G) No. (C) (G) ENV7715333

12. Sponsoring Organization Name and Address	13. Type of Report & Period Covered
Directorate for Engineering (ENG) National Science Foundation 1800 G Street, N.W. Washington, DC 20550	14.

15. Supplementary Notes

Submitted by: Communications Program (OPRM)   *A.E. Fiorato
              National Science Foundation
              Washington, DC 20550

16. Abstract (Limit: 200 words)

In the development of earthquake resistant, reinforced concrete walls, two one-third scale, six-story coupled wall specimens were tested under incremental cyclic loadings. A lightly coupled system which damaged early was first tested and then retested with the damaged coupling beams replaced by stiffer and stronger beams. The heavy coupling beams between walls caused the system to behave as a single isolated wall, and the coupling beams yielded immediately before and after the yielding of the walls. An analytical model was developed to simulate experimental results and was used to calculate the load versus deflection relationship of the coupled wall system. Using this model, inelastic shear action in the walls was found to be a significant factor in the analysis of a lightly coupled system. In heavily coupled systems, use of the model indicated that redistribution of shear and moment between walls was significant, and that interaction of axial and flexural forces is the most important factor to consider in calculating behavior of heavily coupled systems.

17. Document Analysis a. Descriptors

Earthquake resistant structures   Dynamic structural analysis
Concrete construction   Mathematical models
Structural design   Stress analysis
Walls   Dynamic tests

b. Identifiers/Open-Ended Terms

Coupled wall systems

c. COSATI Field/Group

18. Availability Statement	19. Security Class (This Report)	21. No. of Pages
NTIS	20. Security Class (This Page)	22. Price

(See ANSI-Z39.18)   See Instructions on Reverse   OPTIONAL FORM 272 (4-77)
                                                                (Formerly NTIS-35)
                                                                Department of Commerce

TABLE OF CONTENTS

EARTHQUAKE RESISTANCE STRUCTURAL WALLS -

COUPLED WALL TESTS

by

K. N. Shiu, J. D. Aristizabal-Ochoa,
G. B. Barney, A. E. Fiorato, and W. G. Corley*

HIGHLIGHTS

Structural walls coupled by beams in multi-story buildings
are efficient systems for resisting lateral forces from earth-
quake motions. In a properly designed system, coupling-beam
elements provide additional lateral stiffness and energy dissi-
pation capacity.

To determine effects of coupling beam strength and stiffness
on overall behavior of coupled wall systems, a combined experi-
mental and analytical investigation was undertaken by the Con-
struction Technology Laboratories. Effects of axial load
induced by coupling beams on behavior of individual walls were
evaluated. Interaction among individual structural elements,
and redistribution of moment and shear between walls were
investigated.

In this report, two six-story coupled wall specimens were
tested under incremental cyclic loadings. Specimens were about
one-third of prototype size. The two tests showed behavior of
a wall system with relatively weak coupling beams,

---

*Respectively, Structural Engineer, Former Structutal Engineer,
Structural Development Department; Manager, Building Construc-
tion Section; Manager, Construction Methods Section; Divisional
Director, Engineering Development Division, Construction Tech-
nology Laboratories, a Division of Portland Cement Association,
Skokie, Illinois 60077

and a repaired system with stiffer and stronger beams. Applied loads, deflections, rotations, shear distortions, and reinforcement strains were measured.

An analytical model was developed to simulate experimental results. The analytical model was based on a structural system idealized by an inelastic line model. The model accounted for inelastic flexural and shear behavior. Interaction between shear and flexure, as well as axial force and flexure, was also evaluated.

The analytical model was used to calculate behavior of wall systems with weak beams and with strong beams. Calculated results were compared with experimental data. Effects of selected parameters on wall behavior were analyzed. Effects of beam repair were also evaluated.

OBJECTIVES

Objectives of this investigation were to evaluate behavior and develop design recommendations for earthquake-resistant reinforced concrete coupled walls. Behavior of coupled wall systems with weak coupling beams and with strong coupling beams under static lateral in-plane reversing loads was investigated. Specific objectives of the tests were:

(1) To determine effects of beam-strength on the behavior of coupled wall systems.

(2) To evaluate effects of induced axial coupling beam forces on the strength and ductility of individual walls.

(3) To identify critical design parameters for coupled wall systems with weak and strong coupling beams.

(4) To investigate the redistribution of shear and moment between coupled walls.

(5) To evaluate procedures for repairing damaged structural wall systems.

(6) To develop and verify procedures for analyzing structural wall systems.

(7) To determine effects of selected parameters on the behavior of coupled wall systems.

SCOPE

The research investigation for coupled walls was divided into two programs:

(1) Experimental Program

(2) Analytical Program

Experimental Program

In the experimental program, two coupled wall tests were performed. Tests were conducted on a specimen which was approximately 1/3 scale of a selected prototype structure. The specimen represented a coupled wall system in a six-story building. To simulate site conditions, the specimen was built with common construction practices. Lateral incremental reversing loads were applied to the specimen. Throughout tests, deformations and sequence of yielding of individual elements were recorded.

The first test, CS-1, was performed on a coupled wall system with weak coupling beams. As reversing loads were applied, the weak beams suffered heavy damage relatively early before the walls yielded. Soon after the walls yielded, damage to various structural elements was evaluated and the test was stopped. All coupling beams were removed and replaced with stiffer, stronger beams. Walls were not repaired. The resulting repaired system was designated RCS-1.

System RCS-1 with the stiffer, stronger beams represented a "heavily" coupled wall system. Testing of the repaired system followed similar reversing load cycles as for CS-1. Test RCS-1 was stopped when the load carrying capacity of the specimen deteriorated substantially. Behavior of both test specimens was recorded and compared.

Analytical Program

In the analytical program, a mathematical model of a coupled wall system was developed. Inelastic behavior of individual members was calculated by continually updating element stiffness. Validity of the model was confirmed by comparing analytical and experimental results.

Three parameters that affected behavior of wall systems were considered in detail. These parameters are:

(1) Interaction between flexural and axial forces

(2) Inelastic shear effects in beams and walls

(3) Beam end rotations caused by bond slip.

-4-

The significance of each parameter on overall response of wall systems was evaluated. In addition, effects of beam strength on behavior of coupled wall systems was investigated. Redistribution of shear and moment between walls in the inelastic region was calculated. Effects of axial loads induced in walls by coupling beams were also determined.

BACKGROUND

Structural wall systems can be divided into of three major categories as illustrated in Fig. 1. These are wall systems with openings (or pierced walls), coupled walls, and wall-frame systems. In this report, behavior of coupled walls is of particular interest. Coupled wall systems consist of structural walls connected with coupling beams.

The effectiveness and efficiency of coupled wall systems have been demonstrated by their performance in recent earth quakes.[1] Tests of coupling beam elements[2,3,4] and isolated structural walls[5,6,7] indicate that coupled walls are viable structural systems in earthquake-prone regions. However, proper understanding of design philosophy and details are required so that sufficient strength and ductility of individual elements are available to withstand large inelastic deformations. Effects of interaction between individual structural members on the overall behavior of wall systems must be considered.

In coupled wall systems there are two primary structural actions: flexural and shear resistance of individual walls, and coupling resistance caused by axial forces in the walls.
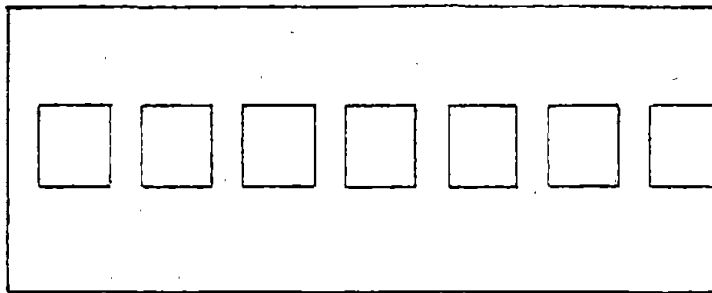
(c) Wall with Openings

(b) Wall Coupled to Frame

Fig. 1 Structural Wall Systems

(a) Coupled Walls

Accumulation of forces transmitted through coupling beams as shear contributes to axial forces in the walls. The amount of coupling is directly related to flexural and shear capacity of beams.

Even though substantial work has been done on evaluation of inelastic behavior of individual elements,[2 - 7] experimental data on overall inelastic behavior of wall systems and effects of interaction between elements are lacking. Information on on deformation capacity of wall systems in relation to possible ductility demands under earthquake motions is limited.[8,9]

Limited data on behavior of coupled structural wall systems has been reported. Data have been obtained from three kinds of tests:

(1) Static monotonic tests

(2) Static reversing load tests

(3) Dynamic tests

Static Monotonic Tests

Three monotonic tests on coupled wall systems were performed by Nguyen at McGill University[10]. Tenth scale micro-concrete models of four-story coupled walls were tested. Variables included coupling beam proportions, coupling beam reinforcement, and wall reinforcement.

Results of the tests indicated that adequate shear reinforcement was required in hinging regions of walls if flexural capacity was to be attained. Results also showed that coupling beams with diagonal reinforcement performed better than beams with conventional reinforcement.

-7-

Static Reversing Load Tests

Paulay and Santhakumar performed two 1/4-scale coupled wall tests[11,12]. The two reinforced concrete models represented two seven-story high structural walls connected by seven coupling beams. Specimens were subjected to repeated cycles of inelastic reversing loads.

Coupling beams of both specimens had shear span-to-depth ratio of 0.7. In one specimen, coupling beams were reinforced with conventional horizontal bars. After several cycles of inelastic loadings, sliding shear failure occurred in the beams. In the other specimen, coupling beams were reinforced with full-length diagonal reinforcement. The diagonally reinforced beams were able to dissipate significant amounts of energy without suffering excessive deterioration. The test was terminated when capacity of the compression wall was reached.

Regardless of beam performance, both wall systems exhibited substantial deformation capacities. Wall systems with conventional reinforced beams lost lateral strength with the rapid deterioration of shear capacity in the tension wall. Wall system with straight diagonals, on the other hand, failed in compression buckling of reinforcement in compression wall.

Experimental results showed the effectiveness of using full-length diagonal bars in short-span coupling beams. Further discussion of the coupling beam reinforcement details is given by Paulay and Binney[13]. Beams should also be selected in light of the capacity of wall elements. Too strong the coupling beams would result in excessive damage in wall elements.

Thereby the capacity of the wall system was limited to that of the walls.

The Portland Cement Association undertook similar approach to investigate individual structural elements[2,5]. Eighteen tests on isolated walls and eight tests on coupling beams were performed. Different wall sections and reinforcement details were investigated. Coupling beam specimens[3] with shear-span to depth ratios of 1.25 and 2.5 were tested. Full length diagonal bars were found to be very efficient in short-span beams. However, the effectiveness of full-length diagonals decreased with increasing shear span-to-depth ratio.

Dynamic Tests

Aristizabal and Sozen[14] have reported results of dynamic tests on four small-scale coupled wall systems. Specimens were ten stories high with wall elements joined at each floor by coupling beams. Span-to-depth ratio of the coupling beams was approximately 2.7. Reinforcement details of wall elements for all specimens were identical. The four specimens were designed with different amounts of beam flexural reinforcement. Specimens were subjected to variations of either 1940 El Centro or 1952 Taft earthquake motions.

Test results indicated that natural frequencies decreased as specimens were subjected to base motions of increasing intensities. It was also observed that for relatively strong base motions, damage could be confined to the coupling beams.

Effects of coupling beam strength and stiffness on the

behavior of wall systems have also been reported by Lybas and Sozen.[15]

Dynamic and static tests of coupled walls have been reported by Irwin and Young.[16] However, dynamic tests were conducted only in the elastic range of very small specimens. A sine wave function was used as the forced vibration. In static tests, the model exhibited a ductility factor in excess of four. Lateral load redistribution between structural wall elements was reported.

EXPERIMENTAL PROGRAM

Two coupled wall tests are presented in this report. These corresponded to tests on a system with weak beams (CS-1) and a system with strong repaired beams (RCS-1).

Test Specimens

Dimensions of the coupled wall specimen are shown in Fig. 2. The 18 ft (5.5 m) high, 1/3 scale, six-story model consisted of two rectangular walls coupled by six beams. Each wall had a horizontal length of 6 ft 3 in. (1.9 m) and a uniform wall thickness of 4 in. (102 mm). Cross section of the wall elements is shown in Fig. 3. The base of each wall was anchored rigidly to the test floor through a common base block. Soil-structure interaction was not considered.

For CS-1, coupling beams spaced 3 ft (0.9 m) on centers had a clear span of 16.7 in. (423 mm) corresponding to a shear span-to-depth ratio of 2.50. The cross section of coupling beams was 4 in. by 6.7 in. (102 mm by 169 mm) as shown in Fig. 3.
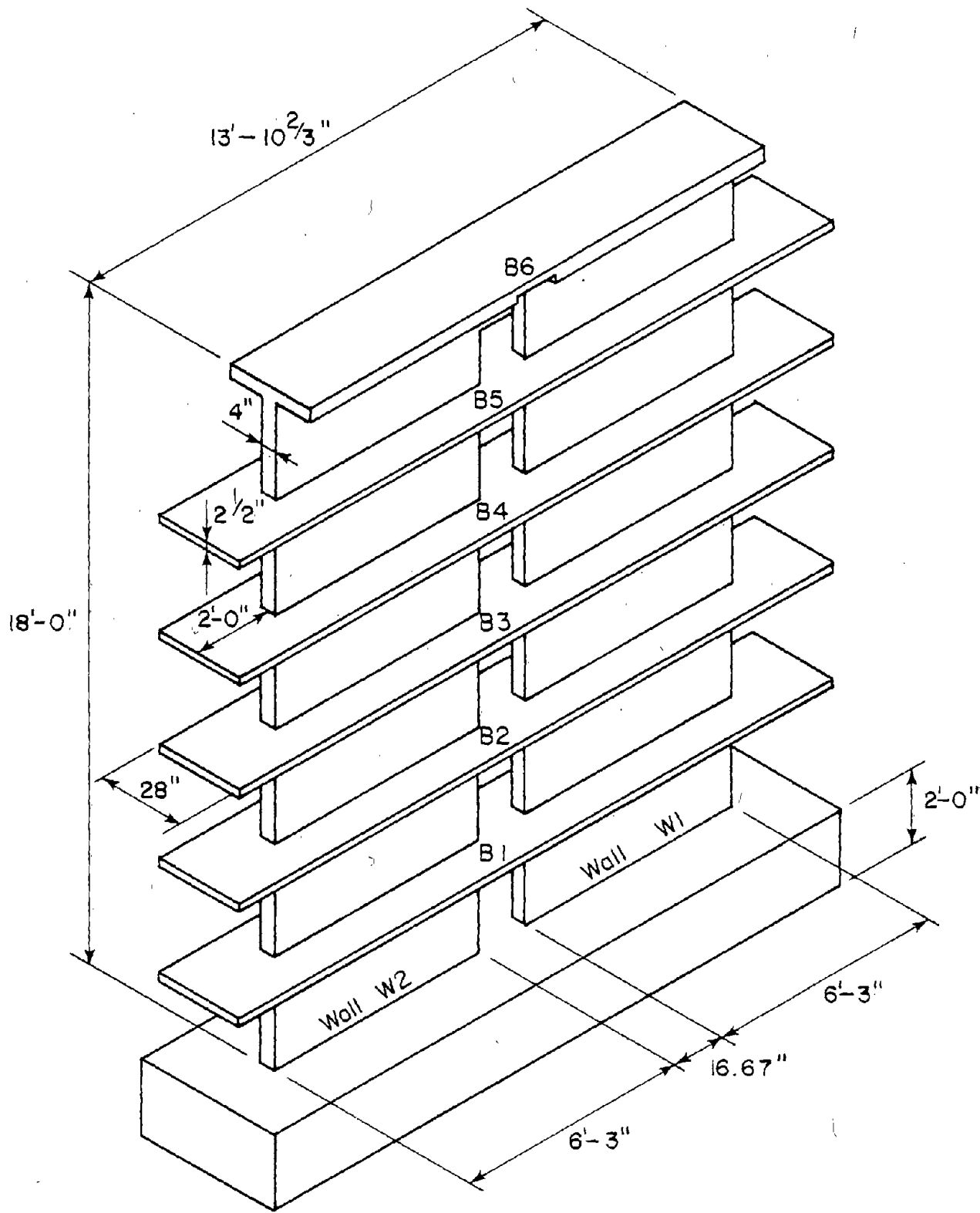
Fig. 2   Dimensions of Coupled Wall Specimen
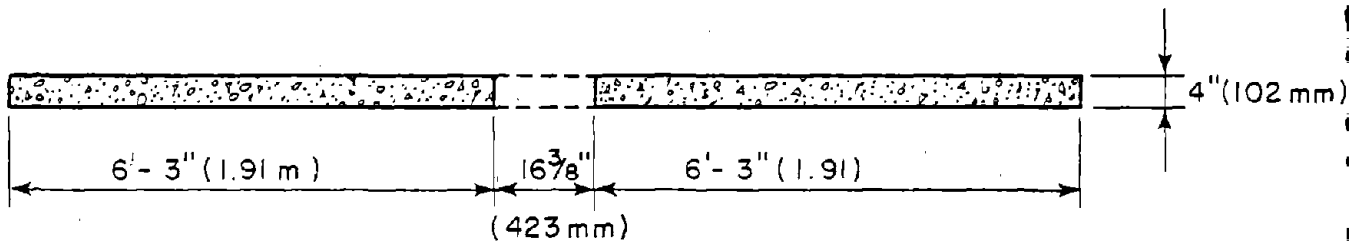
(a) Wall Element
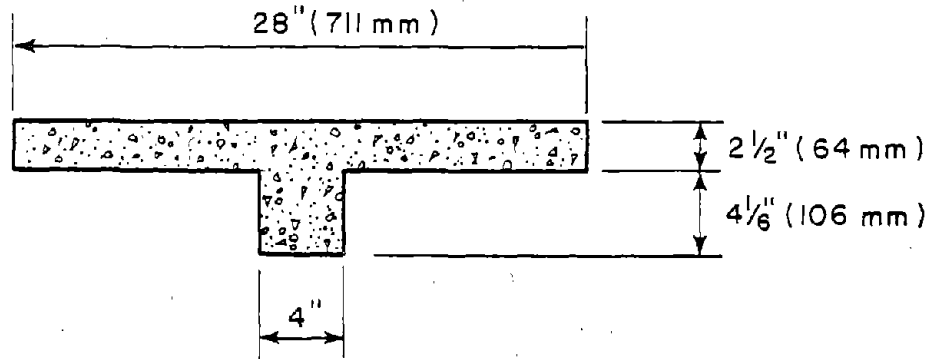
(b) Coupling Beam in CS-1
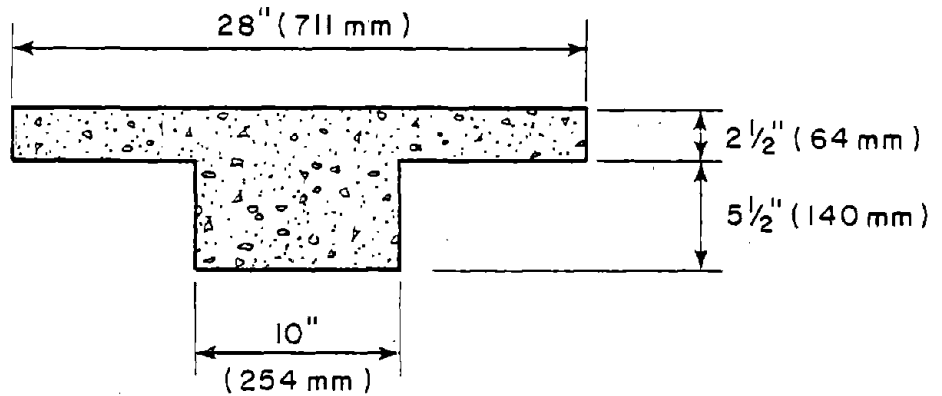
(c) Coupling Beam in RCS-1

Fig. 3 Cross-Sectional Dimensions of
Walls and Coupling Beams

Repaired beams in RCS-1 had a cross section of 10 in. by 8 in. (254 mm by 203 mm) as shown in Fig. 3. Shear span-to-depth ratio of the repair beam was 1.04. At each floor level, slabs were simulated by 2.5 in. (64 mm) by 1 ft (0.3 m) stubs with 2 ft (0.6 m) overhang on both sides of the walls. To prevent out-of-plane wall movements during testing, restraining supports were provided for slab overhangs in the first three floors. Thickness of the top floor slab was increased to 5 in. (127 mm) to accommodate applied lateral forces introduced at that level.

Construction procedures for the specimen were similar to those used in the field. The structure was cast vertically, one story at a time, with construction joints at each floor level. Detailed descriptions of the specimen and construction procedures are given in Appendix A.

Materials and Reinforcing Details

Design compressive strength of concrete was 3,000 psi (20.7 MPa) and Grade 60 reinforcing steel was used. Measured material properties are summarized in Table 1. Specimen CS-1 was tested at the youngest concrete age of 105 days. Therefore, very little change of concrete strength in wall elements were anticipated in RCS-1 tests.

General design of reinforcement details was based on the 1971 ACI Building Code.[17] Reinforcing steel configuration for wall elements is shown in Fig. 4. Primary flexural reinforcement in the wall was provided by 12 No. 4 bars which formed the boundary element at each end of the wall. Confinement at the

Table 1 - Material Properties

Reinforcement	f_y (ksi)	f_{su} (ksi)
No. 3 Bar	70	108
No. 4 Bar	63	101
6 mm Bar	77	103
D-3 Wire	74	85

Concrete	f'_c (psi)	E_c (ksi)
First level	4430	3640
Second level	3390	3350
Third level	3740	3140
Fourth level	3630	3350
Fifth level	3040	2960
Sixth level	3750	3420
Repaired Beams of RCS-1	3500	4070

1000 psi = 1 ksi = 6.895 MPa

f_y = yield strength of reinforcement

f_{su} = ultimate strength of reinforcement

f'_c = compressive strength of concrete

E_c = modulus of elasticity of concrete

-14-
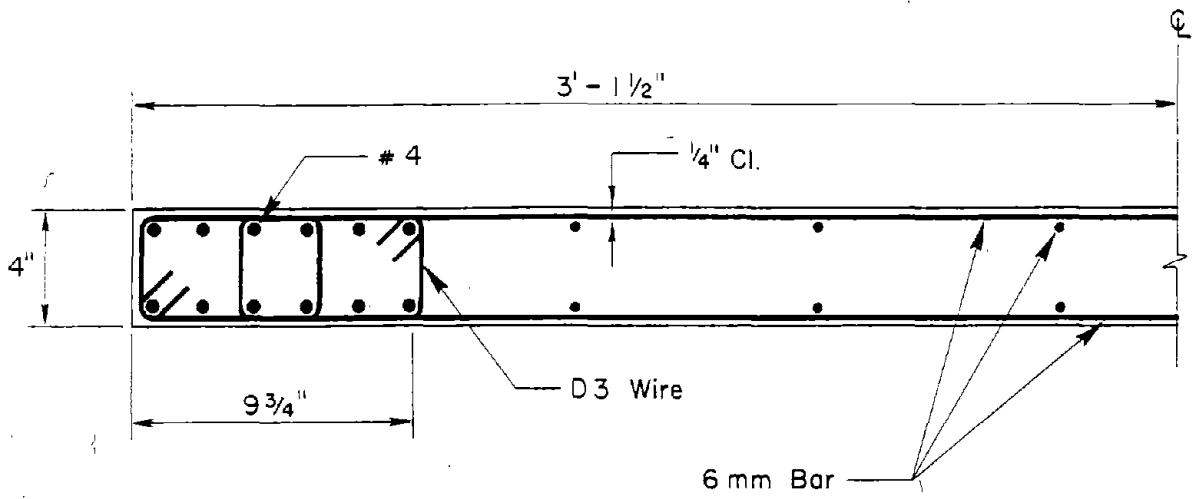
Fig. 4   Reinforcement Details of
          Wall Element

1 in. = 25.4 mm
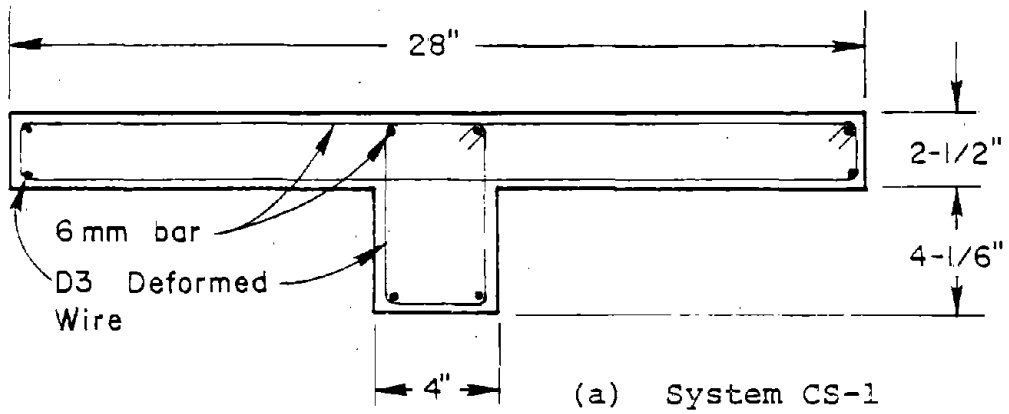
(a)   System CS-1
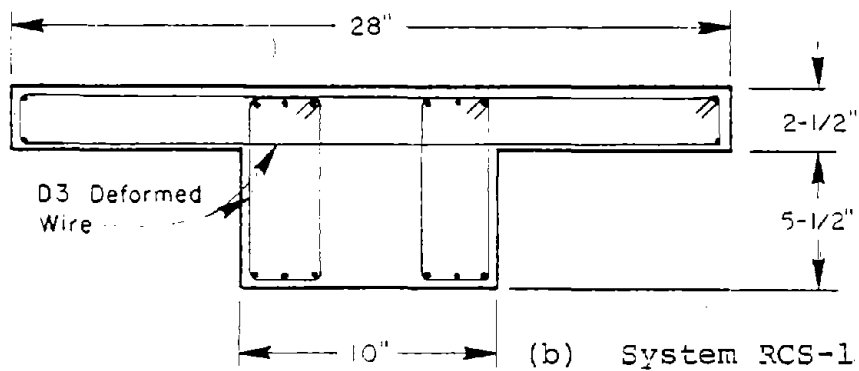
(b)   System RCS-1

Fig. 5   Reinforcement Details of
          Coupling Beams

-15-

boundary element was provided by closed hoops of D-3 deformed wires spaced at 1.33 in. (34 mm) on centers over the first two stories. Hoop spacing in the upper stories was increased to 4 in. (102 mm). Vertical web reinforcement consisted of two layers of 6-mm bars spaced at 9 in. (229 mm). Horizontal shear reinforcement was designed to resist shear forces corresponding to a mechanism consisting of flexural yielding at ends of the coupling beams and 1.25 times flexural yielding at the base of the walls. The 1.25 factor considered in the walls was to account for strain hardening of primary flexural reinforcement. Horizontal reinforcement consisted of the two layers of 6-mm bars spaced at 4 in. (102 mm). No strain hardening was assumed in the coupling beams.

Reinforcement details for coupling beams of CS-1 are shown in Fig. 5(a). Based on experimental results from beam element tests, straight horizontal reinforcement was used.[2,3] Closed hoops of D-3 deformed wire spaced at 1.33 in. (34 mm) were provided in the beams for both shear and concrete confinement. Based on flexural analysis of the coupled wall system, 13% of the total moment capacity at yield was provided by the beams.

Reinforcement details for repaired coupling beams of RCS-1 are shown in Fig. 5 (b). Straight horizontal reinforcement was used. Reinforcement formed two cages to permit anchorage of horizontal reinforcement. Details of the repair procedure are given in Appendix B. Closed hoops of D-3 deformed wire were spaced at 0.83 in. (21 mm) in each cage. Based on the flexural

analysis of the system, the repaired beams provided 30% of the total moment capacity at yield.

Test Setup

The setup for coupled wall system tests is shown in Fig. 6. The specimen, located between two reaction abutments, was loaded laterally at the top as a fixed vertical cantilever.

Forces were applied and distributed equally by crossheads to the top of each wall throughout testing. To monitor behavior, coupled wall specimens were instrumented with both external and internal gages. Applied loads, deflections, rotations, shear distortions and reinforcement strains were measured at selected locations. A detailed description of the tests is given in Appendix A.

Incremental reversing load cycles, as shown in Fig. 7, were applied to the specimens. For CS-1, a total of six reversing load cycles were applied. The weak coupling beams yielded early and suffered severe damage. When wall reinforcement yielded, deterioration of the coupling beams accelerated. At the end of the sixth load cycle, the test was stopped. Although coupling beams were severely damaged, the two walls were still in good condition.

Damaged beams were removed and replaced with stiffer and stronger beams. Wall elements were not repaired. This became the repaired system RCS-1. The resulting wall system was designated as RCS-1. Testing of the repaired system was conducted with similar reversing load cycles as for CS-1. The load
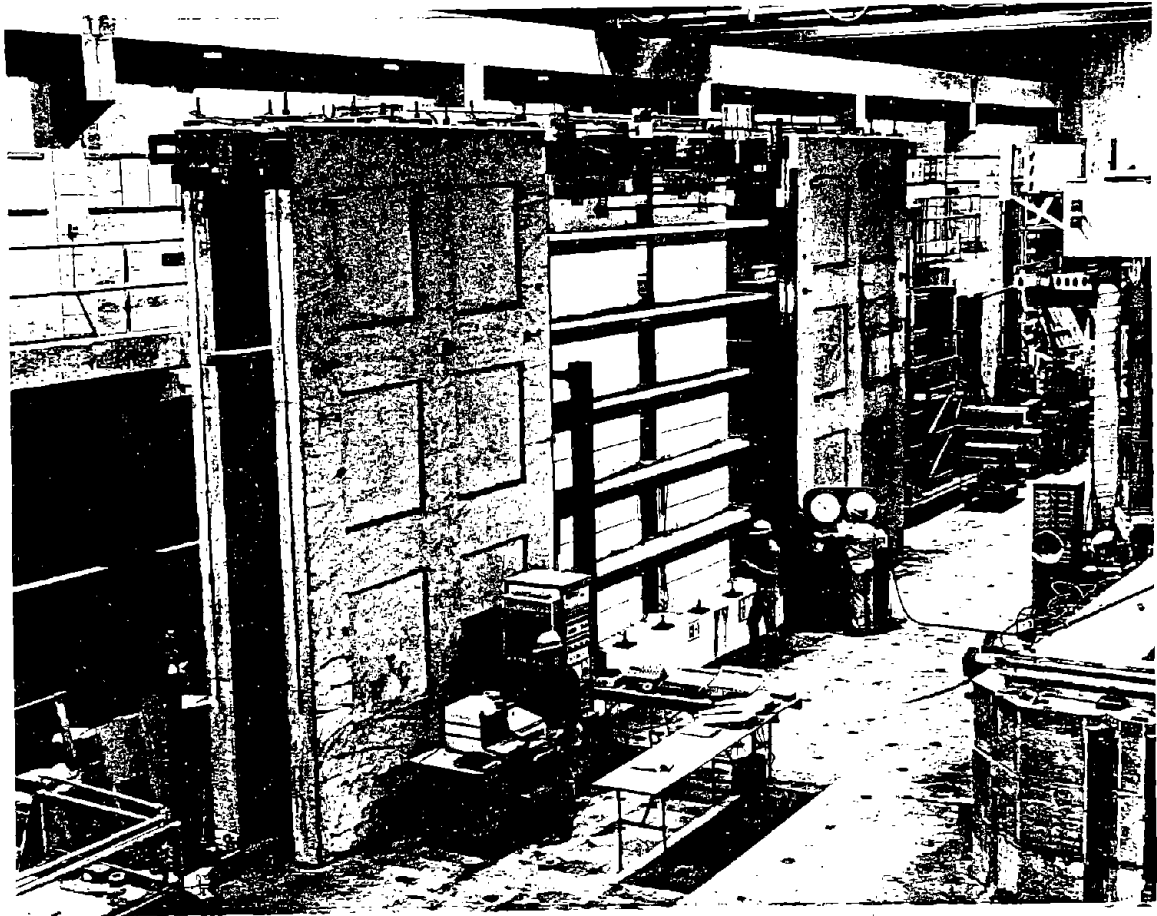
Fig. 6   Coupled Wall Test Setup   1 in. = 25.4 mm
                                       1 kip = 4.448 kN
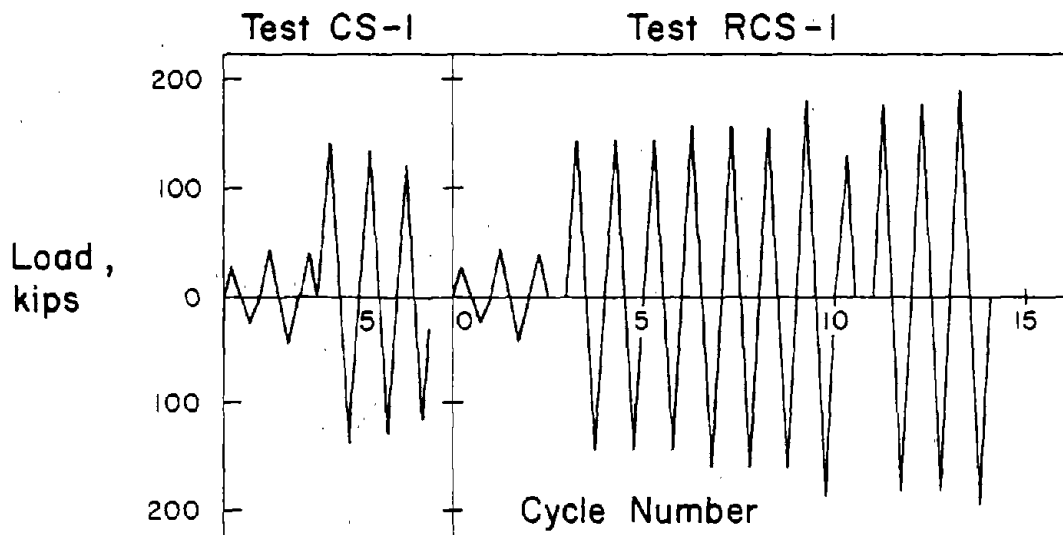
Fig. 7   Load Histories

history for RCS-1 is shown in Fig. 7. The test of RCS-1 was
stopped when load carrying capacity of the specimen deteriorated
substantially. A total of fourteen load cycles were applied to
RCS-1.

SUMMARY OF EXPERIMENTAL RESULTS

Coupling beams selected for the wall systems permitted two
ranges of response to be observed. These ranges were distin-
guished by the magnitude of axial load and shear induced in the
walls. The changes in induced axial loads, and the resulting
redistribution of shear forces, caused two different failure
mechanisms. In this section, observed behavior of CS-1 and
RCS-1 is presented and their load versus deformation character-
istics are discussed. Principal results for both tests are
given in Table 2.

Observed Behavior

Load versus deflection relationships of CS-1 and RCS-1 are
shown in Figs. 8 and 9, respectively. The load and deflection
indicated in the figures represent total applied load and cor-
responding deflection at the top of the specimen. Yielding of
coupling beam elements is identified in Figs. 3 and 9 by shaded
areas. Yielding sequence for coupling beams in both tests is
listed in Table 3.

For CS-1, all coupling beams except the one at the first
level yielded at loads corresponding to 1/3 to 1/2 of the system
yield load. Early yielding of the coupling beams resulted in
excessively high ductility demands. As both wall elements
yielded, all coupling beams had already suffered severe damage.

-19-
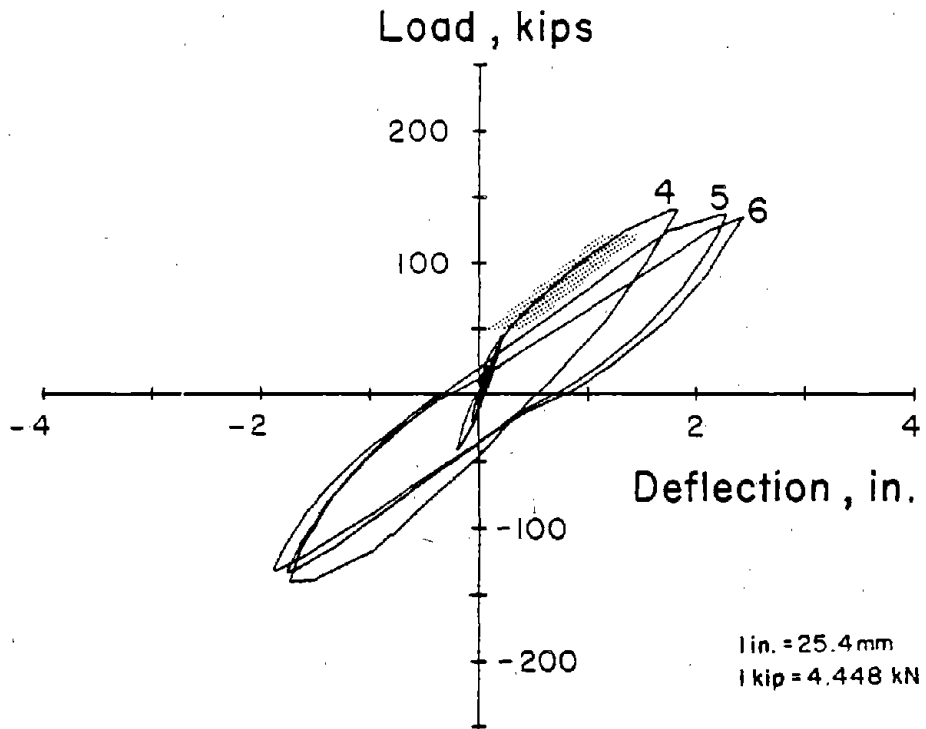
Fig. 8   Load versus Top Deflection for CS-1
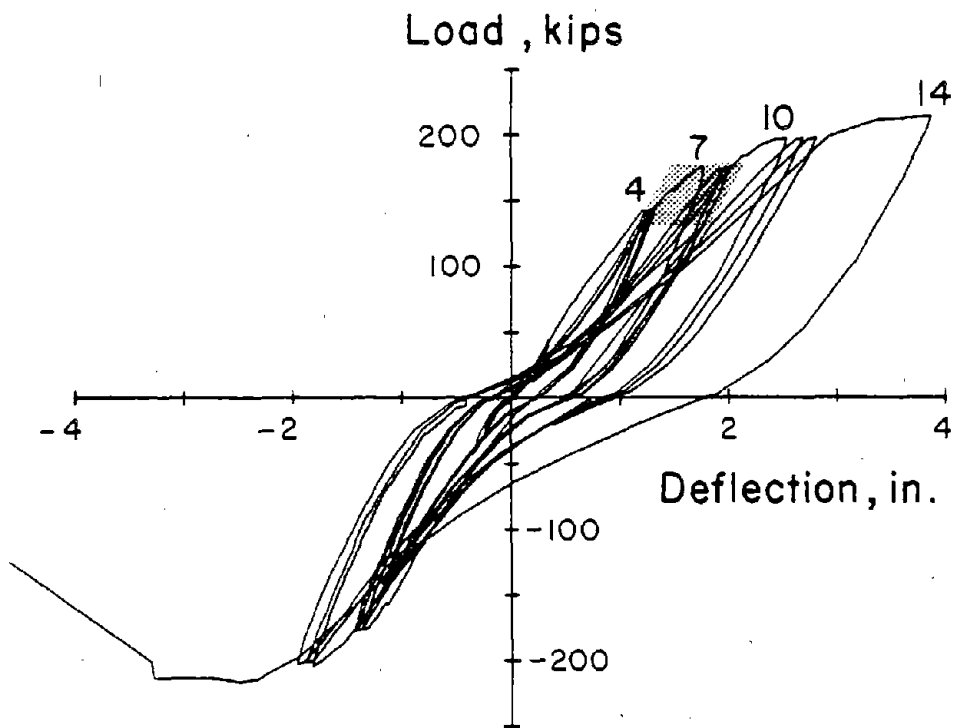
Fig. 9   Load versus Top Deflection for RCS-1

TABLE 2 - PRINCIPAL TEST RESULTS

Item	Test CS-1	Test RCS-1
System Yield Load	120^k (534 kN)	--
System Yield Top Deflection	1.3 in. (33 mm)	--
Maximum Applied Load	143^k (636 kN)	217^k (965 kN)
Maximum Imposed Top Deflection	2.4 in. (61.7 mm)	4.0 in. (101.6 mm)
Max. Nominal Shear Stress	5.4 f'_c psi (0.45 f'_c MPa)	6.7 f'_c psi (0.56 f'_c MPa)

TABLE 3 - YIELDING SEQUENCE OF COUPLING BEAMS

TEST OF CS-1		TEST OF RCS-1	
Load kips (kN)	Coupling Beam Floor Level	Load kips (kn)	Coupling Beam Floor Level
42 (186)	6th	122 (544)	4th
42 (186)	3rd, 4th, 5th,	133 (593)	3rd, 5th
59 (262)	2nd	157 (700)	6th
86 (383)	1st	192 (854)	1st

In addition, a separation of 0.5 in. (13 mm) between walls at the top of the specimen was measured at the end of the fourth load cycle. Wall separation imposed axial deformations in coupling beams which further reduced beam deformation capacity. Thus, under subsequent inelastic reversals, walls became uncoupled and the specimen behaved as two uncoupled walls in parallel. The amount of coupling estimated at yield load during the fourth cycle was 11%. This compared well with the 13% expected at full yield from the design analysis.

The extent of cracking in CS-1 at the end of the sixth load cycle is shown in Fig. 10. Cracks in coupling beams were concentrated at both ends. With repeated inelastic cycles hinges formed in the coupling beams at the wall-beam interface. Eventual deterioration of hinge capacity reduced the coupling action provided by the beams to a simple linkage mechanism. As shown in Fig. 10, the observed cracking pattern of the wall elements was similar to that of an isolated wall under lateral load reversals[15]. Wall elements of CS-1 were in good condition at the end of the test as can be seen in Fig. 11.

A total of fourteen load cycles were applied to RCS-1. Beam yielding occurred at levels higher than 2/3 of the maximum load as shown by shaded areas in Fig. 9. All coupling beams yielded before significant reduction of specimen stiffness occurred.

Axial load in the walls generated by the coupling beams had a significant effect on wall ductility and mode of failure. The nominal axial stress for the compression wall was estimated to be 42% of the balanced flexural failure condition. This estimate was based on calculated axial load versus moment interaction diagram. For the tension wall, uplift represented 63% of the yield capacity under pure axial tension. Because of effects of induced axial load, significant redistribution of shear and moment between walls was expected.

The combination of large axial and shear stresses in the compression wall of RCS-1 was sufficient to cause web crushing at a lateral top deflection of 3.8 in. (97 mm). Deformation capacity of the system was significantly lower than that
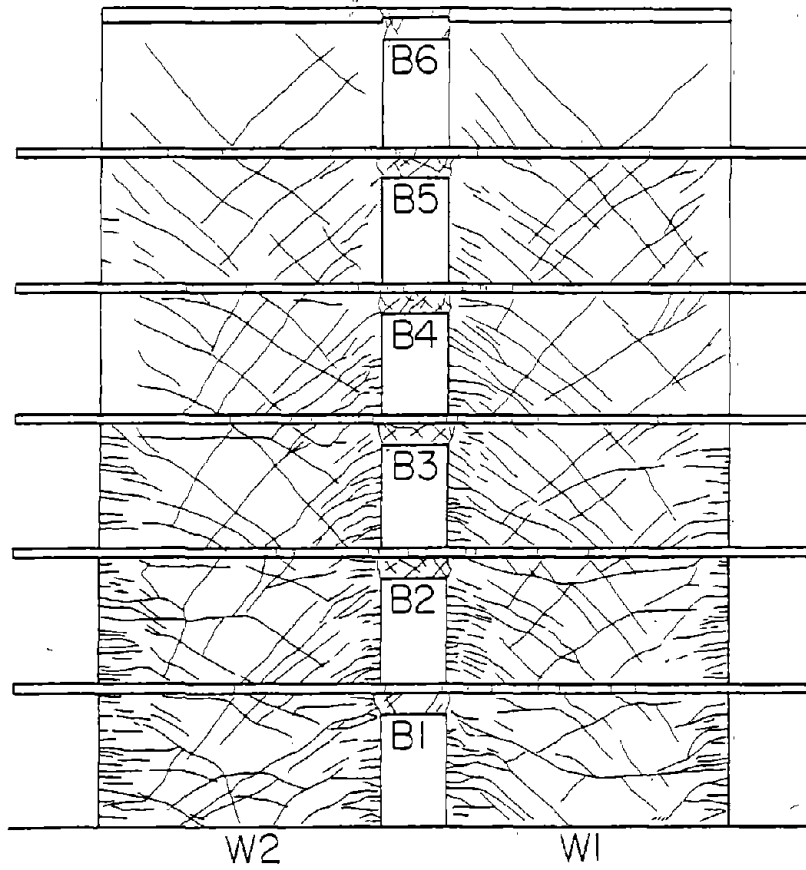
Fig. 10   Crack Pattern in CS-1
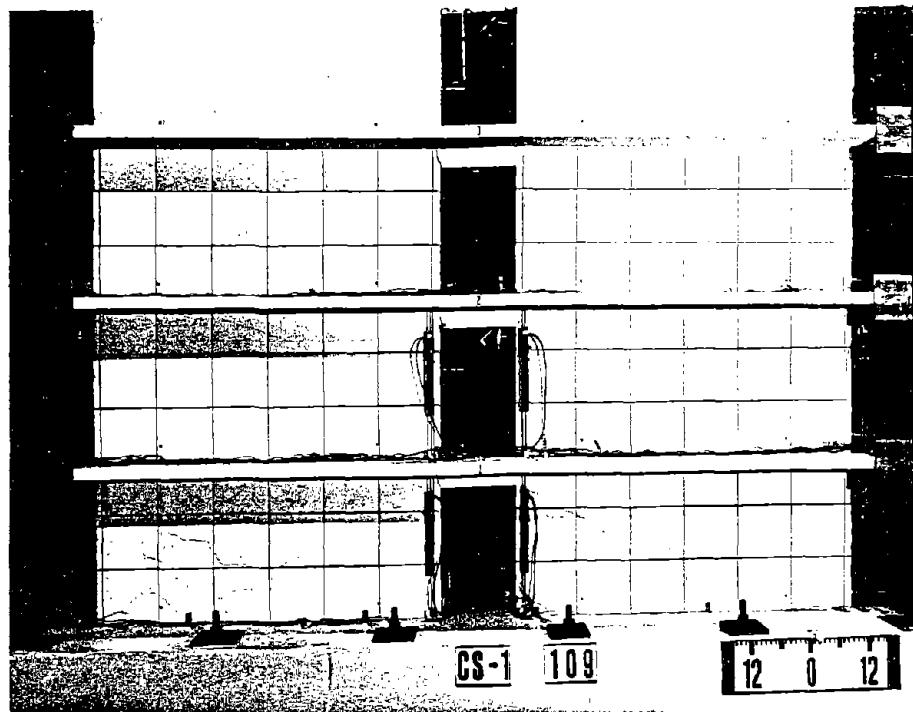
Fig. 11 System CS-1 after Testing

measured in isolated wall tests[18]. Further details on behavior of the coupled wall specimens are given in Appendix B.

The cracking pattern of RCS-1 is shown in Fig. 12. For clarity, only cracks resulting from one direction of loading are shown. Diagonal cracks were observed spreading evenly throughout the height of the specimen. Cracks initiated in the tension wall were seen propagating through the coupling beams unto the compression wall. This indicated that the specimen was behaving very much like a single element in an "overturning" mode. A photograph of RCS-1 after testing is shown in Fig. 13.

Load-deflection envelopes for CS-1 and RCS-1 are plotted in Fig. 14. The broken line in the figure represents the load-deflection envelope of two uncoupled walls in parallel[18].

The initial stiffness of CS-1 and RCS-1 was observed to be about three times the stiffness of two walls in parallel. However, once coupling beams yielded, stiffness of the systems decreased steadily. For CS-1, decrease of specimen stiffness was quite rapid. As can be seen in Fig. 14, the load-deflection envelope of CS-1 approached that of two uncoupled walls. The test was stopped after the walls yielded. For RCS-1, higher load capacity was attained, than for two uncoupled walls acting in parallel. However, the system was less ductile.

Observed behavior of the test specimens can be summarized as follows. Coupling provided by the relatively weak beams in CS-1 was too light. The coupling beams suffered severe damage relatively early which resulted in a "linked" wall system. The
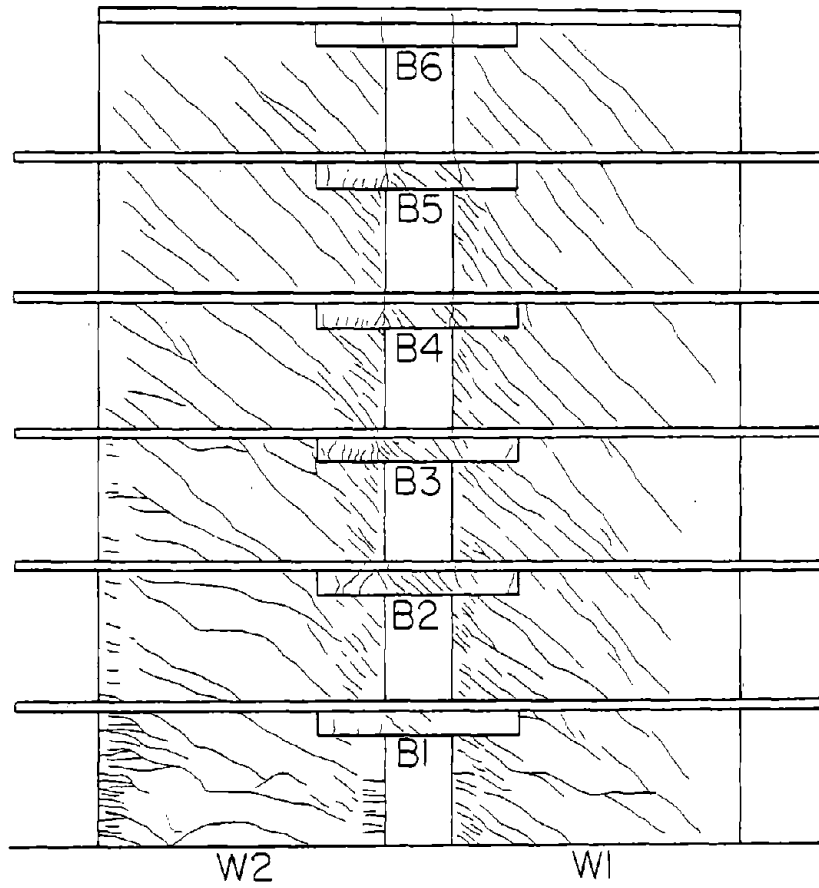
Fig. 12   Crack Pattern in RCS-1
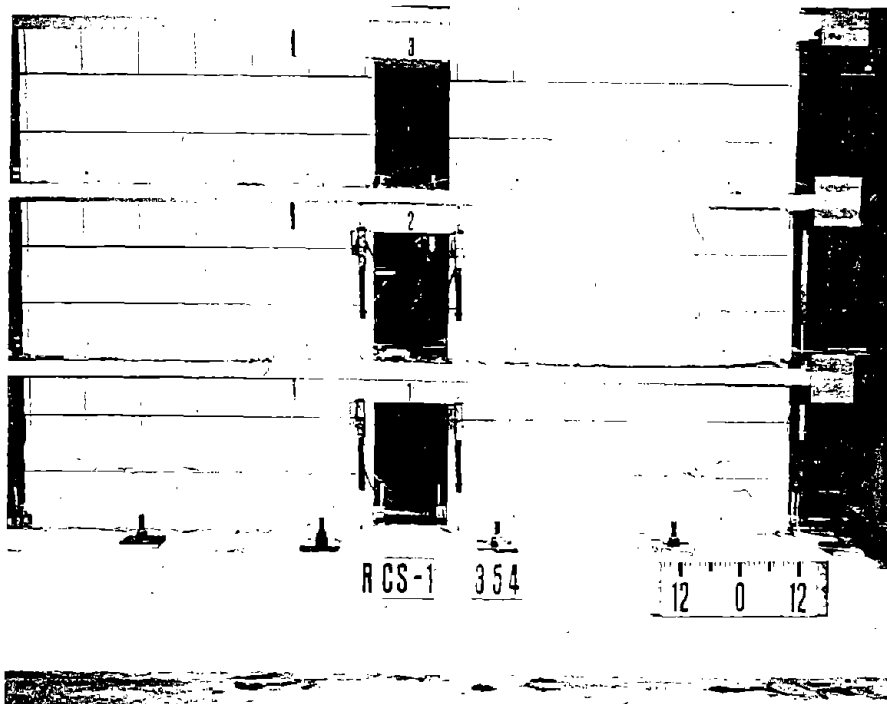
Fig. 13   System RCS-1 after Testing

Top Deflection, mm
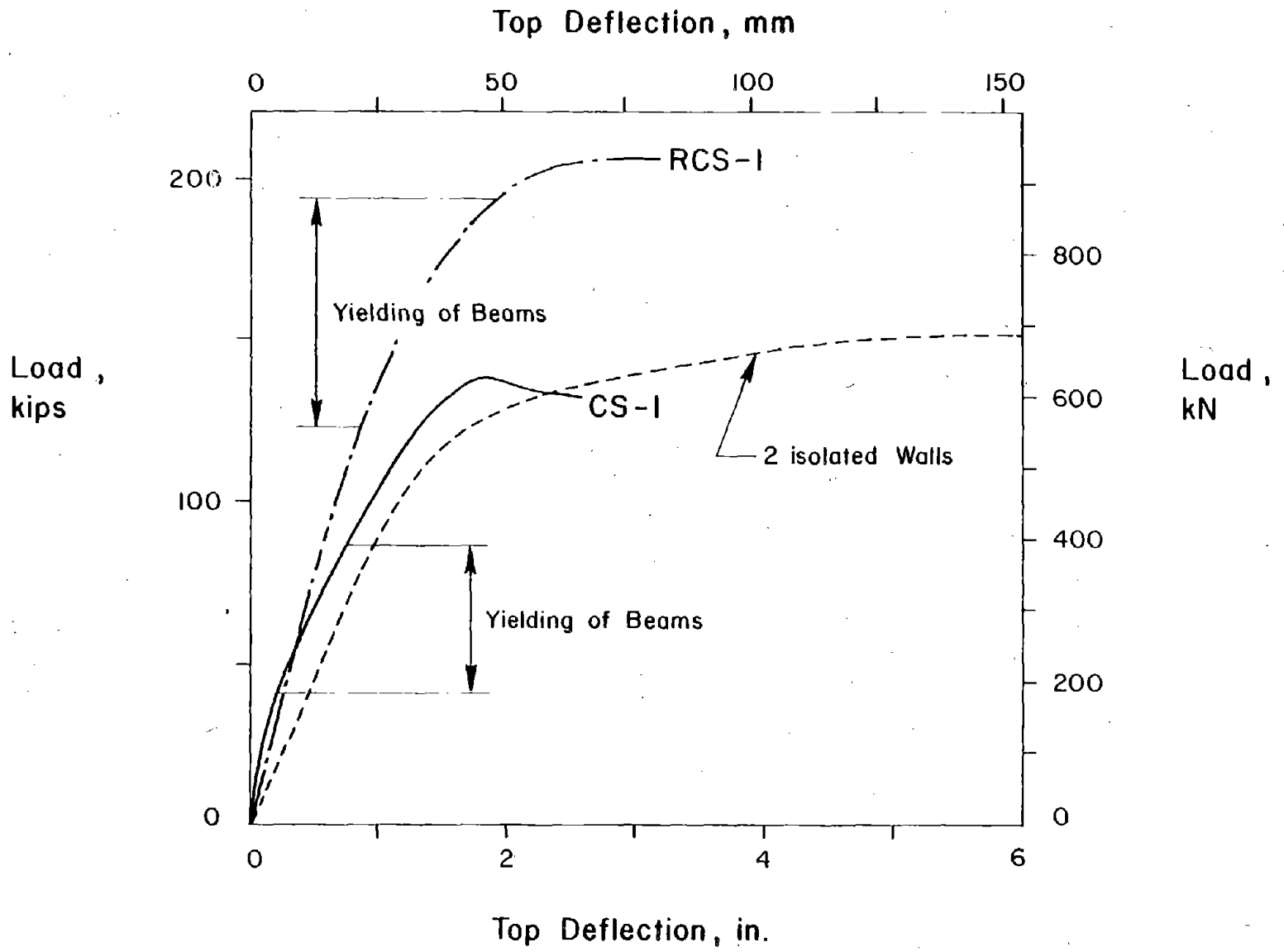
Fig. 14   Load Deflection Envelopes

-26-

advantage of dissipating energy through coupling beams was not efficiently utilized. On the other hand, coupling beams in RCS-1 were too strong relative to the walls. Inelastic behavior of beams was not fully utilized to dissipate input energy. Thus, wall elements became the critical element in the design. In addition, strong coupling beams induced high axial loads on the walls which reduced deformation capacity of the system.

An efficient coupled system should provide the desired load capacity without sacrifice of required deformation capacity. Wall elements should be designed to maintain their integrity while energy is dissipated in coupling beams. At the same time, beams should be selected with sufficient deformation capacity to sustain coupling actions beyond system yielding.

Deformation Characteristics

A maximum top deflection of 2.4 in. (61 mm) was measured in CS-1 when the test was terminated. This corresponds to about 1.1% of the specimen height. A deflection of 4.0 in. (102 mm), 1.9% of the specimen height, was applied to RCS-1. As a point of reference, generally accepted maximum overall drift for design is about 1 to 2%.

Lateral deflection profiles of the two systems at approximately the same top deflection are shown in Fig. 15. Curves on the positive side of the x-axis represent the deflection profile of the compression wall, while curves on the negative side of the x-axis represent deflection profile of the tension wall. The walls acquired different deflected shapes as they were sub-jected to alternating axial tension and compression under load

-27-

Story Level

Test CS-1

Test RCS-1

1 in. = 25.4 mm

-2.0   -1.0   0   1.0   2.0
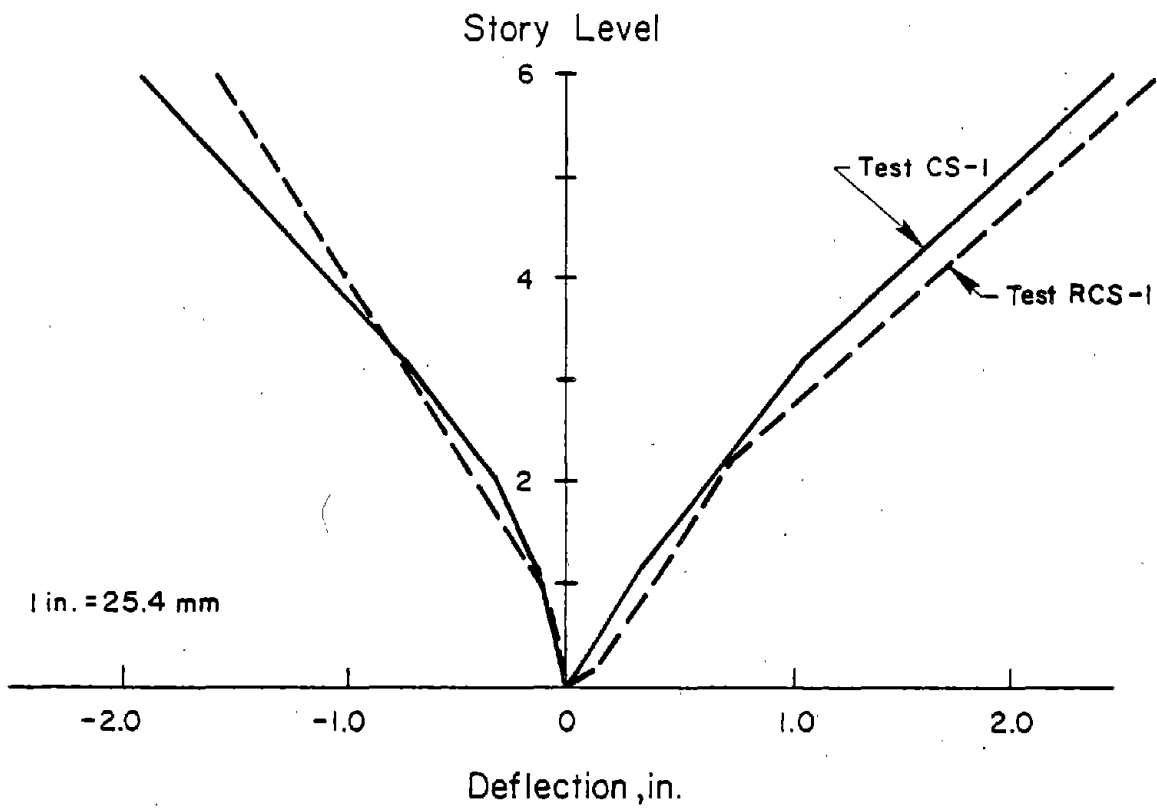
Deflection, in.

Fig. 15   Lateral Deflection Profiles for
          CS-1 and RCS-1

reversals. Walls in compression exhibited larger deflections especially at the first two stories. This can be explained by the fact that shear and moment were redistributed between the tension and compression walls through the coupling beams.

In Fig. 16(a), total lateral load is plotted versus rotation of first story wall elements. Positive loads indicate that compressive axial forces were induced into the wall element being measured. Negative loads indicate tensile axial forces in the wall element. For CS-1 load versus rotation curves under positive loads were similar to those under negative loads. This indicates that wall behavior under different axial forces was essentially the same. Axial forces induced through coupling were not large enough to change wall behavior.

For RCS-1, load versus rotation relationships in tension and compression walls were quite different. Measured rotations for the wall in compression were significantly larger than those of the wall in tension. This indicated that moment resisted by the compression wall was significantly higher than the tension wall. Such redistribution of moment between two walls was attributed to the large induced axial loads. The axial loads induced through coupling were large enough to change wall behavior significantly.

In Fig. 16(b), load versus shear distortions measured in the first story of wall elements are shown. Positive loads indicate that compressive axial forces were present in the wall element while negative loads indicate the presence of tensile axial forces. From Fig. 16(b), it can be seen that load versus shear

-29-

Load,
kips

200

100

-0.010   -0.005   0.005   0.010

-100

Rotation, rad.

-200

θ

Load,
kips

200

100

-0.010   -0.005   0.005   0.010

-100

Rotation, rad.

-200

(a)   CS-1

Load,
kips

200

100

-0.010   -0.005   0.005   0.010

-100

Shear Distortion,
rad.

-200

1 in. = 25.4 mm
1 kip = 4.448 kN

γ

Load,
kips

200

100

-0.010   -0.005   0.005   0.010

-100

Shear Distortion,
rad.

-200

(b)   RCS-1
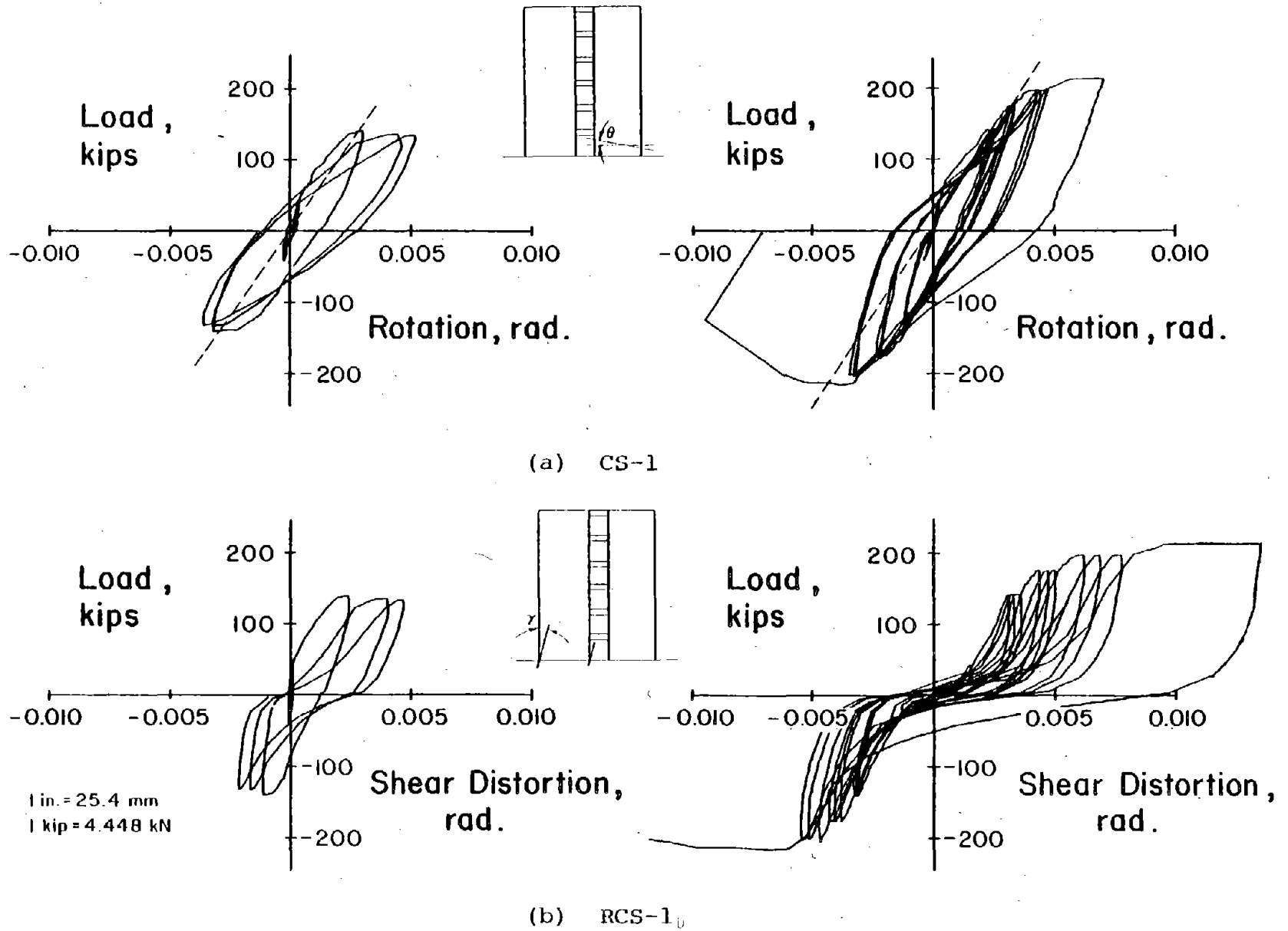
Fig. 16   Rotation and Shear Distortion Measurements
in First Story Wall Elements

distortion relationships for CS-1 and RCS-1 were affected by the direction of applied loads. This indicated that shear was redistributed between wall elements in both tests. Shear forces were transferred from the tension wall to the compression wall through the coupling beams.

In comparing rotations and shear distortions for both tests, shear distortions were found to be more predominant in RCS-1 than in CS-1. As shown in Fig. 16, at load cycles with the same measured rotation, corresponding measured shear distortions in RCS-1 were twice than those of CS-1. This indicated that the amount of deflection made up by shear distortions was larger in RCS-1 than in CS-1.

Rotations in coupling beams were also measured for both tests. Applied load versus end rotation of the coupling beam at the fourth story is shown in Fig. 17. Measured rotation of the coupling beam in CS-1 was 0.0037 rad.[2,3] at yield and maximum rotation recorded was 9.3 times yield rotation. This exceeded the rotational ductility capacity of the relatively weak beams. Observed separation of walls in CS-1 further reduced beam ductility.

Rotation of the repaired beams at yield was 0.0005 rad. Maximum measured rotation was 17 times the yield rotation. Although beams underwent many times of their yield rotation, beam elements were still in good conditions.

Fig. 18 shows the load versus shear distortion relationships for the 4th story coupling beams of both tests. Shear distortions measured in CS-1 were much larger than those measured in

Load.kips

System CS-I

200

100

-0.04   -0.02   0.02   0.04

-100

-200

System RCS-I

200

100

-0.04   -0.02   0.02   0.04

Rotation,rad.

-100

1 in. = 25.4 mm
1 kip = 4.448 kN

-200
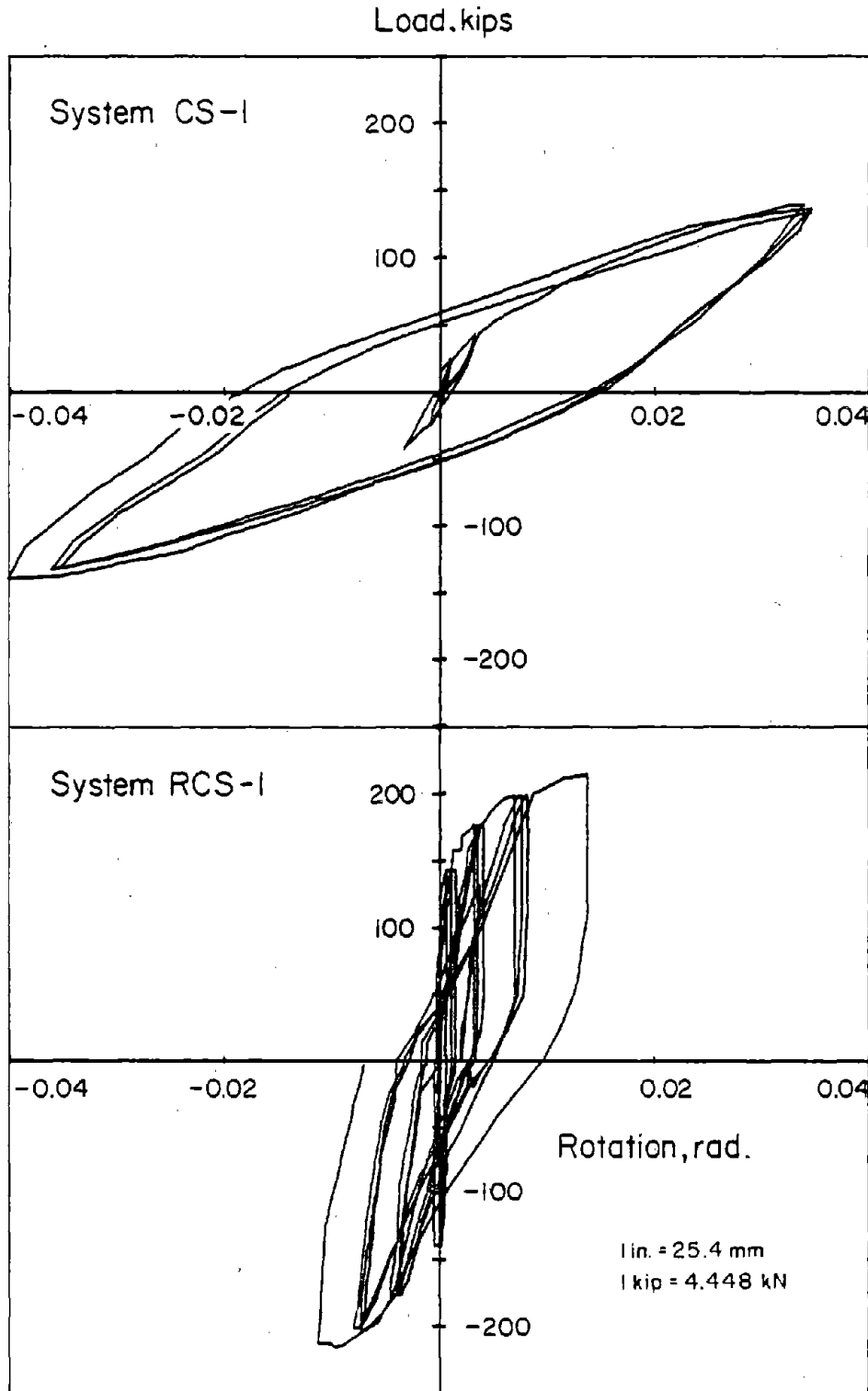
Fig. 17 Load Versus Rotation Relationships
         of Coupling Beams at the 4th Story Level
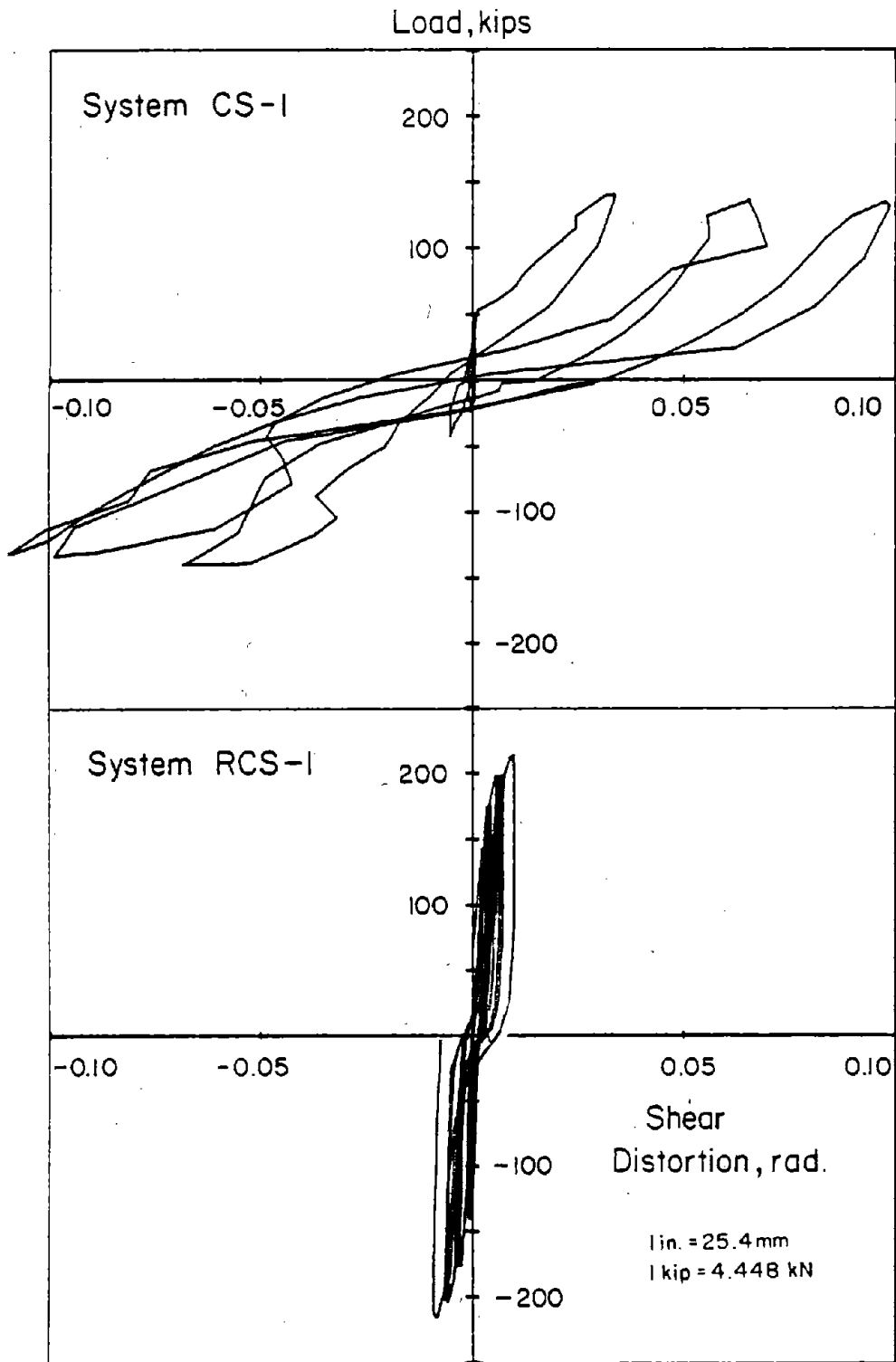
Fig. 18   Load Versus Shear Distortion Relationships
of Coupling Beam at the 4th Story Level

RCS-1. A more detail description of the data is given in Appendix B.

ANALYSIS OF EXPERIMENTAL RESULTS

In this section, coupled wall systems are discussed in light of the experimental data. Load resisting mechanisms of coupled systems are reviewed with respect to the nature of coupling and the redistribution of shear and moment in walls. Components of deflection measurements in wall systems are also presented in this section.

Coupled Systems

In order to understand behavior of the coupled wall systems, attention must be given to interactions of structural elements. A free body diagram of a wall element under axial compression in a coupled wall system is shown in Fig. 19. Shear and moment at the base of the wall element can be expressed as follows:

$$\frac{1}{2} P_O = V_w - \Sigma A_c \tag{1}$$

$$M = \frac{1}{2} P_O H = M_w + \Sigma(M_c + V_c \frac{d}{2}) - \Sigma A_c h_c \tag{2}$$

where P_O = applied load

V_w = shear force at base of wall element

A_c = axial force in coupling beams

H = height of wall system

M_c = moment in coupling beams

M_w = moment in wall element
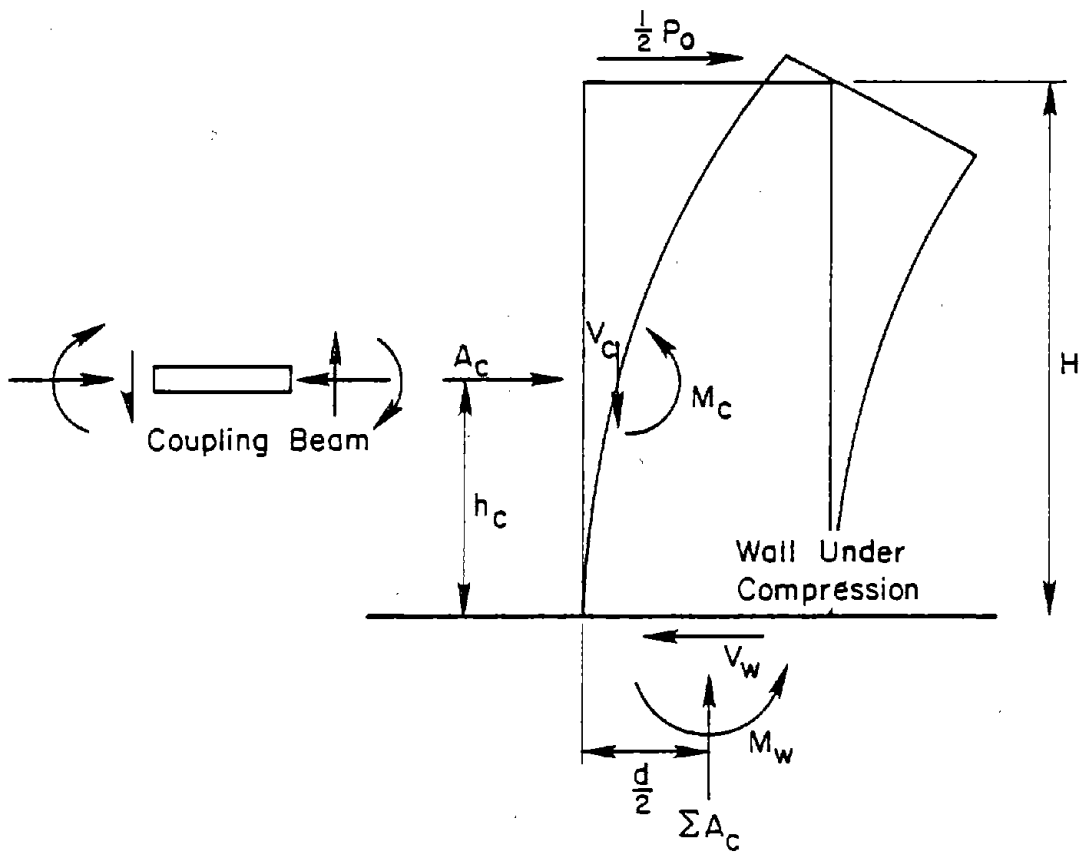
$$\tfrac{1}{2} P_0 = V_w - \Sigma A_c$$

$$M = \frac{P_0 H}{2} = M_w + \Sigma (M_c + V_c \tfrac{d}{2}) - \Sigma A_c h_c$$

Fig. 19   Free Body Diagram of a Wall Element
in a Coupled Wall System

V_c = shear force in coupling beams

h_c = height of coupling beam above base

d = horizontal length of wall element

From Fig. 19, it can be seen that wall elements of a coupled wall system must resist a complicated pattern of forces. Wall elements were subjected to alternating axial tension and compression within one complete load cycle. Shear, moment, and axial stresses were induced into the wall elements through the coupling beams.

It can be seen from Eq. (1) that applied loads were redistributed through axial deformations of coupling beams. Lateral loads were transmitted from tension wall to compression wall. Similarly, moments were also redistributed between the tension and compression walls through the coupling beams as shown in Eq. (2). The last term in Eq. (2) represents the redistributed moments. Therefore, axial forces in coupling beams have to be considered in evaluation of loading conditions in wall elements.

The second term in Eq. (2) represents the coupling moment provided by beams. It is obvious that coupling strength is directly proportional to the strength characteristics of coupling beams.

In order to experimentally evaluate the coupling effects, test results for CS-1 and RCS-1 were compared with isolated wall test data[18]. First, rotation histories of individual walls in CS-1 and RCS-1 were obtained for a selected cycle. Using these rotation histories, lateral loads required to produce a similar rotation history on an isolated wall specimen were

estimated. This estimate was based solely on data from a test of an isolated wall with the same design and details as walls in the system[18]. Effects of load history and inelastic shear characteristics were neglected. Lateral load calculations were made for both tension and compression walls. Load histories obtained for the two walls were then added together and compared with test results. Comparisons of measured and estimated load-deflection relationships for CS-1 and RCS-1 are shown in Figs. 20 and 21 respectively.

As can be seen in Fig. 20, total estimated loads resisted by both wall elements were found to be consistantly smaller than the measured data for CS-1. The discrepancy was attributed to effects of beam coupling. At a top deflection of 1.5 in. (38 mm), the sum of the two estimated wall loads accounted for 84% of the total measured load. This indicated that about 16% of additional load capacity was provided by coupling action. This agrees well with the design calculation which indicated that 13% of full flexural capacity was provided by coupling.

For RCS-1, loads carried by tension and compression walls accounted for about 58% of the total applied load at a top deflection of 3.0 in. (76 mm). This is shown in Fig. 21. Based on design calculations, 42% coupling was predicted. The higher percentage obtained from the comparison in Fig. 21 was due to effects of shear and moment redistribution which were not con-sidered in the design calculations.
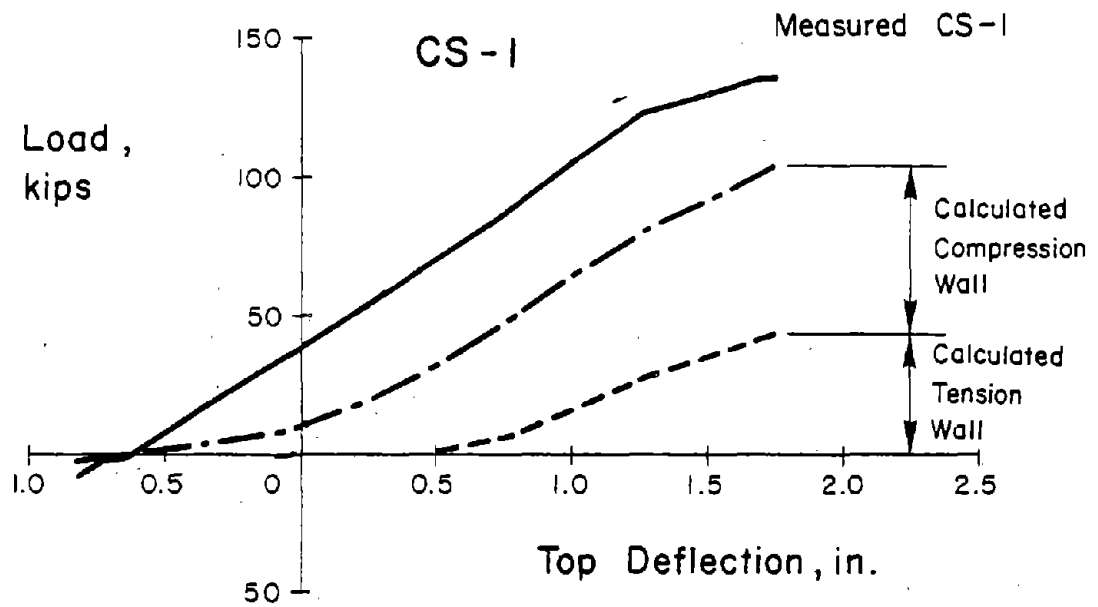
Fig. 20   Estimated Distribution of Loads
for Wall Elements for CS-1

1 in. = 25.4 mm
1 kip = 4.448 kN
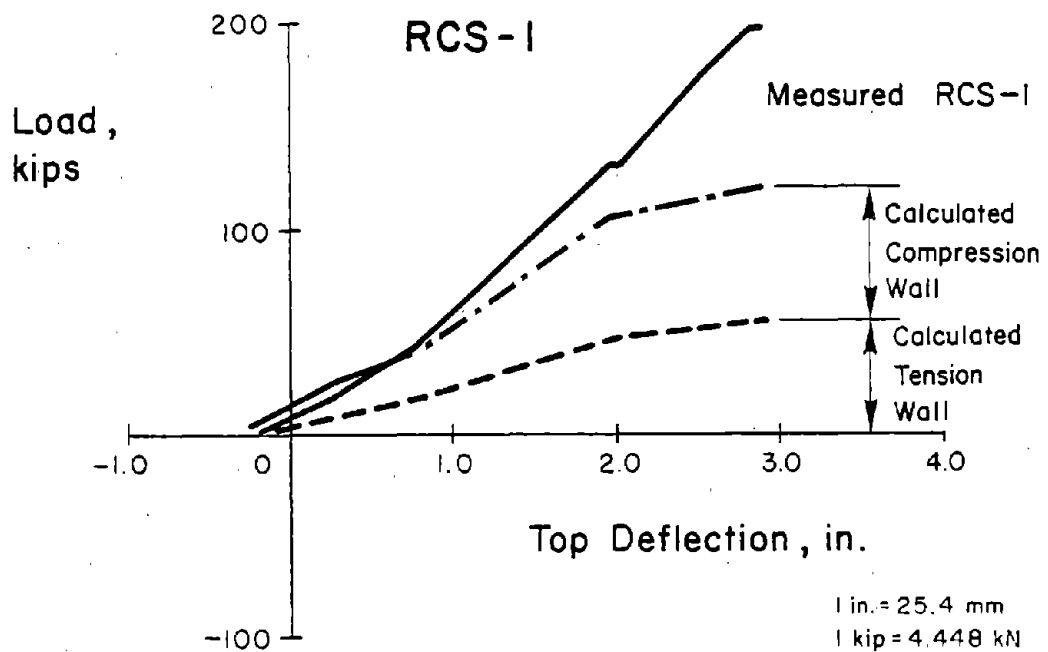
Fig. 21   Estimated Distribution of Loads
for Wall Elements for RCS-1

Deflection Components

Based on rotation and shear distortion measurements at the first two story levels of wall elements, flexural and shear deflections were calculated. Details of calculations are presented elsewhere.[18]

Deflection profiles for CS-1 in Load Cycle 5 and RCS-1 in Load Cycle 12 are shown in Figs. 22 and 23, respectively. Components of measured deflections at the first two stories are also indicated in the figures. It is observed that shear deformation presented a larger portion of measured deflections in RCS-1 than in CS-1.

Since individual walls were subjected to different forces as applied loads were reversed, deflection components versus load stages are plotted in Figs. 24 and 25 for CS-1 and RCS-1, respectively. It was observed that as loads were reversed, the rotation component of deflection did not reverse at the same time as the total deflection. Reversal of deflections attributed to rotations always lagged behind corresponding deflections attributed to shear distortions. This phenonmon is especially obvious for RCS-1.

Relationships between first story deflections and top deflections are shown in Figs. 26 and 27. In CS-1, deflections attributed to shear accounted for 52% of the total measured deflection at the first story level. In RCS-1 deflections attributed to shear accounted for over 65% of the first story deflection. This indicated that inelastic shear behavior was more significant in RCS-1 than in CS-1.

Story Level

6

5

4

3

Measured Deflection
Calculated Rotation and
Shear Component
Calculated Rotation
Component

2

Tension   Compression

-3.0   -2.0   -1.0   0   1.0   2.0   3.0

(a)   Wall Element W1

Deflection, in.

Story Level

6

5

4

3

1 in. = 25.4 mm

2

Tension   Compression

-3.0   -2.0   -1.0   0   1.0   2.0   3.0

(b)   Wall Element W2
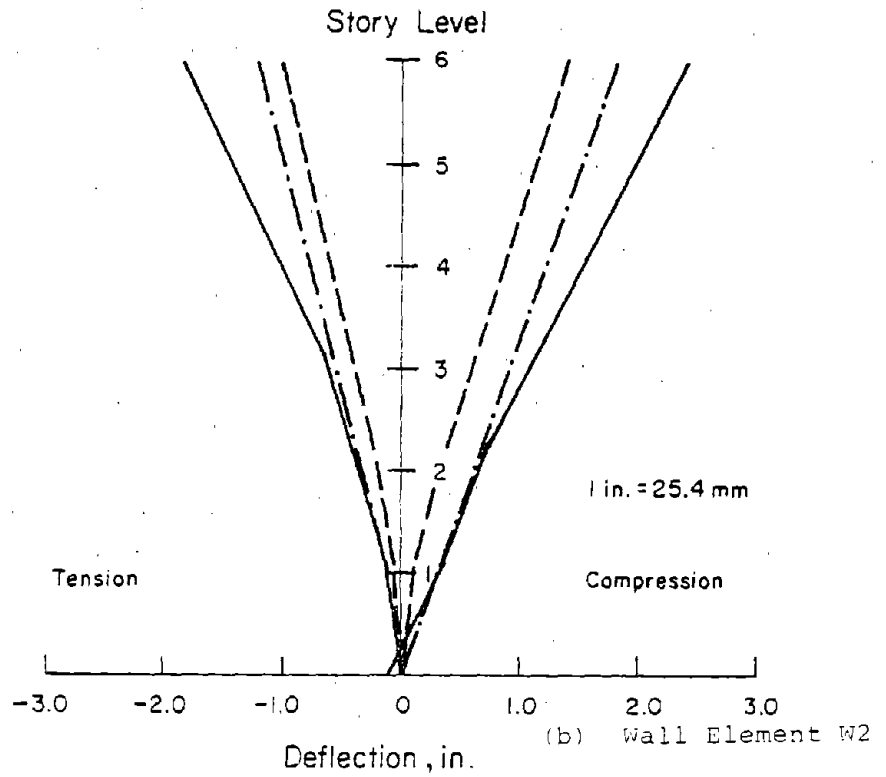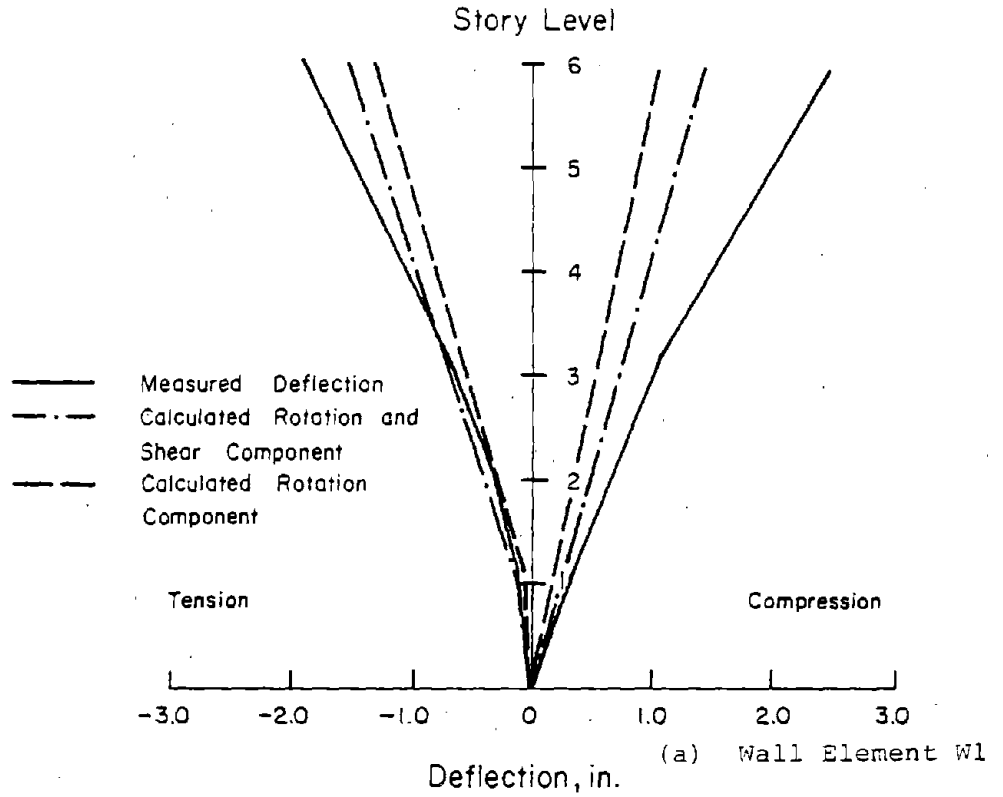
Deflection, in.

Fig. 22   Deflection Profiles for CS-1 at Load Cycle 5

Story Level

Measured Deflection
Calculated Rotation and
Shear Component
Calculated Rotation
Component

Tension   Compression

-3.0   -2.0   -1.0   0   1.0   2.0   3.0

Deflection, in.   (a)   Wall Element W1

Story Level

1 in. = 25.4 mm

Tension   Compression

-3.0   -2.0   -1.0   0   1.0   2.0   3.0

Deflection, in.   (b)   Wall Element W2
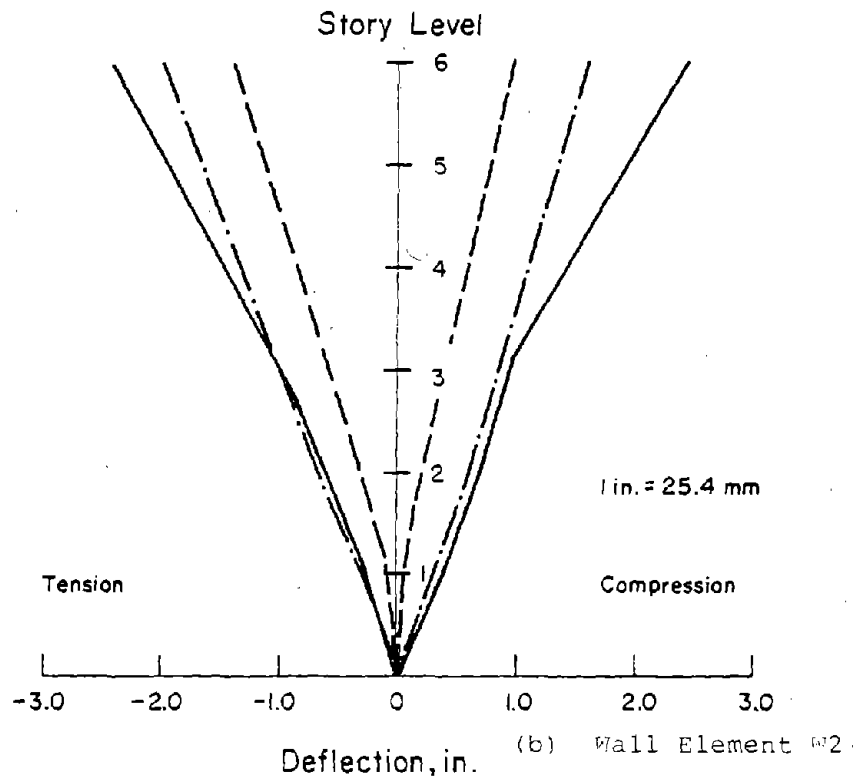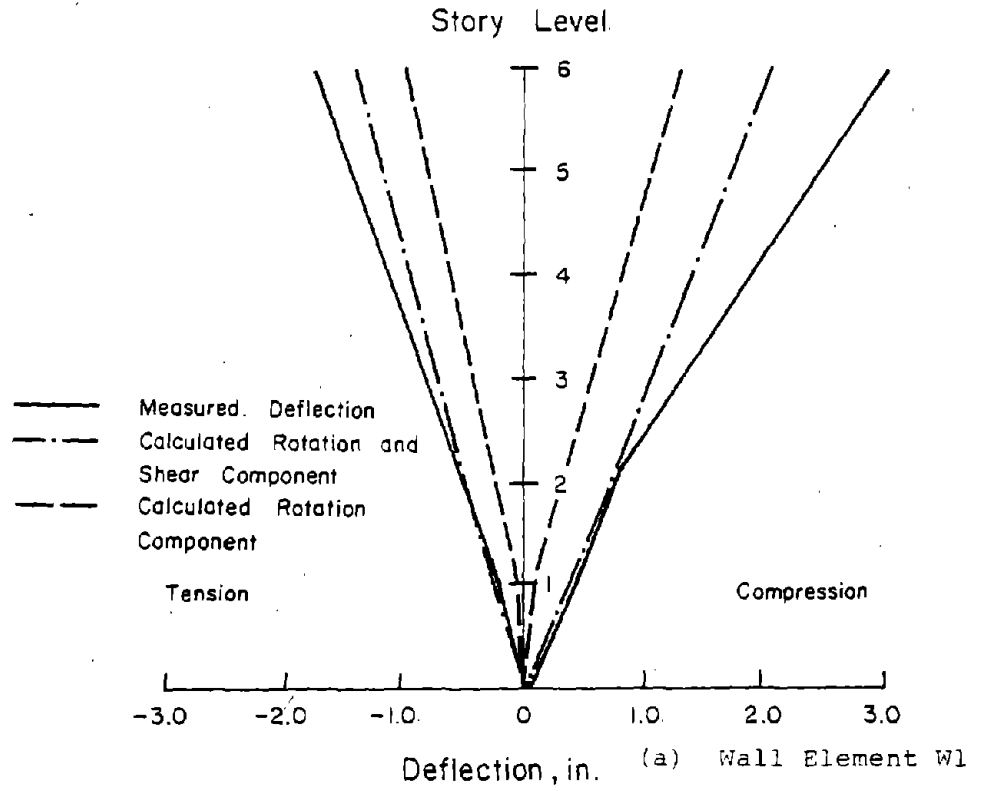
Fig. 23   Deflection Profiles for RCS-1 at Load Cycle 12
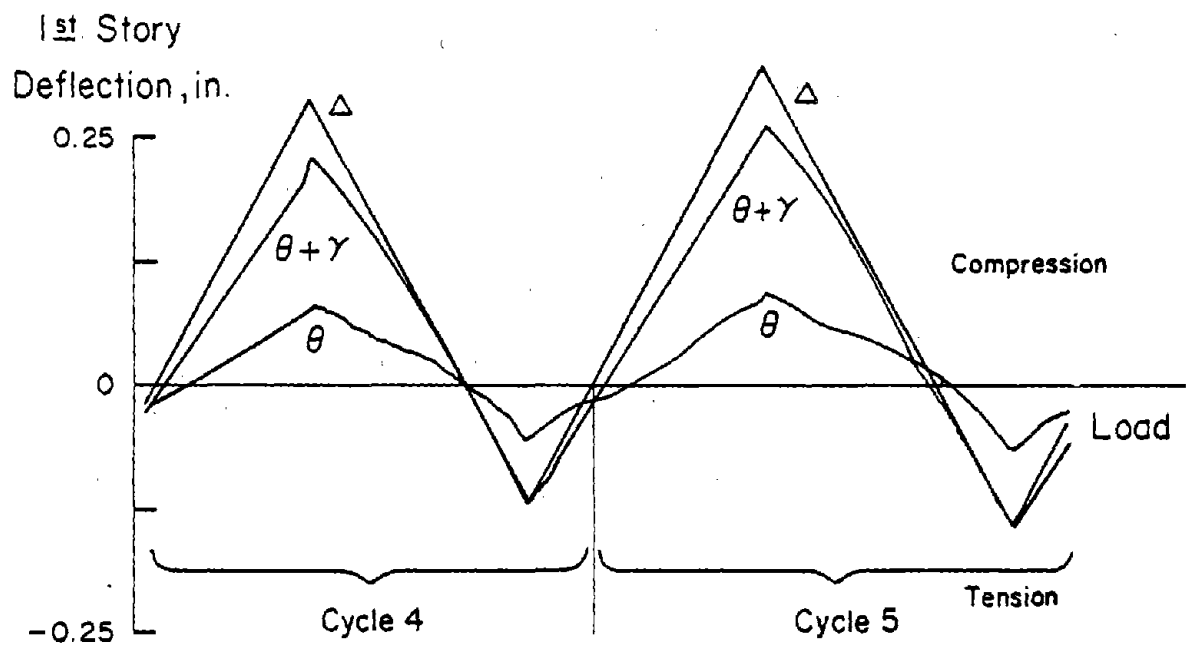
Fig. 24   Deflection Components for CS-1
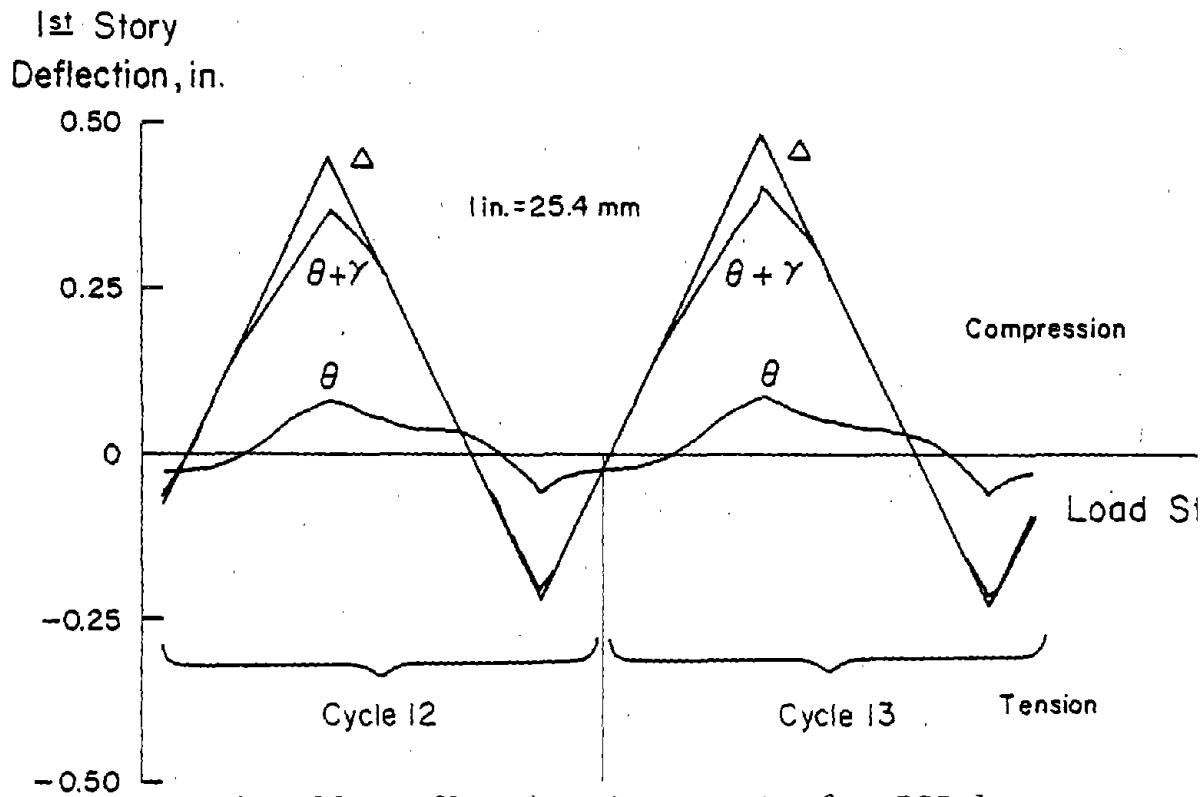
Fig. 25   Deflection Components for RCS-1

1st Story
Deflection

0.50

1 in. = 25.4 mm

0.25

Δ

$\gamma + \theta$

θ

0

0   1.0   2.0   3.0

Top Deflection, in.

(a)   Compression Wall

1st Story
Deflection

0.50

Δ =   Measured Deflection

θ =   Rotational Component

γ =   Shear Distortion Component

0.25

Δ
$\gamma + \theta$

θ

0

0   1.0   2.0   3.0

Top Deflection, in.
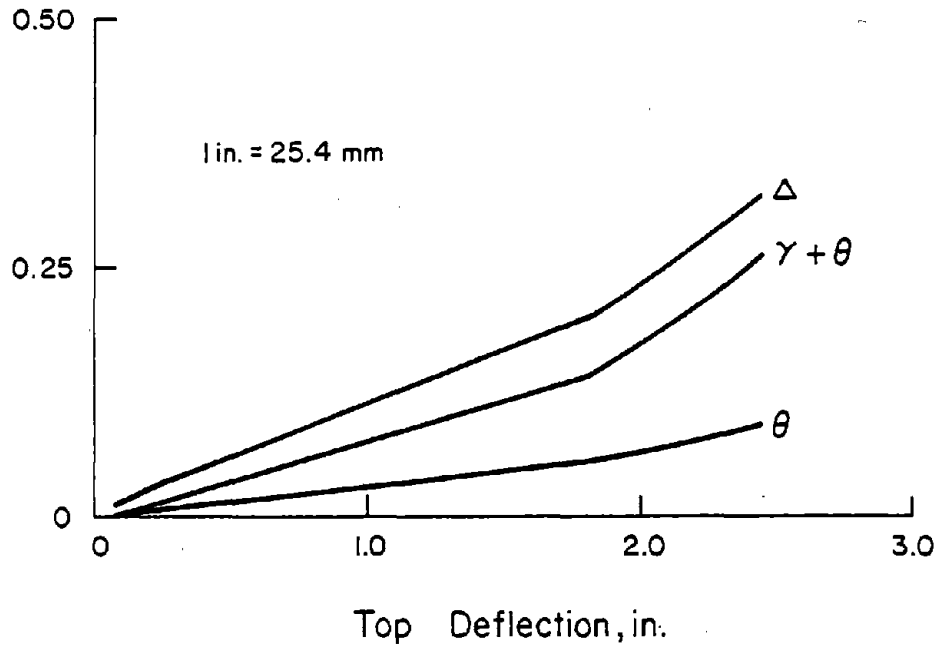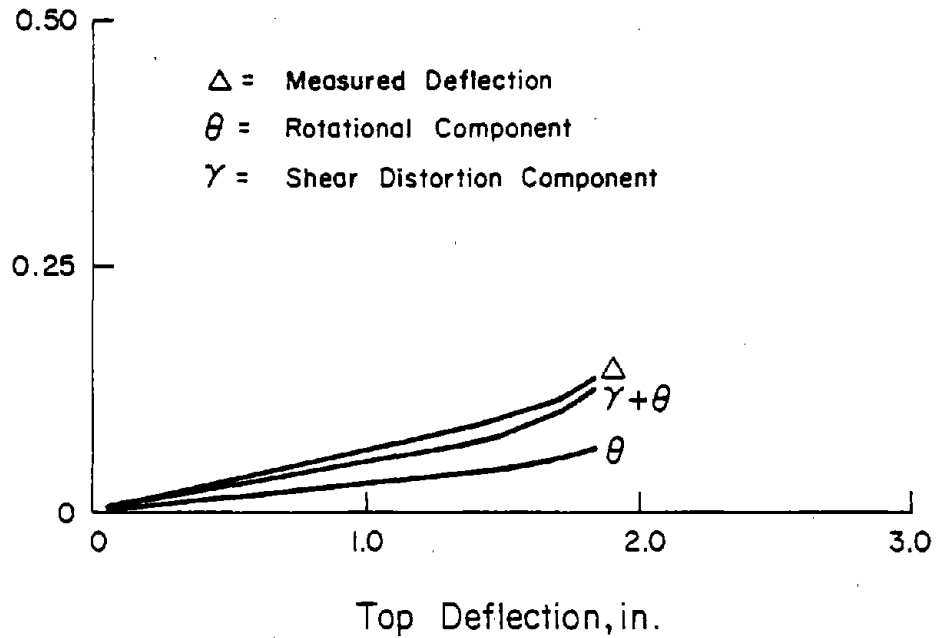
(b)   Tension Wall

Fig. 26   Lateral Deflection Components for CS-1

1st Story
Deflection

0.50

1 in. = 25.4 mm

0.25

0

0   1.0   2.0   3.0

Top   Deflection, in.

(a)   Compression Wall

1st Story
Deflection

0.50

△ = Measured Deflection

θ = Rotational Component

γ = Shear Distortion Component

0.25

0

0   1.0   2.0   3.0

Top   Deflection, in.
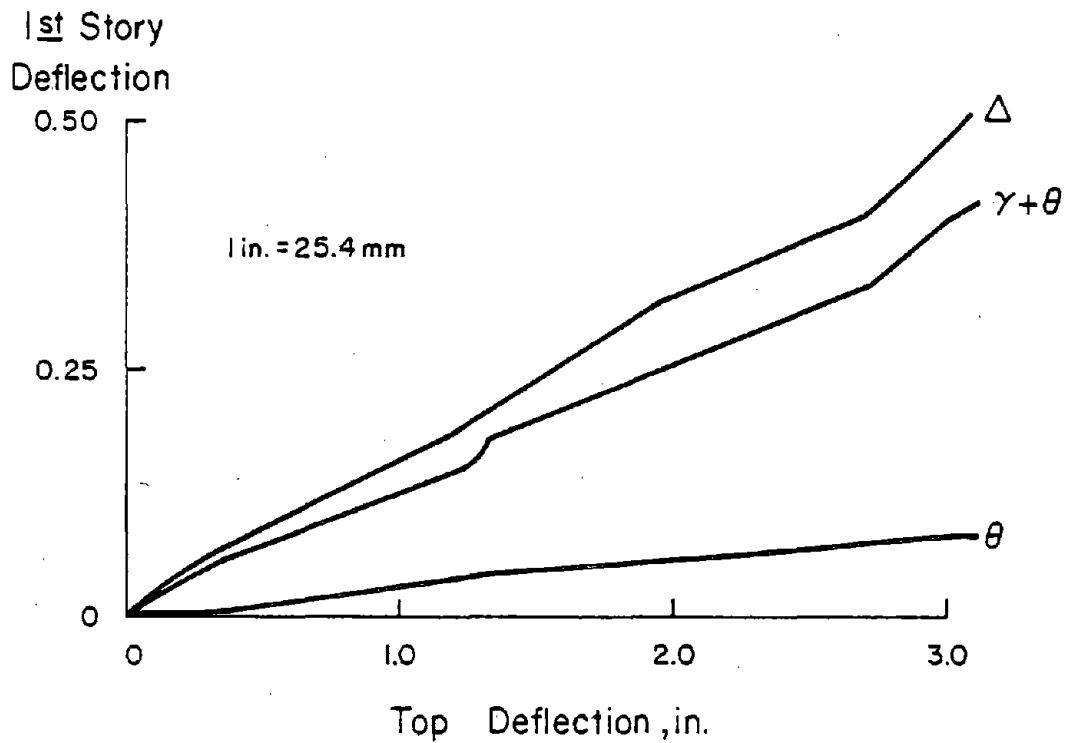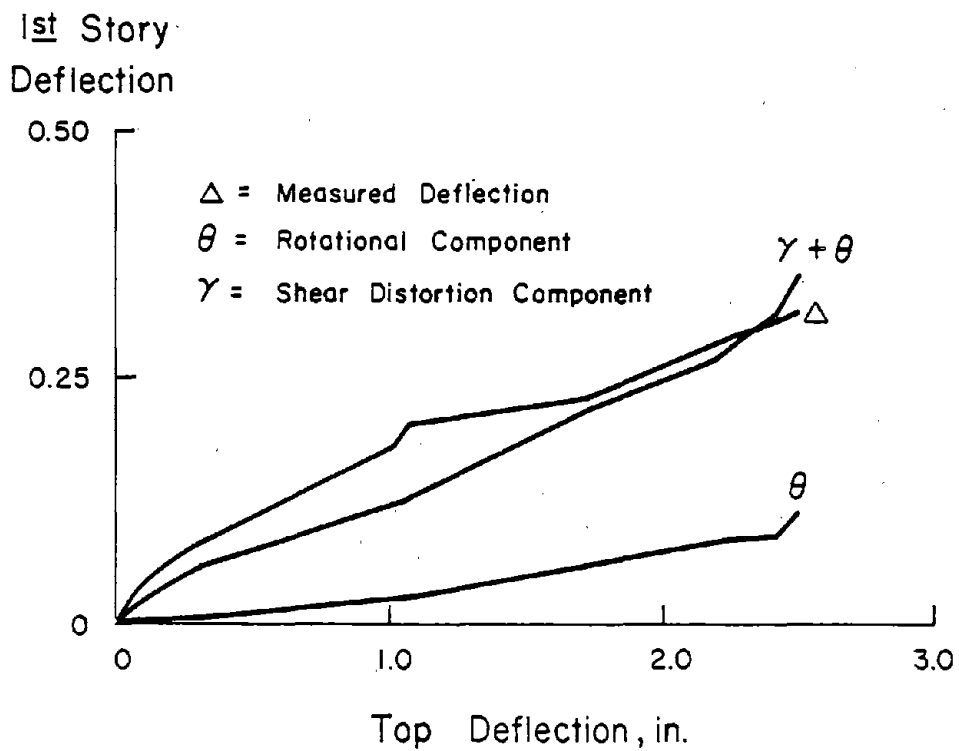
(b)   Tension Wall

Fig. 27 Lateral Deflection Components for RCS-1

ANALYTICAL PROGRAM

In the analytical phase of the investigation, models of coupled wall systems were developed[21]. Three parameters that affected behavior of wall systems were investigated, and the significance of each parameter to the overall response of wall systems was evaluated. Validity of the analytical models was first confirmed by comparison of analytical and experimental results. Then using the developed models, behavior of coupled wall systems was investigated.

In this section, development and verification of the analytical model are discussed.

Structural Model

The structural model developed in this investigation is illustrated in Fig. 28. Structural members were idealized by massless line elements along the centroidal axes of members. All elements except coupling beams were considered to have flexural, axial, and shear rigidity. Axial rigidity of beams was assumed to be infinite because lateral displacement of both walls was assumed to be equal. Separations between walls as observed in the test of CS-1 was not considered in the analysis. At every wall-beam joint, horizontal displacements, vertical displacements and rotations were calculated.

A cantilever beam model was used for simulating coupling beams[19]. The beam model consisted of rigid elements connected to both ends of a flexible member by inelastic rotational springs. The inelastic springs simulated end rotations. In
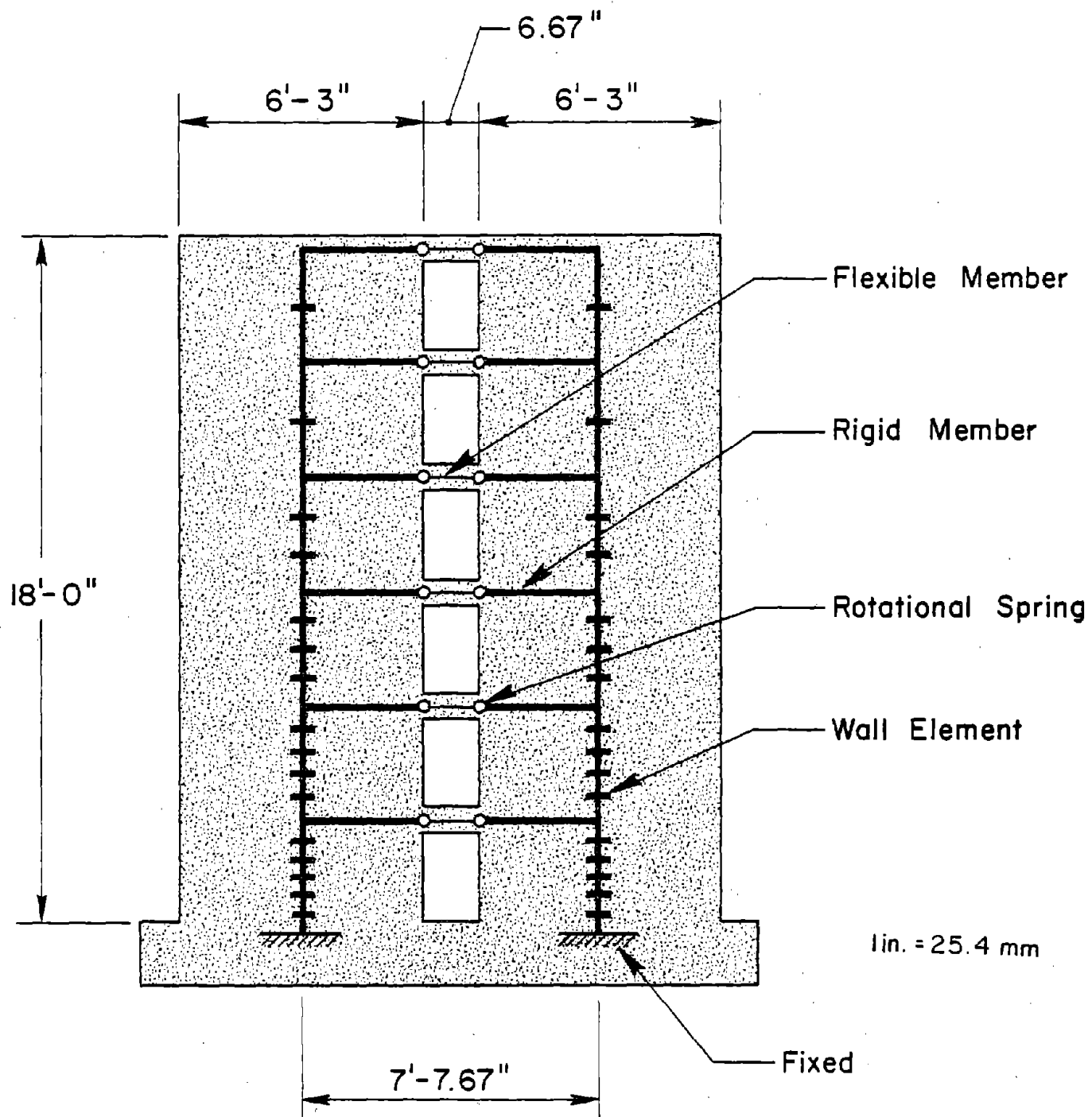
Fig. 28   Analytical Model of Coupled Wall System

addition, inelastic shear behavior in the beams was considered. Calculation of inelastic shear behavior was based on the experimental data.[2]

In wall elements, inelastic flexural behavior was assumed to spread over the lower two stories. To model these inelastic rotations, wall elements in the first two stories were divided into finer line members as can be seen in Fig. 28. The fine division of a story into more line elements allowed better simulation of localized inelastic action. Inelastic shear behavior of the walls was also considered by using calculated shear-versus-shear distortion relationships based on wall tests.[5]

Using the proposed model, a stiffness matrix for the wall system was assembled. Inelastic behavior of the structure was calculated on a step-by-step basis by applying loads in small increments. Within each load increment, stiffness was assumed to be constant. Whenever an element cracked or yielded, the stiffness matrix was updated. Geometric linearity was assumed throughout the analysis.

Analyses were also extended to calculate behavior of wall systems under load reversals. A modified Takeda model for calculating load reversals was used.[20] Detailed development of the analytical model is discussed elsewhere.[21]

Analyses of Systems

Inelastic response of coupled walls CS-1 and RCS-1 under monotonic loads was calculated. Critical parameters pertinent to the behavior of lightly and heavily coupled wall systems

-47-

were identified. Comparisons were made between experimental and analytical results. Parameters considered in the analysis were (1) interaction between flexural and axial behavior, (2) inelastic shear effects in beams and walls, and (3) beam end rotation caused by bond slip. Interaction between flexural and axial behavior was defined as the influence of axial loads on the flexural properties of individual walls.

Comparisons of the calculated load versus top deflection relationships for CS-1 and RCS-1 under monotonic loadings were made with measured load versus diflection envelope. These are shown in Figs. 29 and 30. Experimental data shown in the figures represent the average measured load-deflection envelope of the walls. Parameters included in the analysis are identified in the legend on each figure.

From Fig. 29, inelastic shear behavior of the walls was found to be the most important factor in calculating response of CS-1. Other parameters considered had only a small influence in comparison with the inelastic shear effect. This indicated that for lightly coupled wall systems, wall behavior is the governing factor. Axial and flexural interaction in the walls was not critical because coupling provided by beams was small. Axial loads induced by the weak beams were not large enough to affect response. This agreed with test data which indicated that CS-1 eventually behaved as two isolated walls in parallel.

For RCS-1, interaction between flexural and axial forces was the critical parameter. This can be seen in Fig. 30. Inelastic
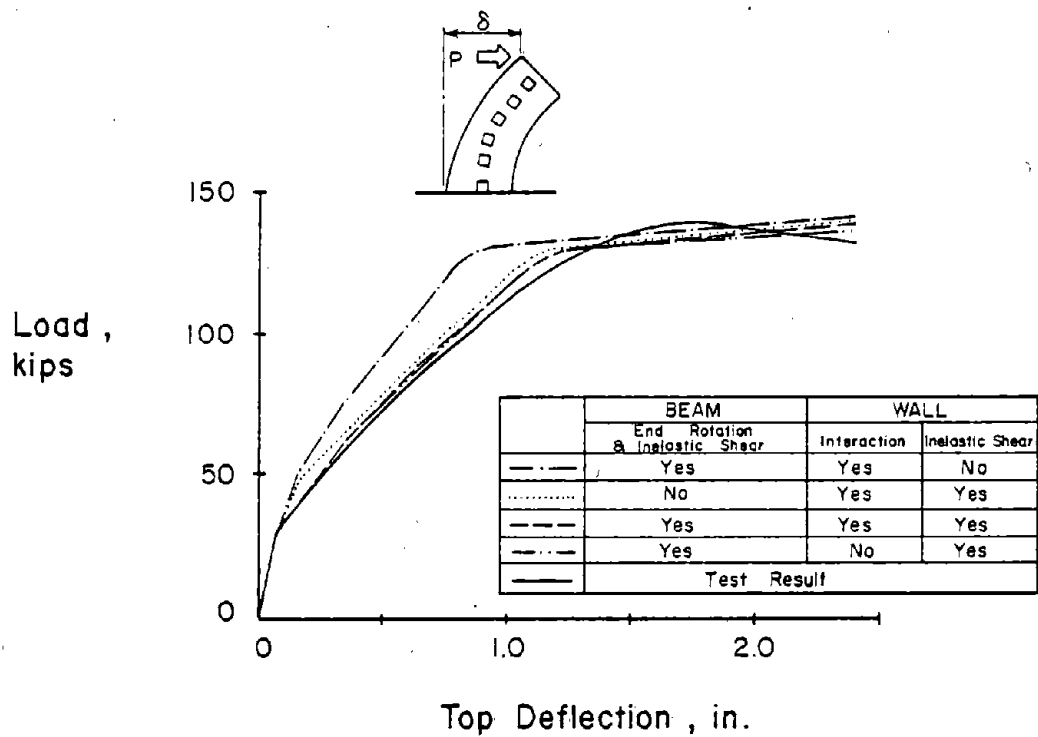
Fig. 29   Effects of Inelastic Shear on
Behavior of CS-1
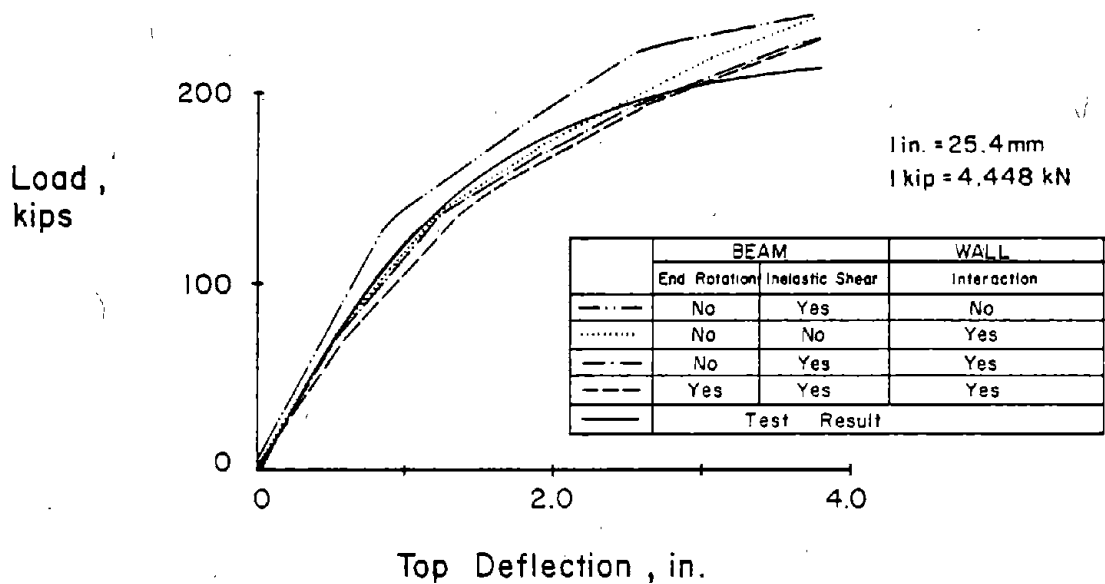
Fig. 30   Effects of Axial Load Interaction
on Behavior of RCS-1

shear in the of walls was included in the analysis. Other
parameters, such as effects of end rotation due to bond slip
and inelastic shear deformation in the beams, were much less
critical. This indicated that strong beams were effective in
coupling walls together and, that high axial forces were induced
in the wall elements. This observation was in agreement with
the experimental results which showed RCS-1 behaved as a single
element in its "overturning" mode.

Load versus deflection relationships of CS-1 under load
reversals were also calculated. Comparison of load-deflection
hysteresis curves for the calculated and measured data are shown
in Fig. 31. It is evident from Fig. 31 that the model was able
to successfully simulate the test of CS-1. The estimated
sequence of coupling beam and wall yielding compared closely
with measured results. No corresponding analysis was performed
for RCS-1 because there was no established procedure to account
for effects of pre-existing damage in the wall elements.

ANALYTICAL RESULTS
Redistribution of base shear and moment are discussed in
this section. Redistribution of shear and moment between walls
was evident in the experimental results. The analytical model
was used to quantify the extent of redistribution. Monotonic
static loads were used in the analysis.

Base Shear Distribution
Calculated distribution of shear for the tension walls of
CS-1 and RCS-1 is shown in Fig. 32. Percentages of total
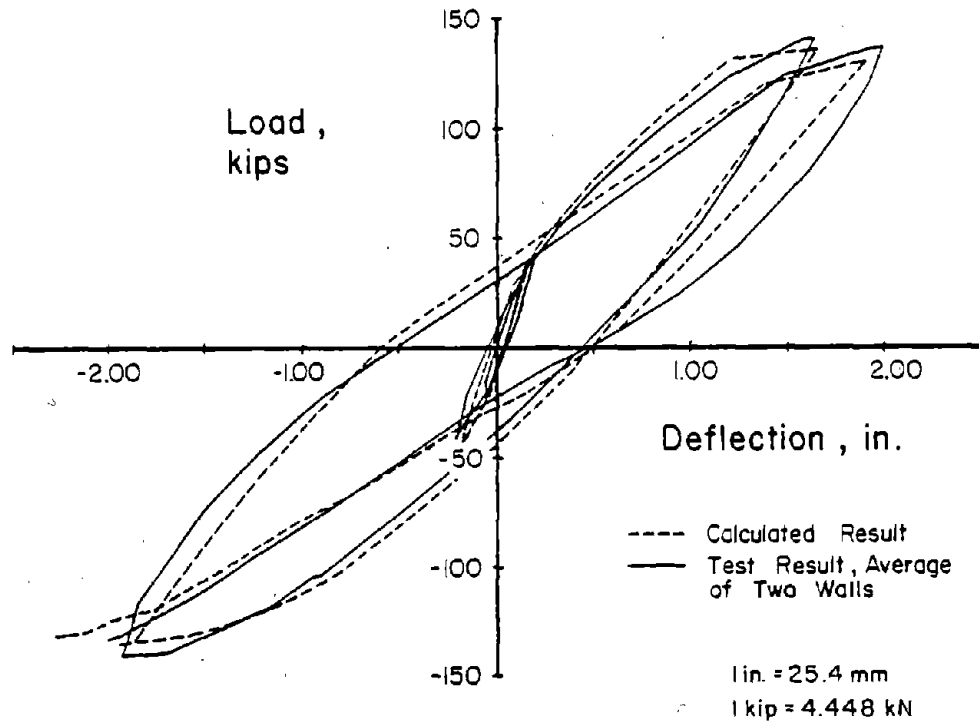
Fig. 31 Comparison of Measured and Calculated Load
versus Deflection Relationship for CS-1
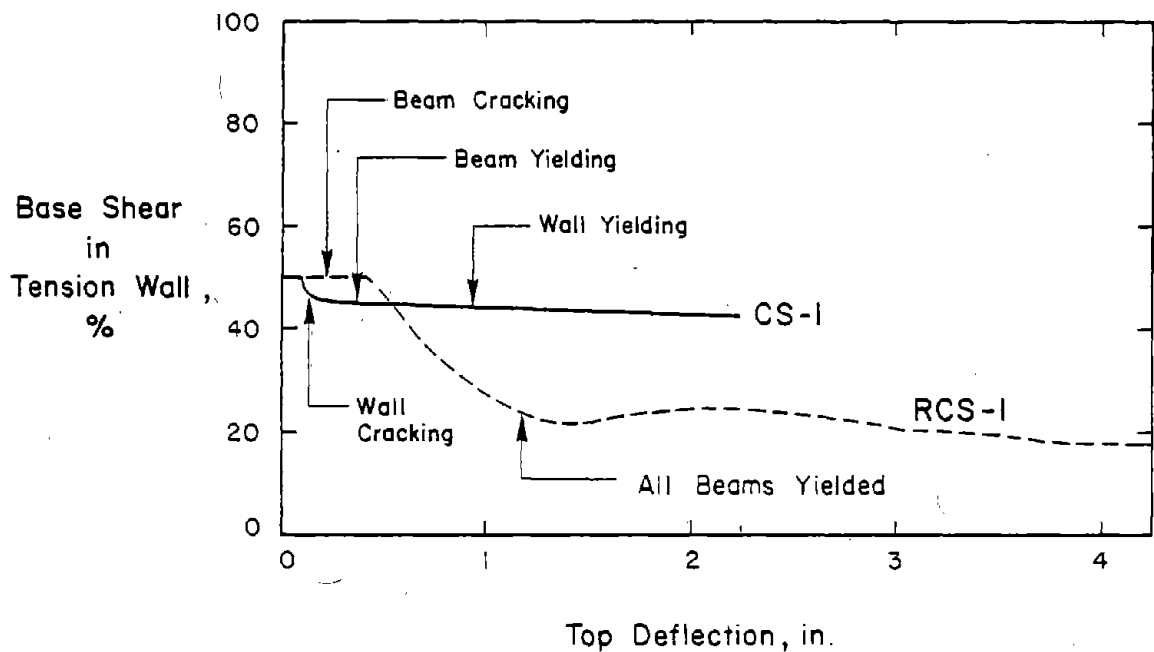
Fig. 32 Redistribution of Shear Stresses for CS-1 and RCS-1

applied shear force resisted by the tension wall of CS-1 are represented by the solid line in Fig. 32. At the beginning of "loading", base shear was distributed equally between walls. Once cracking occurred, shear resisted by the tension wall began to decrease. This shift of shear forces from the tension wall to the compression wall continued as loads increased. At a top deflection of 2 in. (51 mm), 43% of the total applied shear was carried by the tension wall. This indicated that relatively small redistribution of shear was present in the lightly coupled system.

Calculated percentages of total applied shear resisted by the tension wall in RCS-1 are represented by broken curve in Fig. 32. Base shear distribution between walls was assumed to be equal at the beginning of the analysis. As soon as wall system deflected more than 0.5 in. (13 mm), shear redistribution became evident. At a top deflection of 4 in. (102 mm), only 20% of the total shear was calculated to be resisted by the tension wall. Thus, shear was primarily resisted by the compression wall in the heavily coupled system.

Base Moment Distribution

The overturning moment at the first story level of the specimen can be divided into three components: (1) coupling moment due to axial forces in the walls (2) flexural moment provided by the tension wall, and (3) flexural moment provided by the compression wall. Ratios of each moment component to the total

overturning moment at the base were used as parameters to evaluate moment redistribution. Calculated variations of the moment distribution for CS-1 and RCS-1 are illustrated in Figs. 33 and 34, respectively.

For CS-1, the percentage of coupling moment to overturning moment was about 30% at the beginning of loading. This is shown in Fig. 33. As the lightly coupled system went into post yield region, the ratio of coupling moment decreased steadily to 12% and then remained relatively constant. The calculated coupling ratio of 12% is comparable to the measured coupling ratio of 11% at full yield of the system. Some redistribution of flexural moment between tension and compression walls is also evident in Fig. 33. At a top deflection of 2.3 in. (57 mm), moment resisted by the tension wall represented about 42% of the total moment. This indicated that little moment was redistributed between walls in the lightly coupled system.

Redistribution of base moment for RCS-1 is shown in Fig. 34. Ratio of the coupling moment to the overturning moment started at 85% and decreased steadily to 50% at a top deflection of 4 in. (102 mm). Significant redistribution of flexural moment is also noted in Fig. 34. Flexural moment resisted by the tension wall accounted for 10% of the total moment when the repaired beams yielded. In contrast, the compression wall took an increasing proportion of the total moment. In the heavily coupled system the moment resisting mechanism was primarily made up of the coupling moment and the flexural moment of the compression wall.
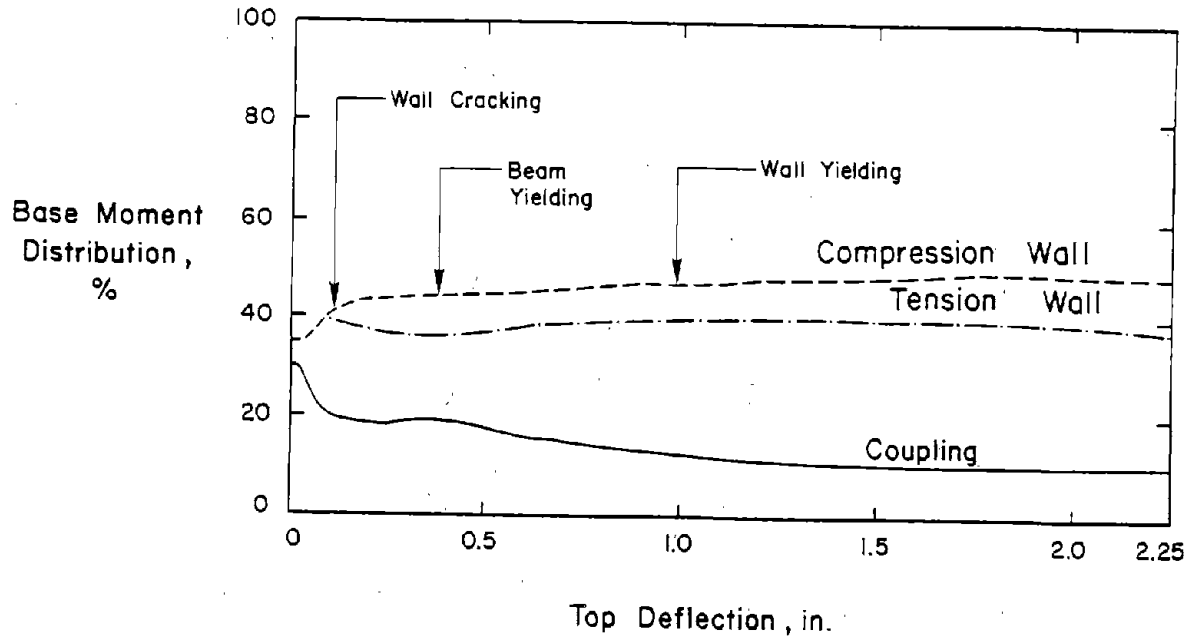
Fig. 33   Moment Distribution for CS-1
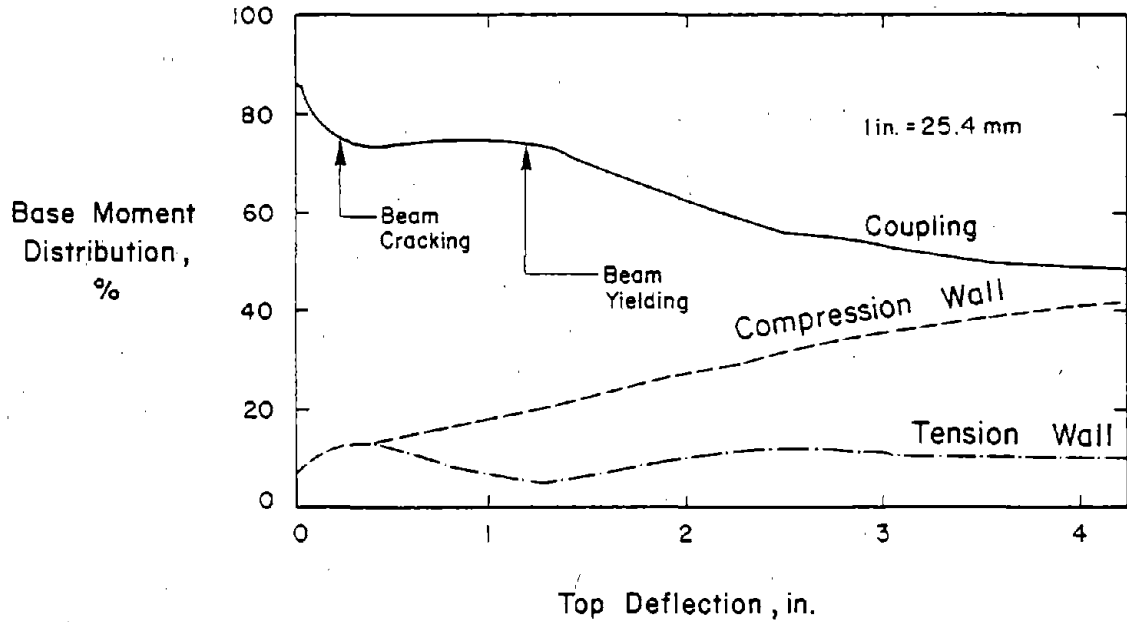
Fig. 34   Moment Distribution for RCS-1

SUMMARY AND CONCLUSIONS

Structural walls coupled by beams are efficient systems for resisting lateral forces in tall structures. A properly designed coupled wall system will dissipate energy through coupling beams without affecting stability of the entire structure.

Two coupled wall tests were reported. Test results showed two kinds of structural response. Initially, a lightly coupled system, CS-1, was tested. The lightly reinforced beams of CS-1 were damaged early under large imposed deformations with repeated load cycles. Plastic hinges formed at the wall-beam interfaces. Subsequently, response of the lightly coupled system was reduced to that of a system of two uncoupled isolated walls in parallel.

Damaged coupling beams in CS-1 were removed and replaced with stiffer and stronger beams. Structural walls in the system were not strengthened or modified. The repaired system, RCS-1, was tested under a load history similar to that for CS-1. The heavy coupling beams between walls caused the system to behave as a single isolated wall. Strong coupling between individual structural elements was evident. Yielding of the coupling beams occurred immediately before and after yielding of the walls. Under repeated reversing loads, the system lost its load carrying capacity by concrete crushing in the web of wall elements.

An analytical model was developed to simulate experimental results.[21] Three parameters that affected behavior of wall systems were investigated. Static analyses were used and comparisons between analytical results and experimental data were

made. Using the same analytical model, redistribution of shear and moment between walls through coupling beams was evaluated.

Based on the experimental and analytical results reported herein, the following conclusions were obtained.

(1)   The amount of axial load in walls created by accumulation of shear forces in coupling beams significantly influences behavior and deformation capacity of the individual walls.

(2)   In the lightly coupled system, CS-1, the measured amount of coupling at full yield was 11%. Beams in this system deteriorated rapidly with most of the inelastic action occurring in the coupling beams before the walls yielded. Axial load in this lightly coupled system did not significantly affect wall performance.

(3)   In lightly coupled wall systems, the critical parameter is deformation capacity of coupling beams. Deformation capacity must be sufficient to insure proper coupling action beyond yielding of the system.

(4)   Repair of CS-1 by replacing the coupling beams with stronger elements was simple and effective. Repaired system RCS-1 had a greater strength than the original system CS-1.

(5)   Conventionally reinforced beams with a shear span-to-depth ratios of 1.25 and 1.04 were effectively used to couple walls. Assuming a shear capacity reduction factor of one ($\varphi = 1.0$), design nominal shear levels in the beams at yield were 5.8 $\sqrt{f_c'}$ psi (0.48 $\sqrt{f_c'}$ MPa) and

9.8 $\sqrt{f_c'}$ psi (0.81 $\sqrt{f_c'}$ MPa) for CS-1 and RCS-1, respectively.

(6) In the repaired coupled wall system RCS-1, measured amount of coupling at ultimate was 30%. With repeated inelastic load reversals, the specimen lost its load carrying capacity by web crushing of the compression wall.

(7) In the repaired coupled wall system RCS-1, strong coupling beams created large axial stresses in the walls. Presence of axial loads significantly affected performance of the walls. Wall elements of system RCS-1 showed less deformation capacity than obtained in individual walls without axial load.

(8) Based on measured deformation characteristics of the wall systems, substantial redistribution of shear and moment between wall elements was indicated. Depending on the effectiveness of the coupling mechanism, shear and moment were transmitted from the tension wall to the compression wall through the coupling beams. The heavier the coupling in the system, the larger the amount of shear and moment redistributed.

(9) Two distinct deflection profiles were observed in the tests. The wall element under compressive axial loads exhibited more deflection in the first two stories than the wall subjected to tensile axial loads. In effect, as loads were reversed, each wall element assumed two distinct deflected shapes within one complete load cycle.

(10) In a heavily coupled wall system, critical parameters are strength and deformation capacity of the walls.

(11) Design of systems to obtain heavy coupling is not recommended because the system does not maximize the use of every structural element. Wall elements will be damaged before energy dissipation capacity of the coupling beams is fully utilized. Moreover, if strength and deformation capacity of walls are exhausted, damage to the structure may be beyond repair.

(12) Design of coupled wall systems should relate the amount of coupling to strength and deformation capacity of beams and walls. Deformation capacity of coupling beams will be critical in a design requiring early yielding of the beams. Strength and deformation capacity of walls will be critical in a design requiring beam and wall yielding at approximately the same level.

(13) An important characteristic in observed behavior of each test specimen was lateral separation between the walls. In lightly coupled system CS-1, separation between walls occurred. This separation was related to axial deformation in the coupling beams and may have caused a substantial reduction in the moment and shear capacity of the beams. In heavily coupled system RCS-1, separation of walls was caused by lateral growth of the walls resulting from the diagonal cracking pattern. Little axial elongation of the beams was observed in RCS-1.

(14) An analytical model was developed in this investigation and was successfully used to calculate the load versus deflection relationship of the coupled wall systems.

(15) Using the analytical model, behavior of a lightly coupled wall system was found to be governed by individual walls. Specifically, inelastic shear action in the walls was a significant factor to consider in analysis of the lightly coupled system.

(16) The analysis also indicated that redistribution of shear and moment between walls was significant in heavily coupled systems. In RCS-1, the compression wall was estimated to be resisting 80% of the applied shear forces and over 40% of the total overturning moment.

(17) The analytical investigation showed that interaction of axial and flexural forces is the most important factor to consider in calculating behavior of heavily coupled systems.

REFERENCES

1. Sozen, M. A. and Shibata, A., "An Evaluation of the Performance of the Banco de America Building Managua, Nicaragua," Conference Proceedings on the Managua, Nicaragua Earthquake of December 23, 1972, Earthquake Engineering Research Institute, San Francisco, Vol. II, November 29-30, 1973, pp. 529-550.

2. Barney, G.B., Shiu, K.N., Rabbat, B.G., Fiorato, A.E., Russell, H.G., and Corley, W.G. "Earthquake Resistant Structural Walls - Tests of Coupling Beams." National Technical Information Service, U.S. Department of Commerce, Springfield, Virginia 22162 (NTIS Accession No. NSF/RA-780501 PB-281733)

3. Shiu, K.N., Barney, G.B., Fiorato, A.E. and Corley, W.G., "Reversing Load Tests of Reinforced Concrete Coupling Beams," Proceedings, Central American Conference on Earthquake Engineering, Central America, January 1978.

4. Paulay, T., "Coupling Beams of Reinforced Concrete Shear Walls," Proceedings, Structural Division, ASCE, Vol. 97, No. ST3, March 1971, pp. 843-862.

5. Oesterle, R. G., Fiorato, A.E., Russell, H. G., and Corley, W. G., "Earthquake Resistant Structural Walls - Tests of Isolated Walls - Phase III," Report to National Science Foundation, Construction Technology Laboratories, A Division of Portland Cement Association, Skokie, July 1981.

6. Paulay, T., "Design Aspects of Shear Walls For Seismic Areas," Research Report 74-11, Department of Civil Engineering, University of Canterbury, Christ Church, New Zealand, October 1974.

7. Bertero, V. V. and Popov, E. P., "Hysteretic Behavior of Reinforced Concrete Flexural Members With Special Web Reinforcement," U.S. National Conference on Earthquake Engineering, Ann Arbor, Mich., June 1975, pp. 316-326.

8. Srichatrapimuk, Thirawat and Chopra, Anil K. "Earthquake Response of Coupled Wall Buildings" Earthquake Engineering Research Center, University of California, Berkeley, Report No. EERC 76-27, November '76 pp. 1-117.

9. Mahin, S.A. and Bertero, V.V., "Nonlinear Seismic Response of a Coupled Wall System," Journal of the Structural Division, ASCE, Vol. 102, No. ST9, September 1976, pp. 1759-1780.

10. Nguyen, Tien Dich, "An Investigation of the Behavior of Coupled Shear Wall Structures," Department of Civil Engineering and Applied Mechanics, McGill University, March 1976, 209 pages.

11. Paulay, T. and Santhakumar, A.R., "Ductile Behavior of Coupled Shear Walls," Journal of the Structural Division, ASCE, Vol. 102, No. ST1, Proc. Paper 11852, January 1976, pp. 93-108.

12. Paulay, T. and Santhakumar, A.R., "Ductile Behavior of Shear Walls Subjected to Simulated Seismic Loading," Preprints, Vol. 3, Sixth World Conference on Earthquake Engineering, New Delhi, 1977, pp. 227-232.

13. Paulay, T. and Binney, J.R., "Diagonally Reinforced Coupling Beams of Shear Walls, Shear in Reinforced Concrete, Special Publication SP-42, Vol. 2, American Concrete Institute, 1974, pp. 579-598.

14. Aristizabal-Ochoa, J.D. and Sozen, M.A., "Behavior of Ten-Story Reinforced Concrete Walls Subjected to Earthquake Motion," Structural Research Series No. 431, University of Illinois, Urbana, October 1976, 378 pages.

15. Lybas, J.M. and Sozen, M.A., "Effect of Beam Strength and Stiffness on Dynamic Behavior of Reinforced Concrete Coupled Walls," Structural Research Series No. 444, University of Illinois, Urbana, July 1977, 569 pages.

16. Irwin, A.W. and Young, R.W., "Tests on a Reinforced Concrete Model Shear Wall Building," Proceedings, Institute of Civil Engineers, Part 2, Vol. 61, March 1976, pp. 163-177.

17. "Building Code Requirements for Reinforced Concrete (ACI 318-71)," American Concrete Institute, Detroit, 1971.

18. Shiu, K.N., Daniel, J. I., Aristizabal-Ochoa, J. D., Fiorato, A. E., and Corley, W. G., "Earthquake Resistant Structural Walls - Tests of Walls With and Without Openings," Report to National Science Foundation, Construction Technology Laboratories, A Division of Portland Cement Association, Skokie, Illinois, July 1981.

19. Otani, S. and Sozen, M. A., "Behavior of Multistory Reinforced Concrete Frames During Earthquakes," Structural Research Series No. 392, Civil Engineering Studies, University of Illinois, Urbana, November 1972.

20. Takayanagi, T. and Schnobrich, W. C., "Computer Behavior of Reinforced Concrete Coupled Shear Walls," Structural Research Series No. 434, University of Illinois, Urbana, December 1976, 192 pages.

21. Takayanagi, T., Scanlon, A. and Corley, W. G., "Analysis of Coupled Wall Test Specimens," Report to National Science Foundation, Construction Technology Laboratories, A Division of Portland Cement Association, Skokie, Illinois, July 1981.

22. Hognestad, E., Hanson, N. W., Kriz, L.B., and Kurvits, O.A., "Facilities and Test Methods of PCA Structural Laboratory", PCA Research and Development Laboratories, Bulletin D-33, pp. 32.

23. Uzumeri, S. M., Otani, S. and Collins, M. P., "An Overview of the State-of-the-Art in Earthquake Resistant Concrete Building Construction in Canada," University of Toronto, Department of Civil Engineering, ISSN 0316-7968 Publication 77-09, May 1977.

24. Aristizabal-Ochoa, J.D., Shiu, K.N. and Corley, W.G., "Effects of Beam Strength and Stiffness on Coupled Wall Behavior," Proceedings, U.S. National Conference on Earthquake Engineering - 1979, Stanford, California, August 1979.

25. Shiu, K. N., Takayanagi, T., and Corley, W. G., "Non-Linear Behavior of Coupled Wall Systems Under Cyclic Loadings," Paper to be Submitted to ASCE, Journal of the Structural Division.

ACKNOWLEDGEMENTS

APPENDIX A - EXPERIMENTAL PROGRAM

Two coupled wall specimens, one with weak and the other with strong coupling beams, were tested. The lightly coupled wall was designated CS-1 and the heavily coupled wall was designated RCS-1. A detailed description of the test specimens and test setup is presented in this Appendix. Construction procedures for specimens and repair methods used for replacing coupling beams are also described.

Test Specimen

The coupled wall specimen was modeled after a prototype structure. Dimensions of this prototype are shown in Fig. A1. They are typical for common residential buildings. Each floor is laid out in 20 ft (6.1m) bays. Lateral rigidity was provided by coupled walls located at every third bay. Forces in the other direction are resisted by other wall elements.

Overall horizontal length of the coupled walls in the prototype structure is 41 ft 8 in. (12.7 m) with individual wall lengths of 18 ft 9 in. (5.7 m). Individual walls are connected by coupling beams as shown by dotted lines in Fig. A1. Span length of coupling beams corresponds to a standard fire-door opening and size of coupling beams is typical for lintels over doorway openings.

Because of the size limitation of the laboratory facilities, the test specimen was built at approximately 1/3 scale.[22]

18'9"   4'2"   18'9"

6 @ 20'0" = 120'0"

Coupled Walls

1 in. = 25.4 mm
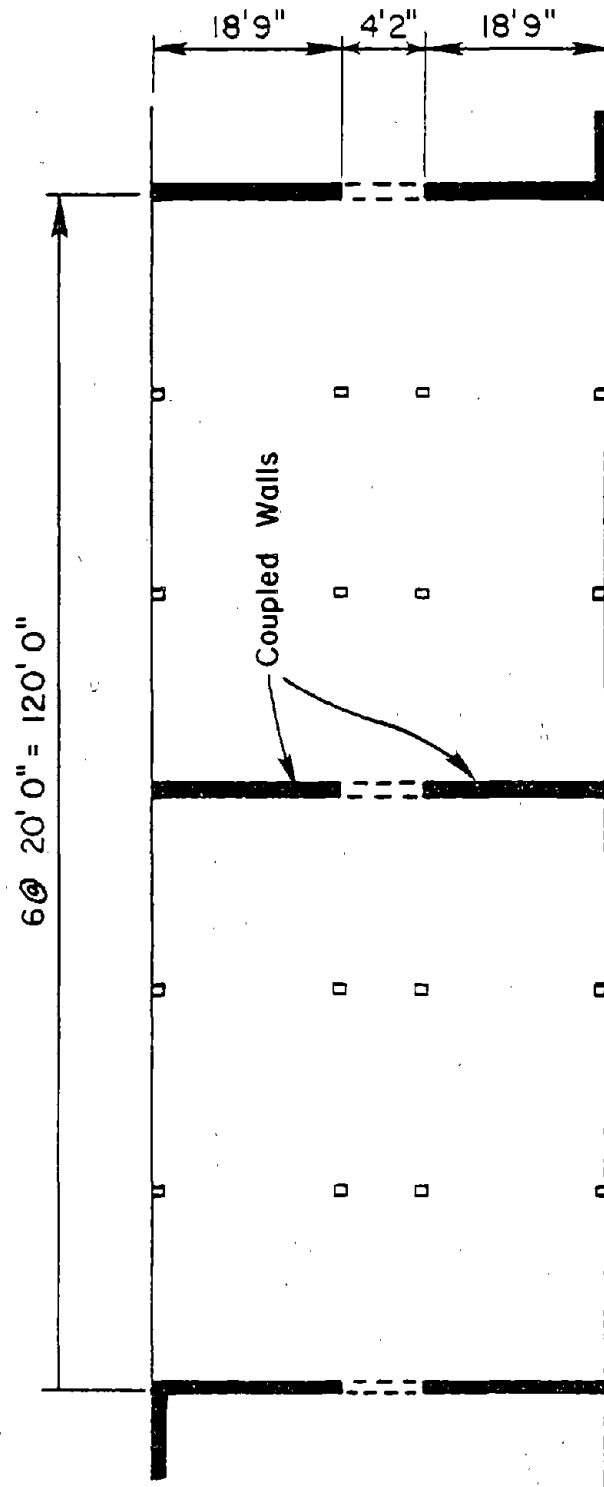
Fig. A-1   Prototype Floor Plan

General Description

Overall dimensions of the coupled wall specimen are shown in Fig. A2. The specimen was an 18 ft (5.5 m) high six story model. It consisted of two rectangular walls in parallel coupled by six beams. Each wall had a horizontal length of 6 ft 3 in. (1.9 m) and a uniform thickness of 4 in. (102 mm). A cross-section of the wall element is shown in Fig. A3. At each story, walls were jointed together by coupling beams. The clear span length of coupling beams was 16.7 in. (423 mm). Cross-sections of coupling beams in Test CS-1 and RCS-1 are shown in Figs. A4 and A5, respectively. Coupling beams of CS-1 had a beam width of 4 in. (102 mm) and a depth of 6.7 in. (169 mm). Beams used in RCS-1 had a width of 10 in. (254 mm) and depth of 8 in. (203 mm).

Floor slabs were simulated using 2.5-in. (64 mm) deep by 1-ft (0.3 m) wide stubs running full length on both sides of the walls. As shown in Fig. A2, the slabs had overhangs of 2 ft (0.6 m) at both ends of the specimen. Thickness of the top slab was to 5 in. (127 mm). The additional thickness of the top slab was to facilitate even distribution of applied loads into the walls.

The coupled wall specimen was anchored rigidly to the test floor through a 2x4x17 ft (0.6x1.2x5.2 m) base block. Soil-structure interaction was not considered and is outside the scope of this investigation.

Overall views of the two specimens before testing are shown in Fig. A6.

Fig. A-2 Dimensions of Coupled Wall Specimen

4"(102 r

6'- 3"(1.91 m)   16⅜"   6'- 3"(1.91)

(423 mm)
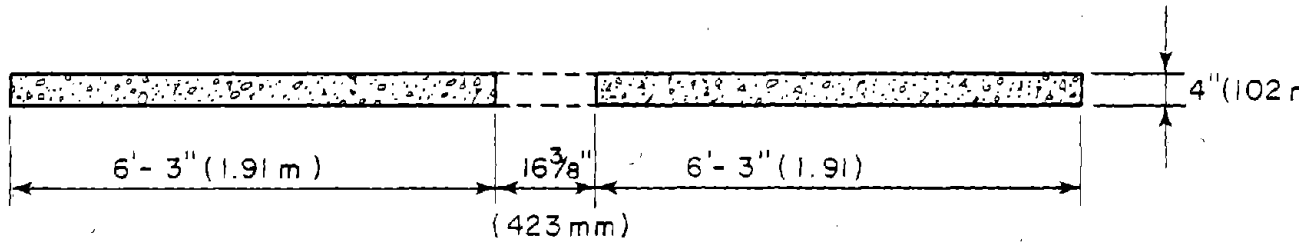
Fig. A-3   Cross Section of Wall Elements

28"(711 mm)

2½"(64 mm)

4⅙"(106 mm)

4"
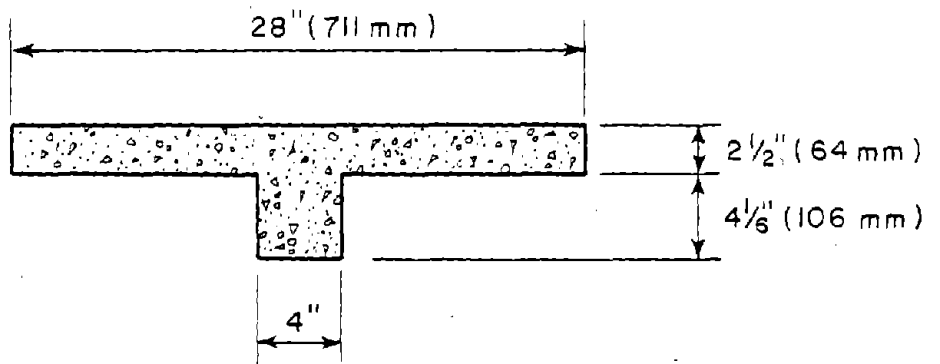
Fig. A-4   Cross Section of Beams in CS-1

28"(711 mm)

2½"(64 mm)

5½"(140 mm)

10"

(254 mm)
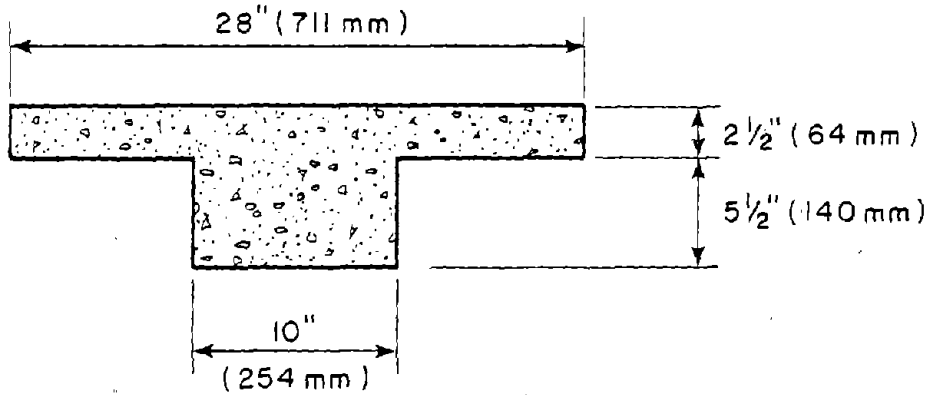
Fig. A-5   Cross Section of Beams in RCS-1

(a) CS-1
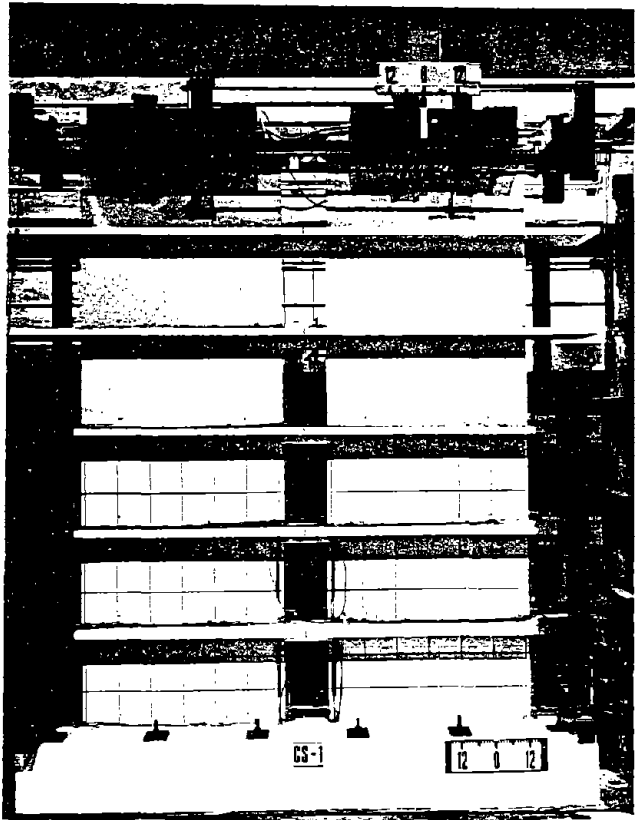
(b) RCS-1
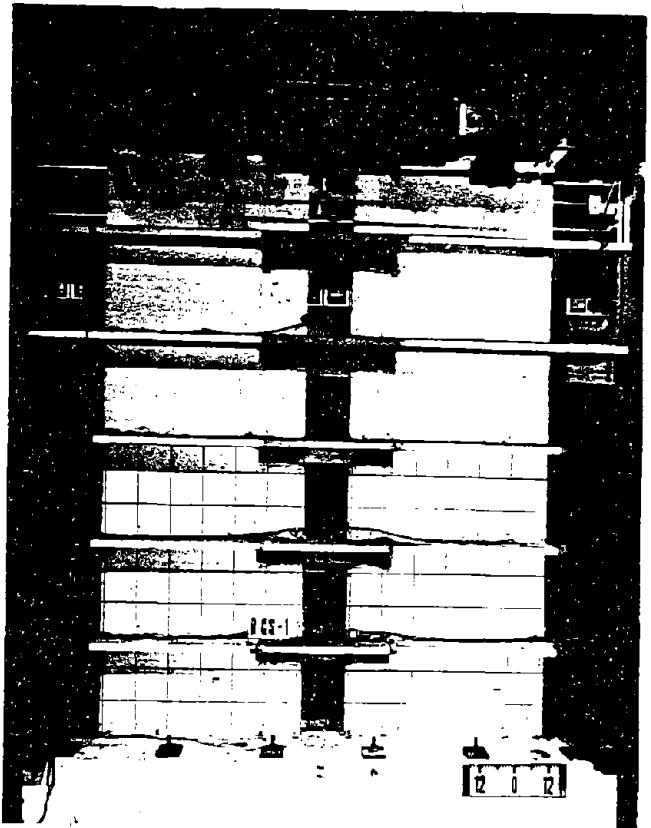
Fig. A6   Specimens before Testing

Material Properties

Design concrete strength was 3,000 psi (20.7 MPa) and steel yield strength was 60,000 psi (414 MPa). Measured stress versus strain relationships for concrete and steel used in the specimens are shown in Fig. A7. Measured material properties are given in Table 1.

Reinforcement Details

Reinforcing steel details for the wall elements are shown in Fig. A8. Primary flexural reinforcement at the extremities, or boundary elements, of each wall was provided by 12 No. 4 bars of Grade 60 steel. The reinforcement percentage of these bars with respect to surrounding concrete is approximately 6%. This percentage is the maximum allowed inthe 1971 ACI Building Code for columns in earthquake resistant structures.[17] Confinement around the primary reinforcement was provided by closed hoops of D-3 deformed wire. These hoops were spaced at 1-1/3 in. (34 mm) in the first stories in accordance with Appendix A of the 1971 ACI Code.[17] Above the second story, spacing was increased to 4 in. (102 mm) in accordance with Chapter 7 of the ACI Building Code.

Horizontal web reinforcement was provided by two layers of 6 mm bars spaced at 4 in. (102 mm). Horizontal shear reinforcement in wall elements was also two layers of 6 mm bars at 6 in. (152 mm). Reinforcement was designed to resist shear forces corresponding to flexural yielding conditions when yielding occured at both ends of the coupling beams and at 1.25 times flexural yielding at the base of the wall. The factor 1.25
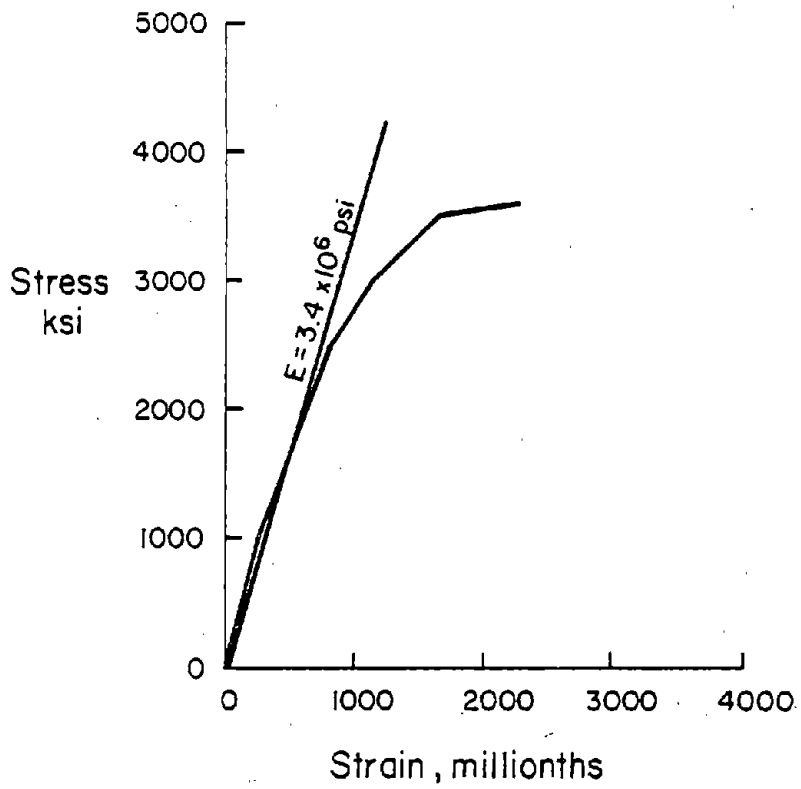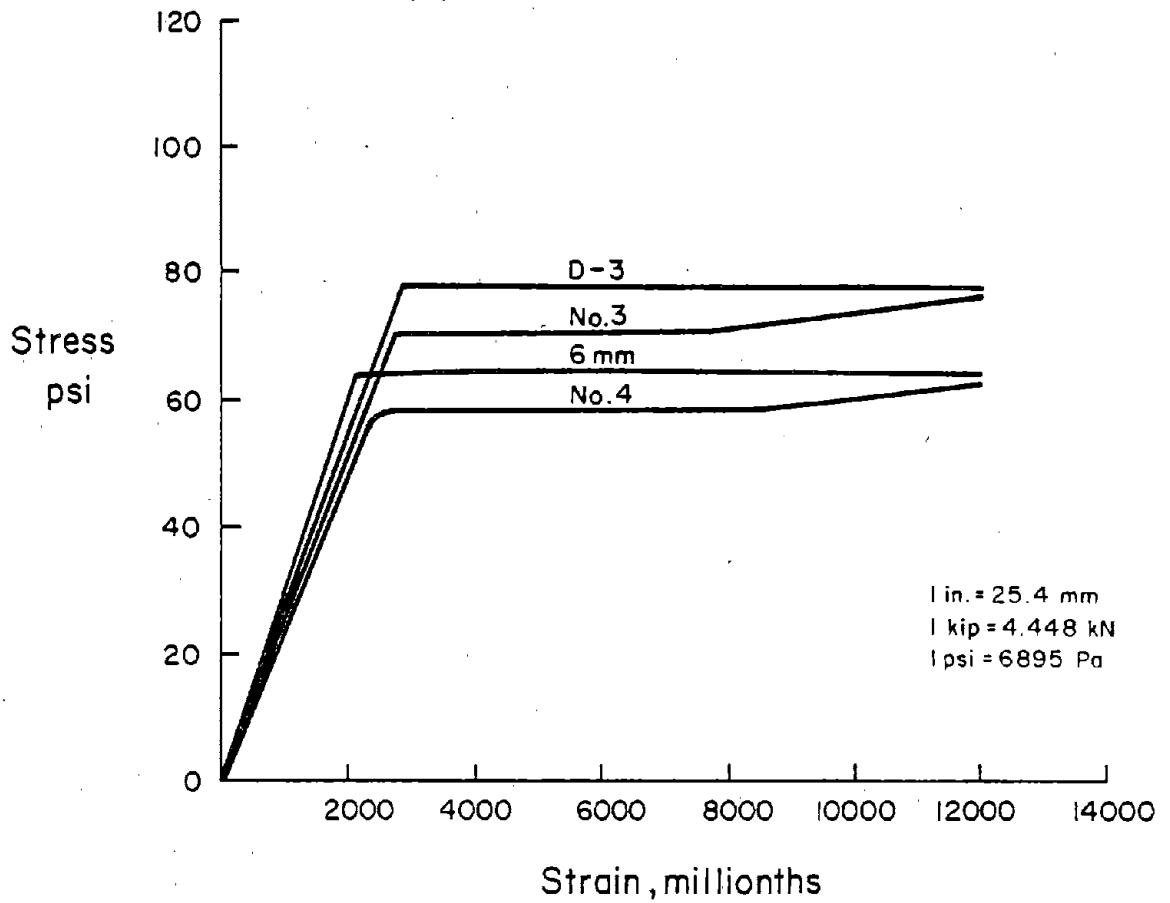
Fig. A-7   Measured Stress versus Strain Relationships
for Concrete and Reinforcement

(a)   Cross Section

3' – 1 ½"

4

¼" Cl.

4"

D3 Wire

9 ¾"

6 mm Bar

1in. = 25.4 mm

CI-1
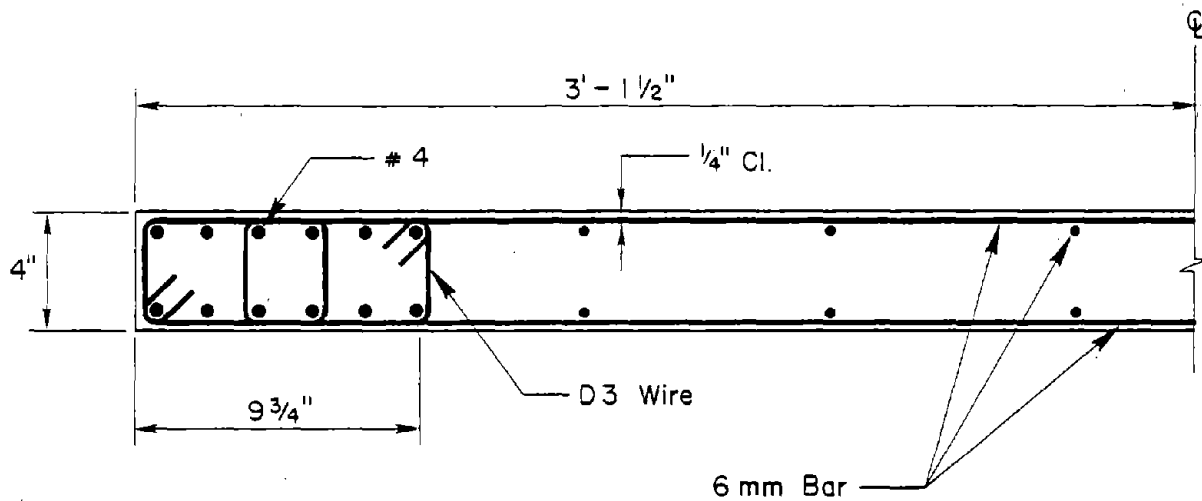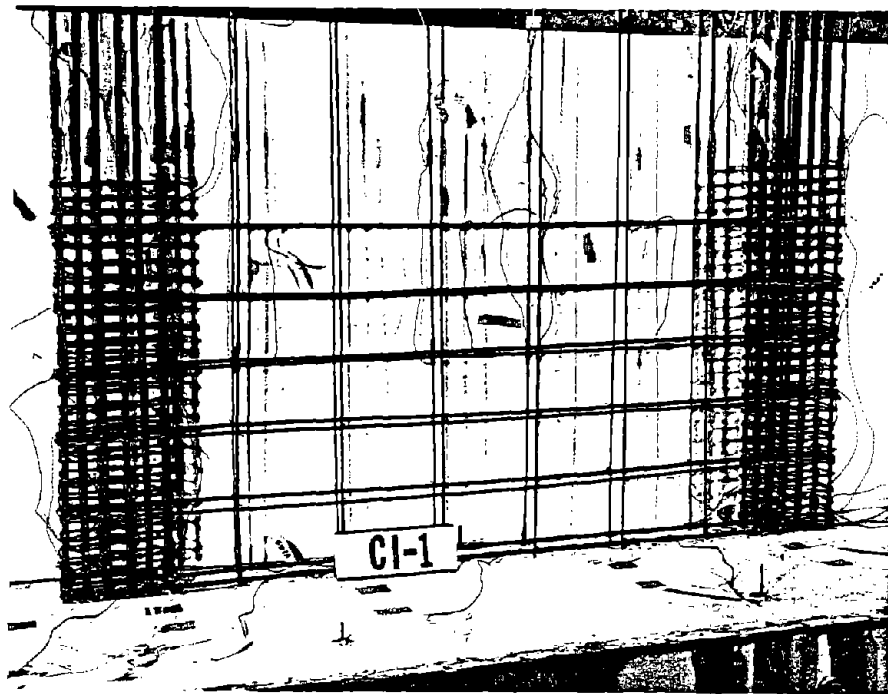
(b)   Photograph of First Story Reinforcement

Fig. A8   Wall Reinforcement Details

considered in the walls accounted for strain hardening of the primary reinforcement. However, based on experimental results no strain hardening was assumed in the design of coupling beam reinforcement.

Coupling beam reinforcement was designed based on test results for conventionally reinforced coupling beams.[2,3]

Reinforcement details and dimensions of coupling beams for the two tests are shown in Figs. A-9 and A-10.

As shown in Fig. A-9, straight horizontal bars were used as flexural reinforcement for System CS-1. Two 6-mm bars were used as top and bottom flexural reinforcement. Shear reinforcement and concrete confinement were provided by closed D-3 deformed wire hoops spaced at 1.33 in. (34 mm).

Beams of RCS-1 were also reinforced with conventional straight reinforcement. Six No. 3 bars were used as primary flexural reinforcement. Closed D-3 deformed wire hoops spaced at 1.33 in. (34 mm) were to provide concrete confinement. Cross section of the beams was 10x8 in. (254x203mm) as shown in Fig. A-10. Additional ties made of D-3 wires were provided to resist shear stresses. Reinforcement details for beams in RCS-1 are shown in Fig. A-10.

Reinforcement details for floor slabs are shown in Fig. A-11. Reinforcement parallel to walls was provided by four D-3 deformed wires located near the edge of the slabs. Reinforcement perpendicular to the walls was selected based on slab analysis of the prototype structure using the "equivalent frame method" as specified in 1971 ACI Building Code.[17] The selected reinforcement consisted of 6 mm bars spaced at 4-in.

28"

2-1/2"

4-1/6"

6 mm bar

D3 Deformed
Wire

1 in. = 25.4 mm

4"

Sec A-A Closed Hoops

Wall   Original Beam   Wall

66-2/3"

8-1/3"   25"

A

A
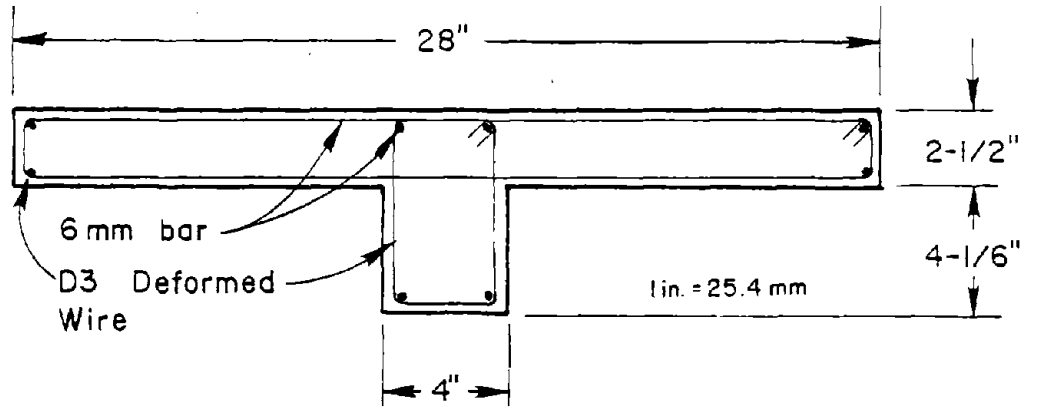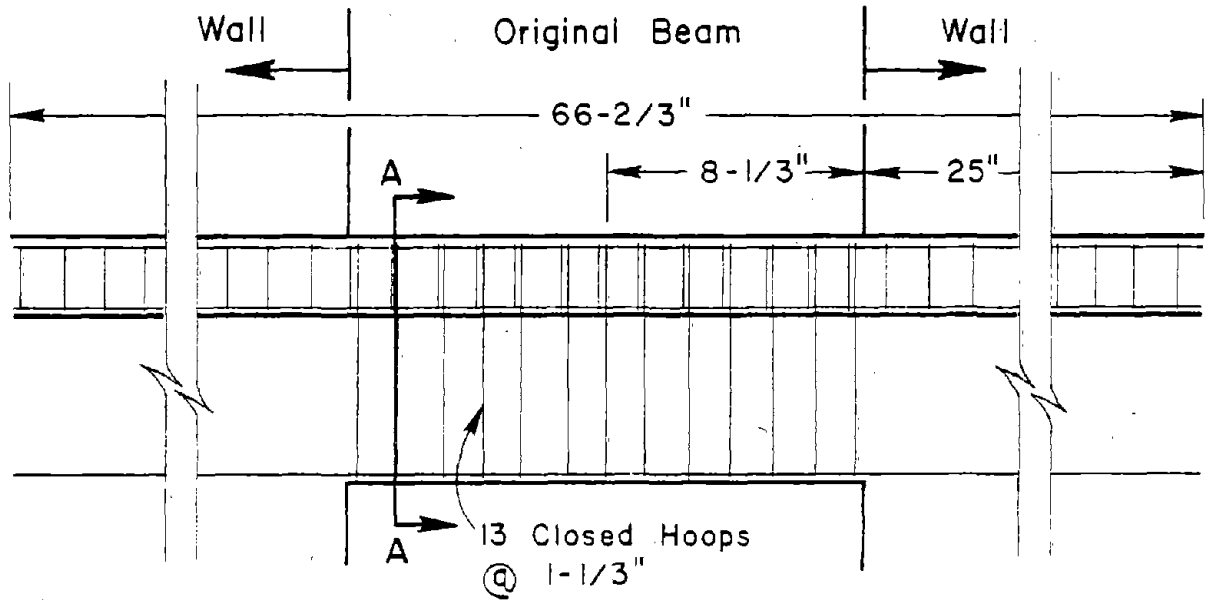
13 Closed Hoops
@ 1-1/3"

Fig. A9   Coupling Beam Reinforcement Details for CS-1

28"

2-1/2"

5-1/2"

D3 Deformed
Wire

10"
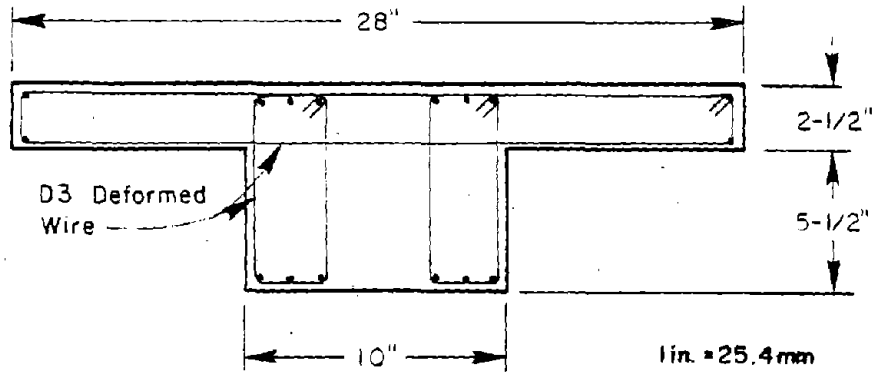
1in. =25.4mm

Sec A-A Closed Hoop D3 Wire

D3 Deformed
Wire

#3 Bar (12)

1/4" CL
(all sides)

Sec B-B 1 Pair ⌐ Tie D3 Wire

48-2/3"

8-1/3"   16"

A   B

A   B

23 Closed Hoops
@ 1-2/3"

10 Pair ⌐ Ties
@ 1-2/3"

Wall   Replaced Beam   Wall
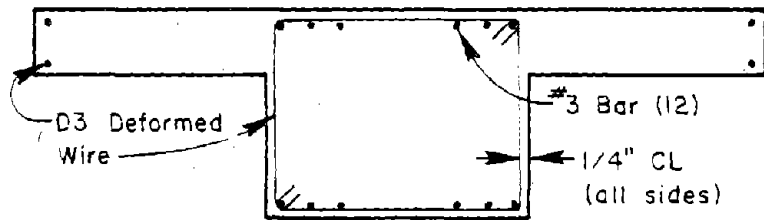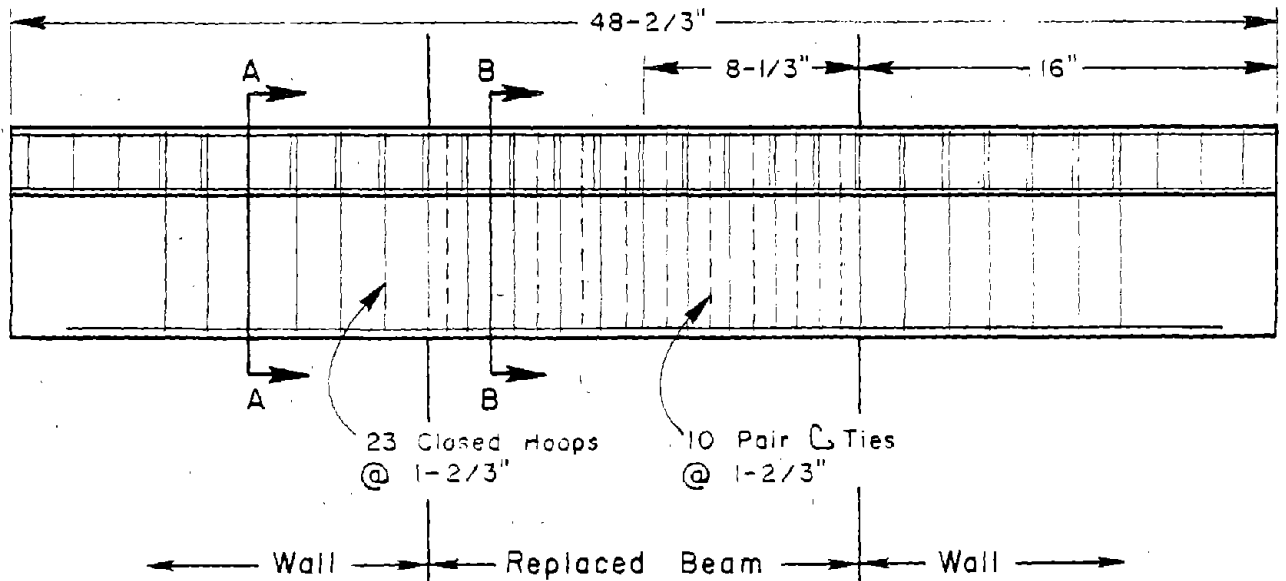
Fig. A10   Coupling Beam Reinforcement Details for RCS-1

6 mm bars

D3 wires

A   B

A   B

3 ½"   52 @ 4"= 17'-4"   3½"

28"

₵-wall

¼" cover

2½"

D-3 wire

6 mm bar

Slab

Wall

4"

1"

Section AA

28"

₵-wall

¼" cover

4"

2½"

6 mm bars

D3 wire

Slab

Wall

1"

Section BB
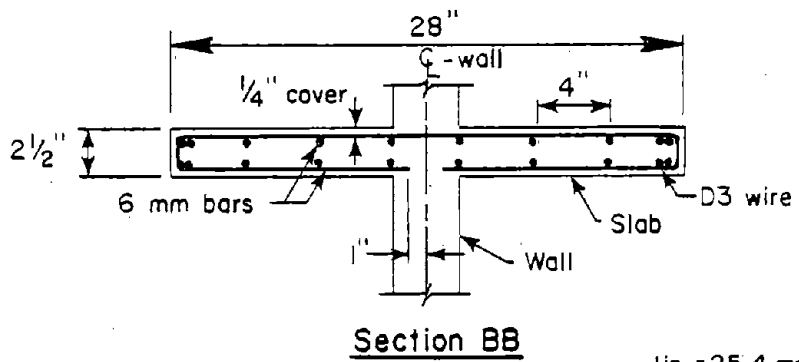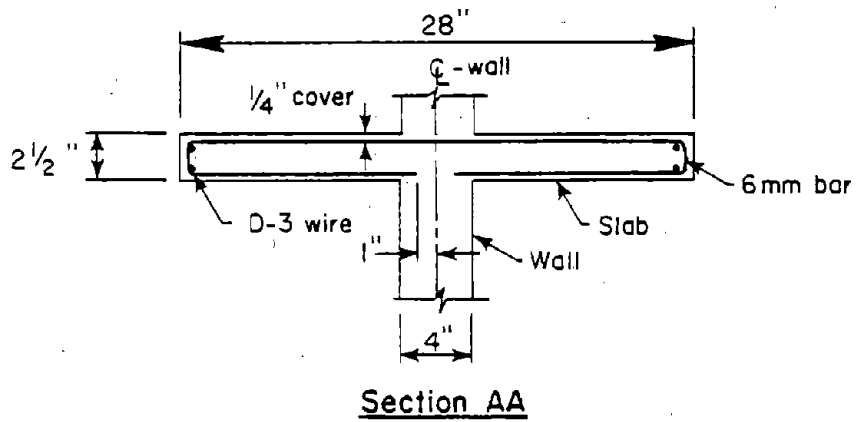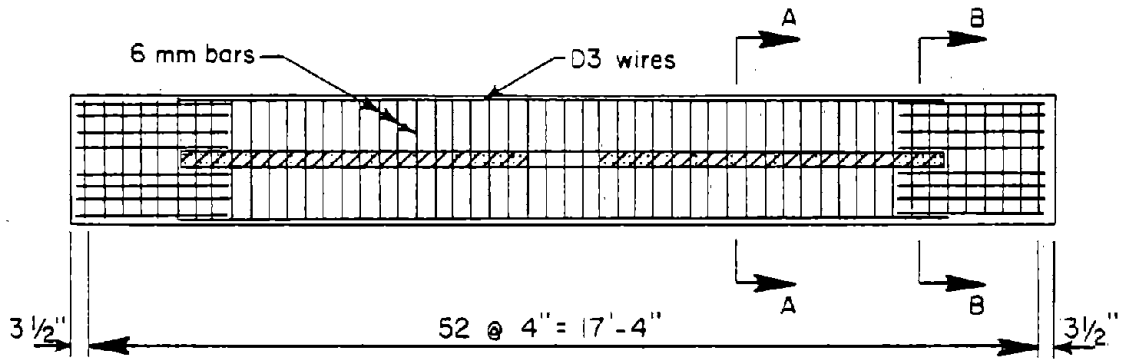
1in. = 25.4 mm

Fig. All   Slab Reinforcement Details

(132 mm), and placed at the top and bottom of the slab. Additional heavier reinforcement was provided in the 2 ft (0.6 m) slab overhang at both ends of the specimen. This extra reinforcement was designed to strengthen the slab section against restraining forces induced by vertical frames used to prevent possible out-of-plane movements.

Test Setup

The test setup for the coupled wall specimen is shown in Fig. A-12. The wall specimen, located between four reaction abutments, was post-tensioned to the test floor. Lateral loads were applied to the specimen through the top slab as a fixed vertical cantilever. A detailed schematic drawing of the coupled wall test setup is also shown in Fig. A-12.

To ensure sufficient lateral restraint against out-of-plane movement, external vertical frames were used to guide the specimen. Vertical frames consisted of steel tubings located at both ends of the test specimen. The tubings were securely fastened to the base block and to the top access platform. Ball casters, mounted on the side of the tubing were used to guide the floor slabs at the first three stories. Throughout testing, ball casters were maintained in contact against steel plates mounted on the 2 ft (0.6 m) slab overhangs. In this way out-of-plane movement in the walls during loading reversals was minimized.

Loading System

Test specimens were loaded laterally in the plane of the structure. Concentrated reversing loads were applied at the top

Test Specimen

Reaction Wall

Test Floor
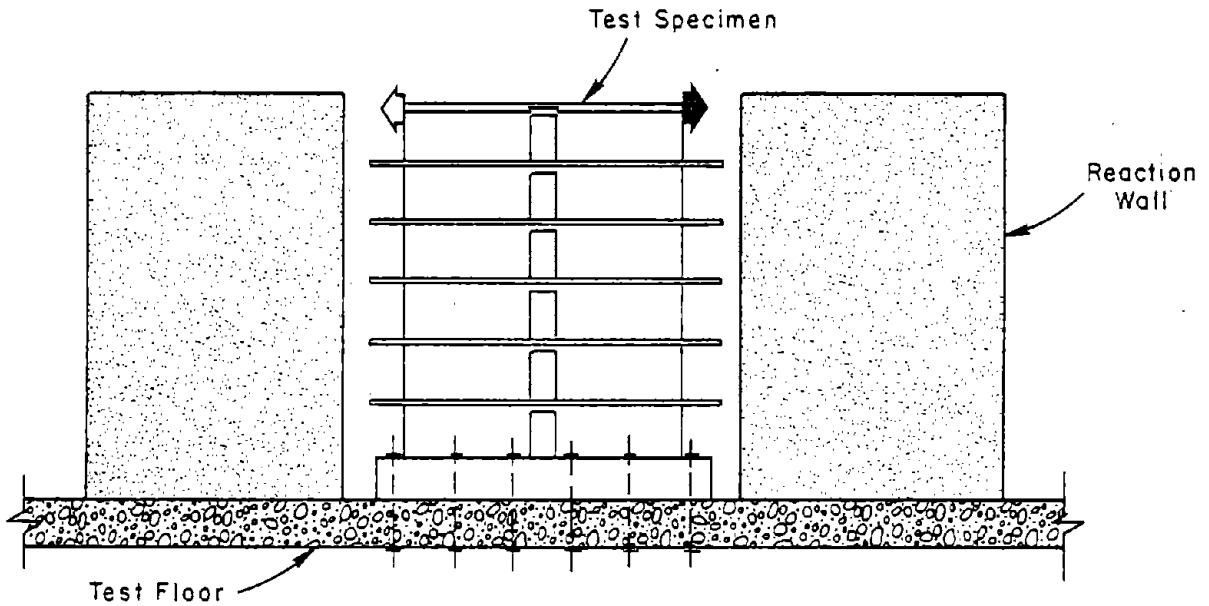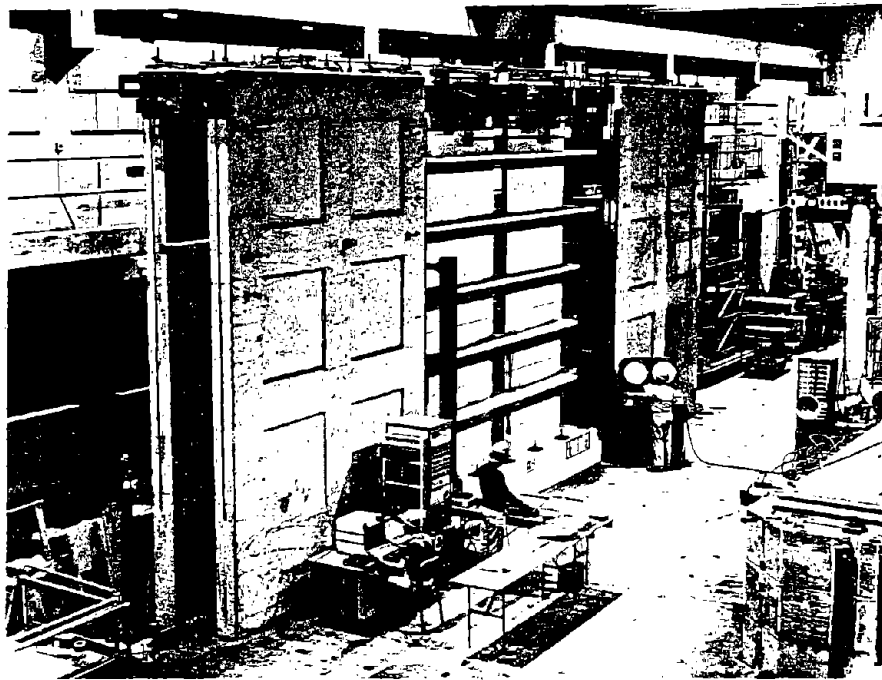
Fig. A12   Test Setup for Wall Systems

of the specimen by four hydraulic rams. Each ram was a double
acting hydraulic load applicator with two-ton load capacity and
a maximum stoke of 36 in. (90 mm). Rams were located between
the reaction walls on both sides of the specimen as shown in
Fig. A-13. Rams on each side of the specimen were hydraulically
coupled together so that applied loads were distributed equally
to both sides of the specimen. Loading pistons of both rams
were connected to a common crosshead and in turn to specially
designed loading assemblies.

The loading assemblies for applying forces to the specimen
are illustrated in Fig. A-14. Each assembly consisted of a
steel box within a box. The outside box was fastened directly
to the top slab. The inside box was connected to the outside
box through a pin. Thus, the inside box was free to rotate
about its center. Forces applied by the rams were transmitted
to vertical crossheads attached to the inside box. In this way
equal forces were applied to each wall.

Lateral loads were applied by pulling against the reaction
abutments. Pulling action was used because it provided natural
restraining forces against out-of-plane wall movements.

Instrumentation

Specimens were instrumented with both external and internal
measuring devices. These measured applied loads, deflections,
rotations, shear distortions, and reinforcement strains in walls
and coupling beams.

Locations of external gages are shown in Fig. A-13. Four
load cells were used to monitor loads applied to the specimen.
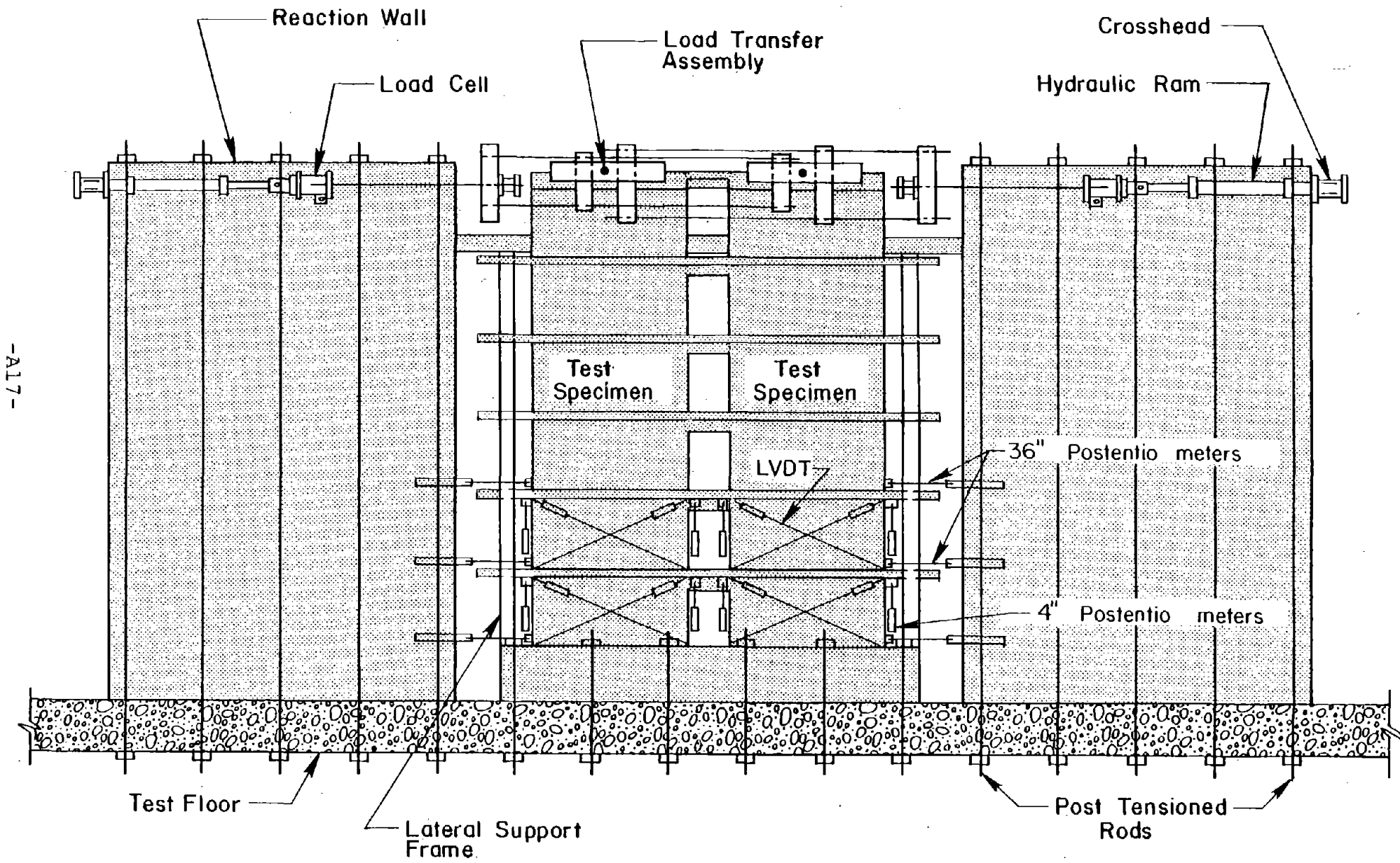
Fig. B13 Schematic Drawing for Test Setup
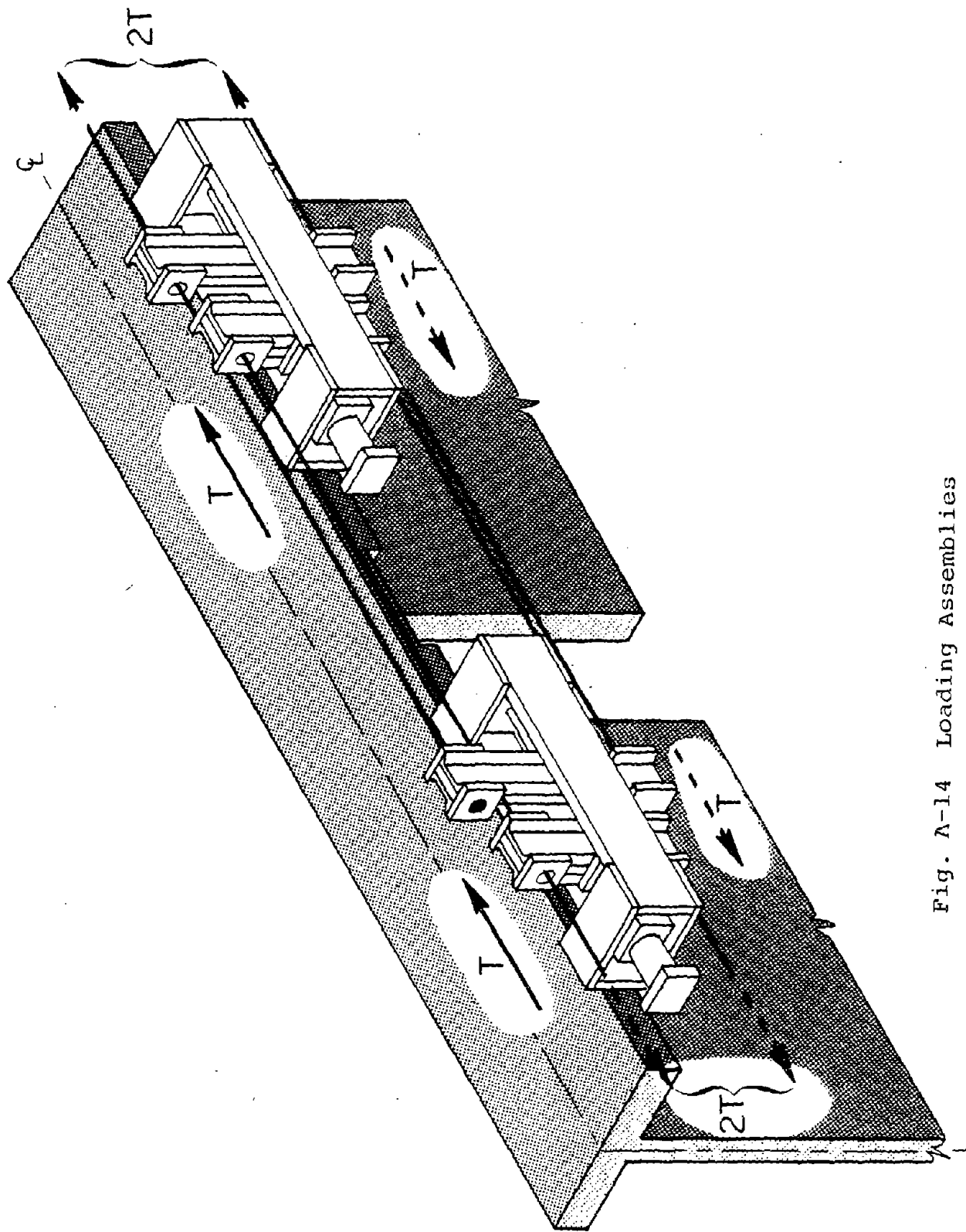
Fig. A-14 Loading Assemblies

They were positioned at the end of each ram piston. Lateral
deflections were recorded on both sides of the specimen by 36 in.
(914 mm) stroke potentiometers located at the first, second,
third, and sixth floor levels. In addition, lateral displace-
ments at 3 in. (76 mm) above the base of the walls and movements
of the base block were also recorded by 4 in. (102 mm) stroke
potentiometers.

Rotations over a given section were measured by two 4 in.
(102 mm) potentiometers. Based on displacements measured by the
potentiometers, average rotations over a given section were
calculated. Procedures for determining rotations from the
potentiometer readings are given in Fig. A-15. Rotations of
wall elements at the first story, second story and over a 3-in.
(76 mm) section above the base block were measured. A photo-
graph of external instrumentation in the wall element is shown
in Fig. A-16. Rotations at the top of the specimens were also
recorded. However instead of using potentiometers rotational
meters developed at Construction Technology Laboratories were
used.

Rotations at end regions of the coupling beams were also
measured. Instrumentation was installed on coupling beams at
the second, fourth, and sixth floor. A photgraph of the rota-
tion instrumentation on coupling beams is shown in Fig. A-17.

Shear deformations were determined from measurements along
diagonals. Using measured displacements along diagonals, aver-
age shear strain of the instrumented section was calculated.
The method used for calculating shearing strains from recorded

-A19-

$$\theta = \frac{r_1 + r_2}{h}$$
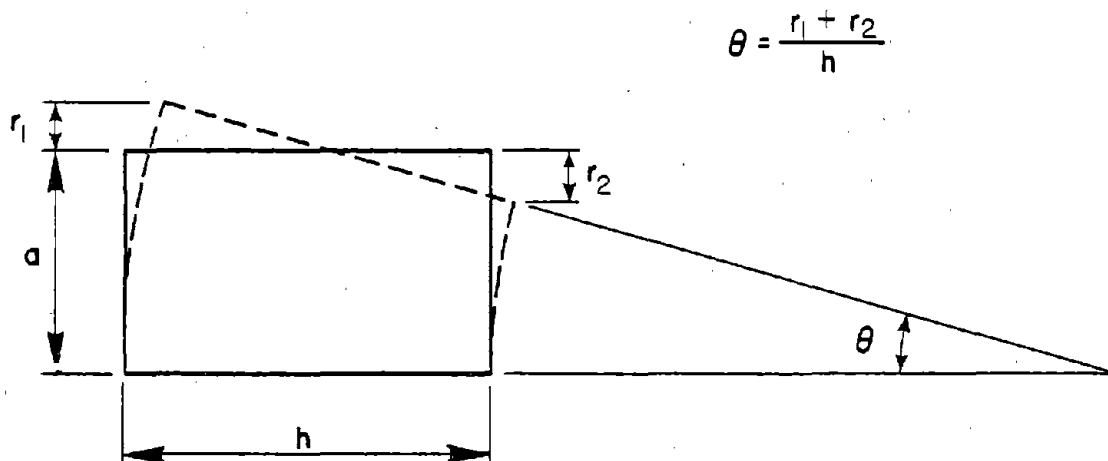
Fig. A-15 Rotation Calculation
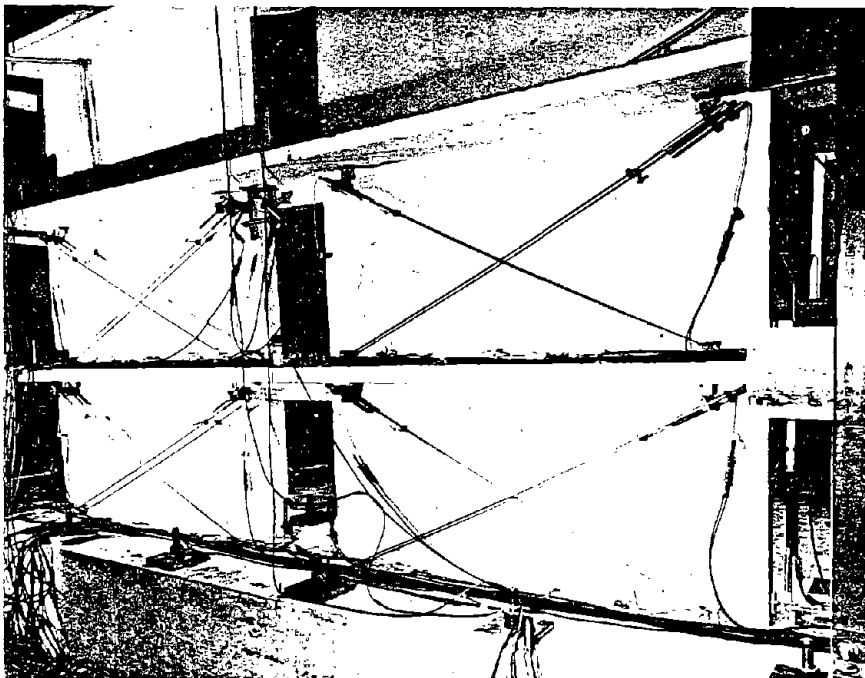
Fig. A-16 External Wall Instrumentation

readings is shown in Fig. A-18. Two 6-in. (152 mm) stroke Direct Current Differential Tranducers (DCDT) were used to measure the first and second story shear deformations. Details of the instrumentation are shown in Fig. A-16. Similar instrumentation was used to measure shear deformation at the end regions of coupling beams. Shear strain measurements on coupling beams were made at the second, fourth, and sixth floor levels.

Strains in steel reinforcement at selected locations were measured by electrical resistance strain gages. Strain gages were attached to the surface of the steel reinforcement before casting.

Locations of strain gages on vertical and horizontal wall reinforcement are shown in Fig. A-19. In addition, reinforcement in floor slabs at the first, second, and third level was instrumented strain gages at locations shown in Fig. A-20. Reinforcement in coupling beams at the second, fourth, and sixth floor was also instrumented. Strains in wall confinement hoops in the first two stories were also measured. Strain gage locations for the coupling beams and hoop reinforcement are shown in Fig. A-21 and A-22, respectively. Over 300 electrical resistance strain gages were used. This instrumentation provided a detailed record of the yielding sequence in each structural element during testing. It also indicated the strain history at specific locations.

Throughout the test program three X-Y plotters were used to obtain continuous records of selected parameters.
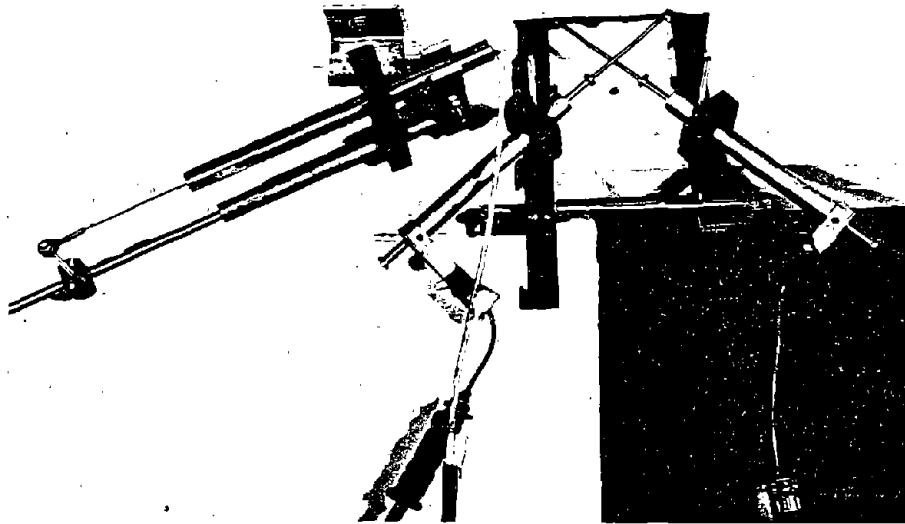
Fig. A17   External Coupling Beam Instrumentation
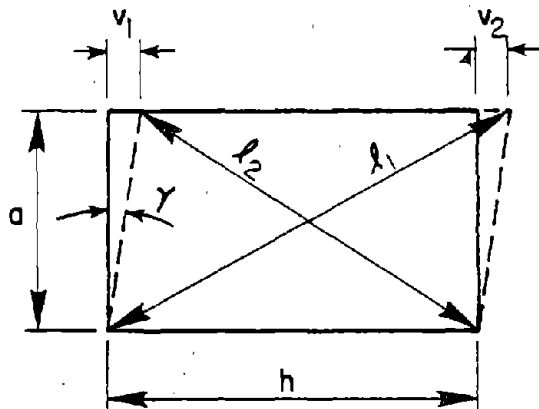
$$\gamma = \frac{v_1 + v_2}{2a} = \frac{\sqrt{\ell_1^2 - a^2} - \sqrt{\ell_2^2 - a^2}}{2a}$$

Fig. A18   Shear Distortion Calculation
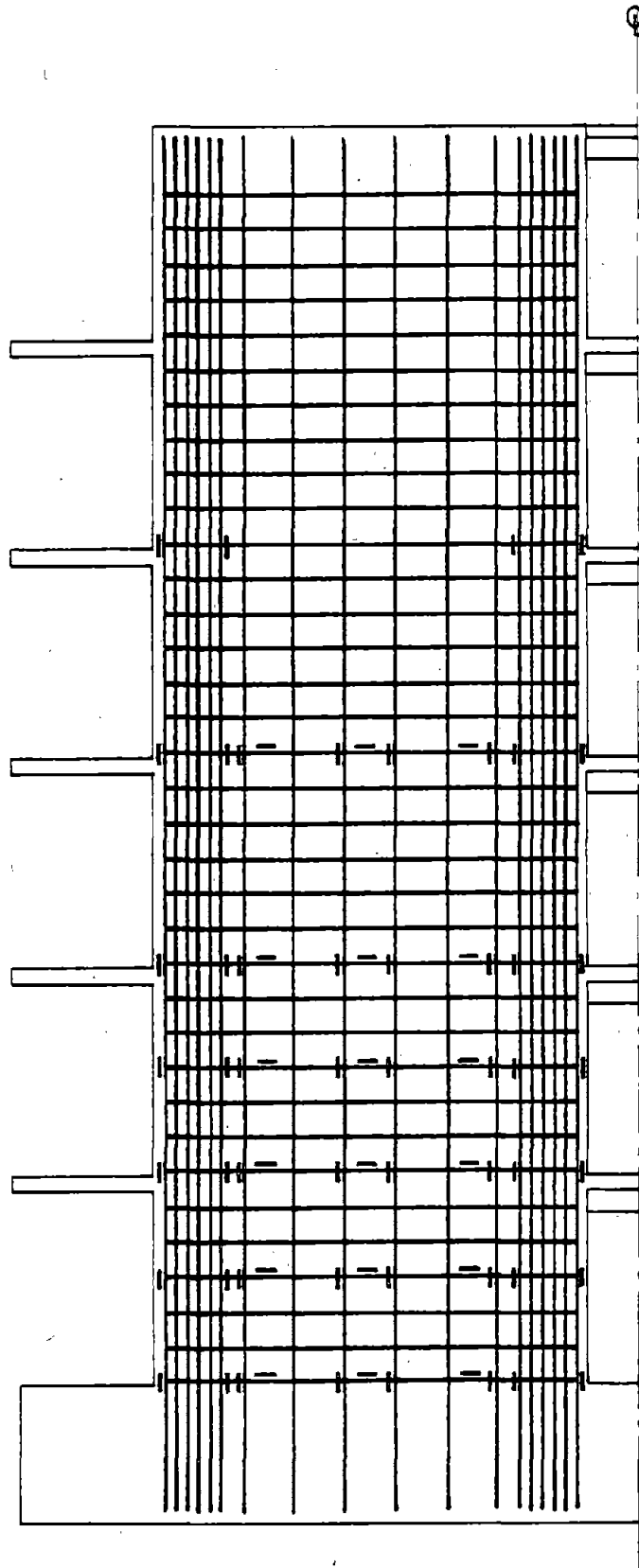
Fig. A19   Location of Internal Strain
Gages in Wall Element

Strain Gages

3½" | 52 @ 4" = 17'-4" | 3½"

I in. = 25.4 mm

Plan
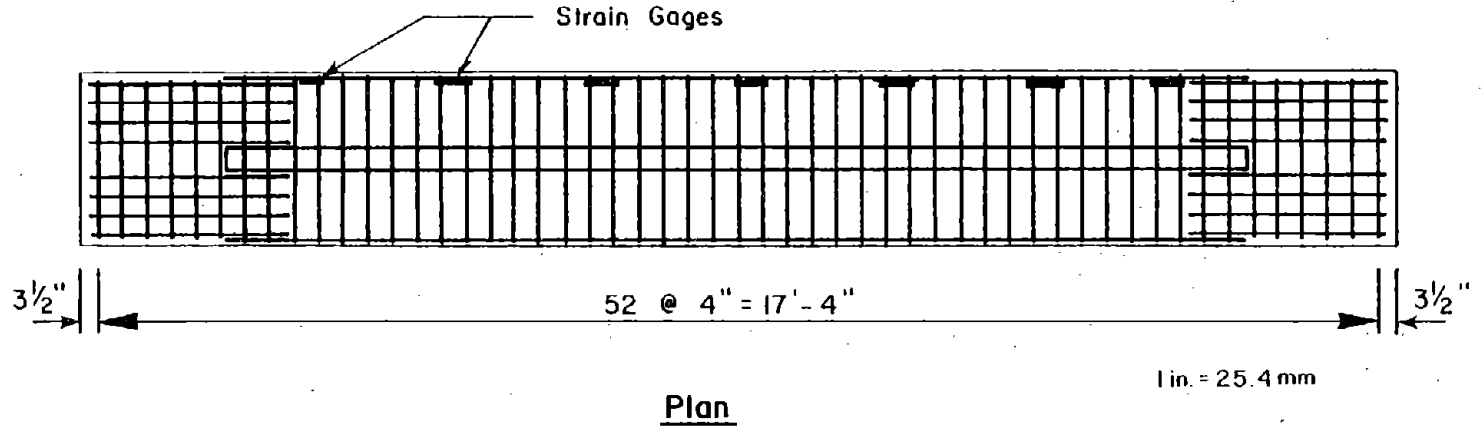
Fig. A-20   Locations of Strain Gages on Slab Reinforcement

Strain Gages

D-3 wire

16⅔"

2 - 6 mm bars

Specimen CS-1

Strain Gages

D-3 wire

16⅔"

6 -#3 bars

Specimen RCS-1
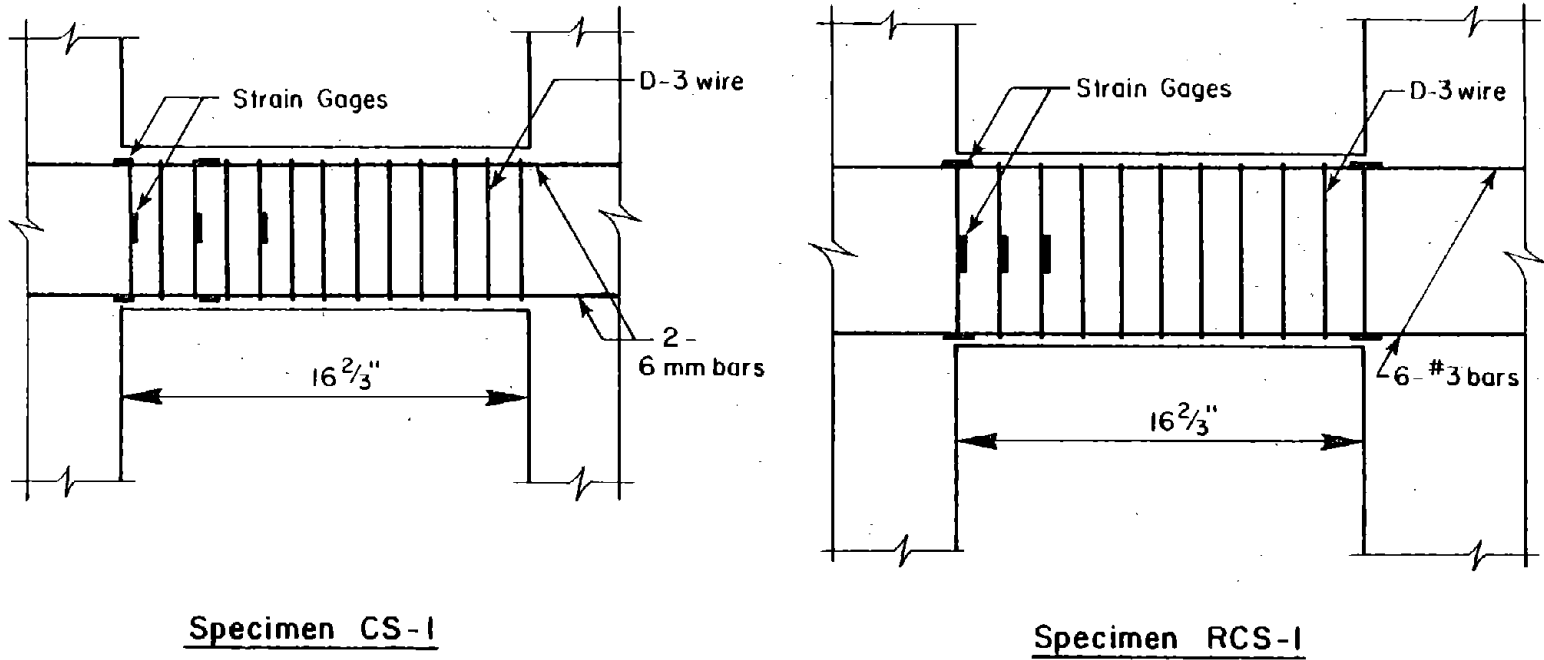
Fig. A-20   Locations of Strain Gages for Coupling Beams

Wall

D-3 wire hoops

Strain Gage

20"

1st floor

$10\frac{5}{8}$"

$10\frac{5}{8}$"

36"

$10\frac{5}{8}$"

Boundary
element

— Base block —
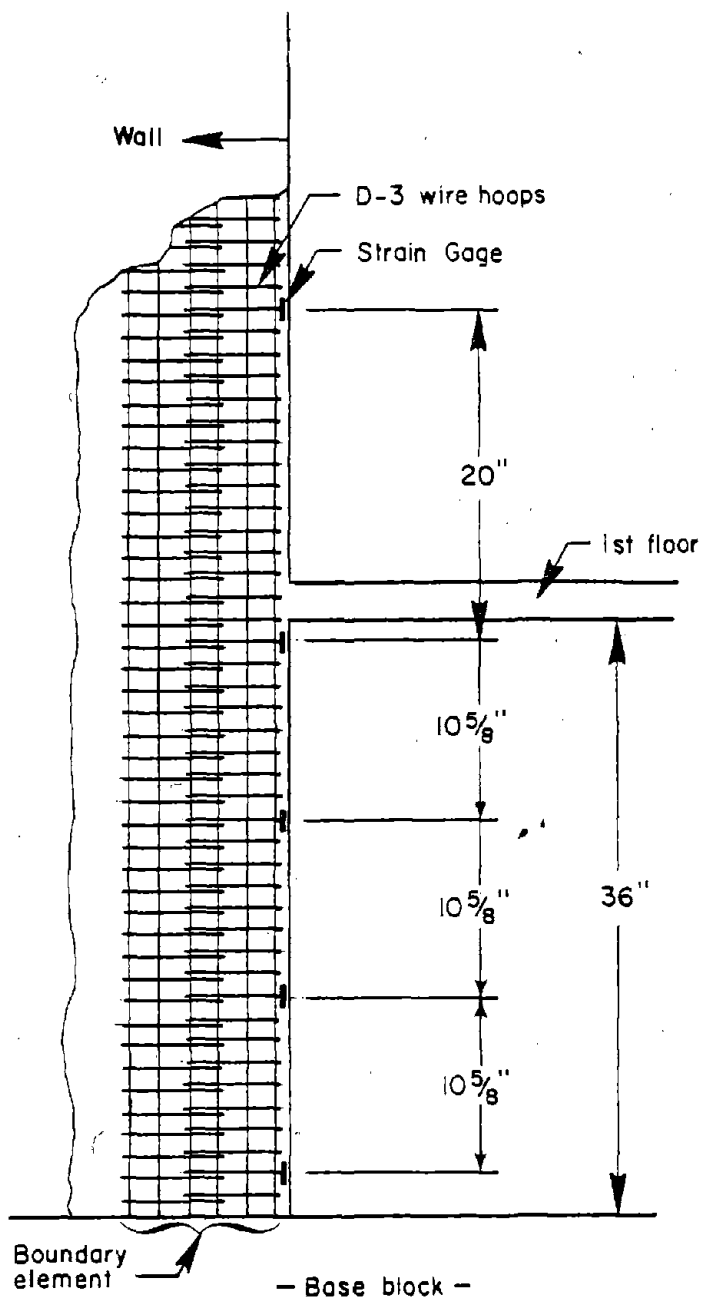
Fig. A22 Strain Gages on Wall Hoop Reinforcement

Construction and Repair Procedures

Construction procedures for the specimens were common field practices. In this section procedures for constructing specimen CS-1 are presented. Methods used to replace damaged coupling beams after CS-1 was tested are also described.

Construction Procedures

Construction of specimen CS-1 began with casting of the 2x4x17-ft (0.6x1.2x5.2-m) base block. Prior to testing, the specimen was post-tensioned to the laboratory floor through the base block. All vertical wall steel was anchored in the base block and extended continuously to higher stories as shown in Fig. A-23.

The specimen was cast vertically, one story at a time, with construction joints at the top of every floor slab. Prior to setting forms at each story, horizontal steel in the walls and floor slabs was tied in position.

A photograph of the specimen showing the base block, first story, and second story formwork is shown in Fig. A-24. Initially, formwork was fastened to inserts in the base block to maintain proper spacing. For stories above the first floor level, forms were secured to the floor slab at the preceeding floor level. Vertical alignment of the wall was maintained by tying laterally to a rigid frame before and after casting. Vertical and horizontal alignment was checked by a theodolite.

After casting, concrete was cured for four days before formwork was stripped. During this period reinforcement for the next story was tied in place.
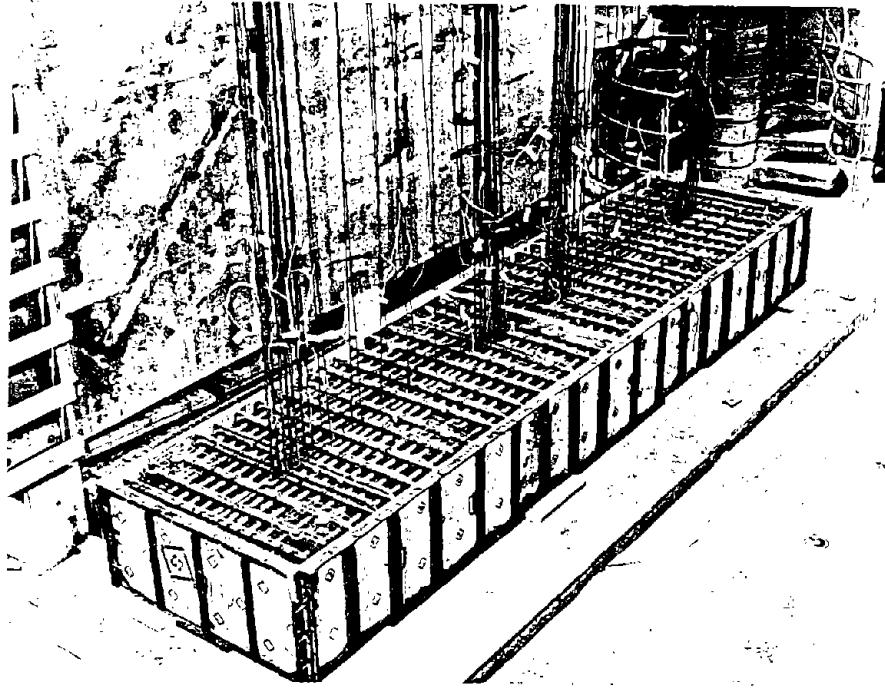
Fig. A-23 Base Block of Coupled Wall Specimen
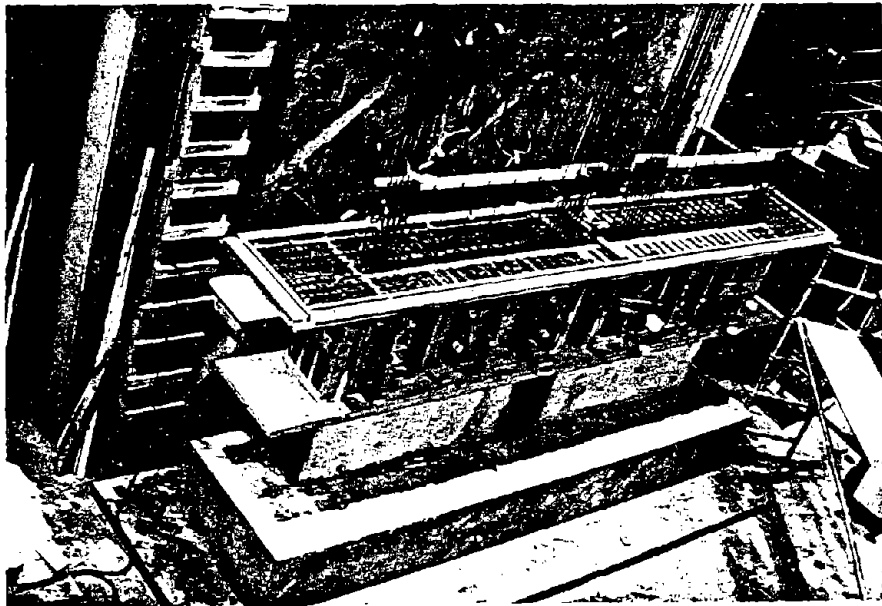
Fig. A-24 Specimen During Construction

Construction joints between lifts were prepared according to specifications in the 1971 ACI Building Code.[17] Concrete surfaces were roughened with a chisel. Laitance and loose particles were then removed prior to placing adjoining concrete.

Coupling Beam Repair Procedures

The following method was used to replace damaged beams with new beams after the test of CS-1. Steps for removing damaged beams are schematically illustrated in Fig. A-25.

1. Slabs along the length of coupling beams were removed. Longitudinal bars in slabs were left in place.

2. Coupling beams were removed. Longitudinal reinforcements in the coupling beams was cut close to the wall-beam interface.

3. Wall elements were checked to be sure that they were perpendicular to the floor. Residual displacement of individual walls was corrected.

4. Concrete cover over boundary elements in wall elements next to coupling beams was chipped off and cleaned. Holes were drilled in the web of the wall beyond the boundary elements. The openings allowed flexural reinforcement for the repaired beam to be bent and anchored around the boundary element.

5. Formwork was put in place. New coupling beams were cast. After four days of concrete curing, forms were stripped.

A view of the specimen after removal of the coupling beams and with the reinforcement cage for new beams in place is shown in Fig. A-26. A view of the repaired beam after casting is shown in Fig. A-27.
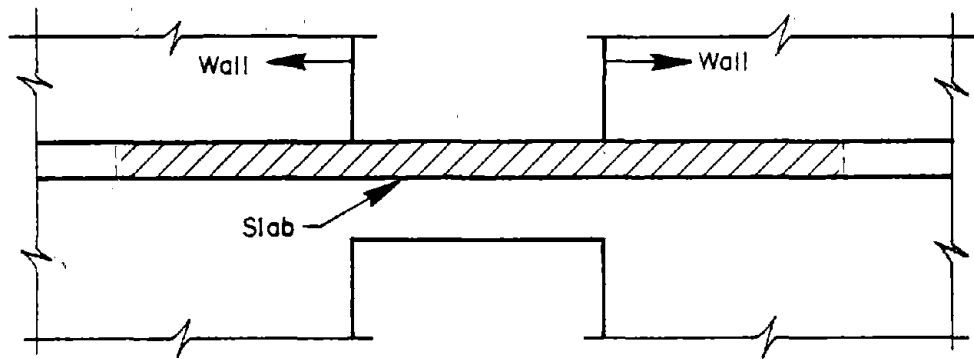
a) Removal of Floor Slab
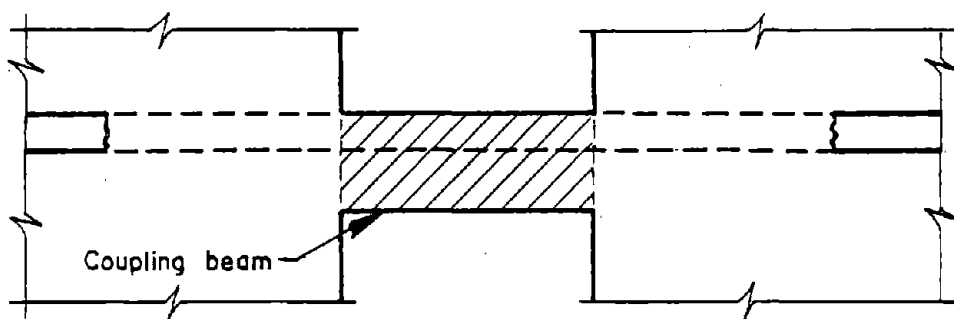
b) Removal of Coupling Beam
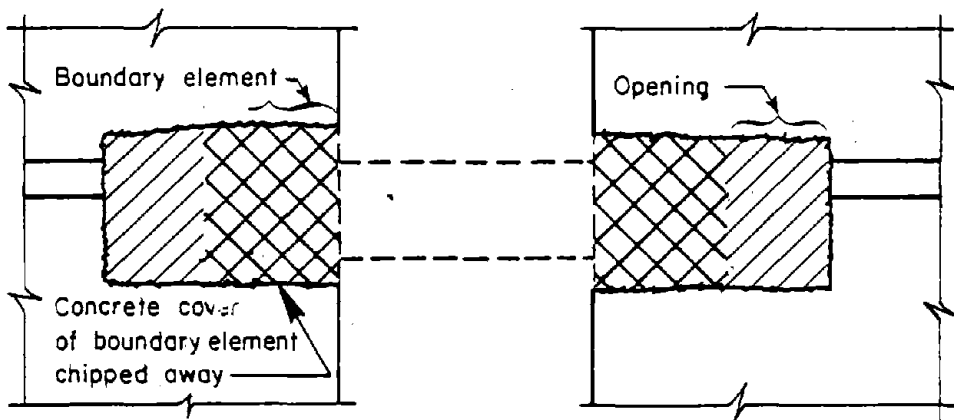
c) Openings in the Web for
Reinforcement of Replaced Beam

Fig. A25   Removal of Damaged Coupling Beams
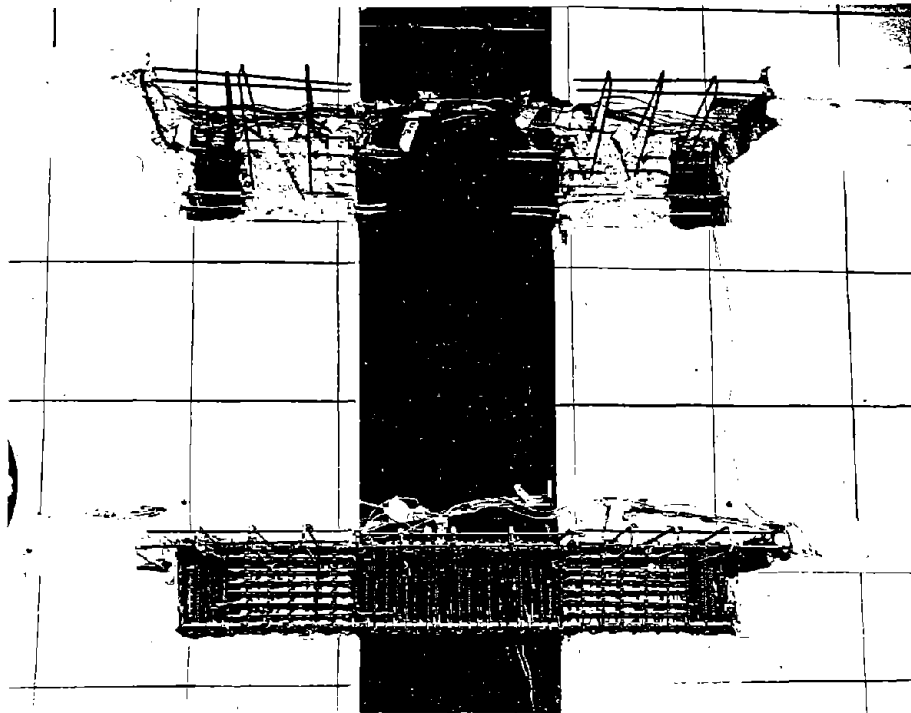
Fig. A26   Reinforcement Cages for Repaired Beams
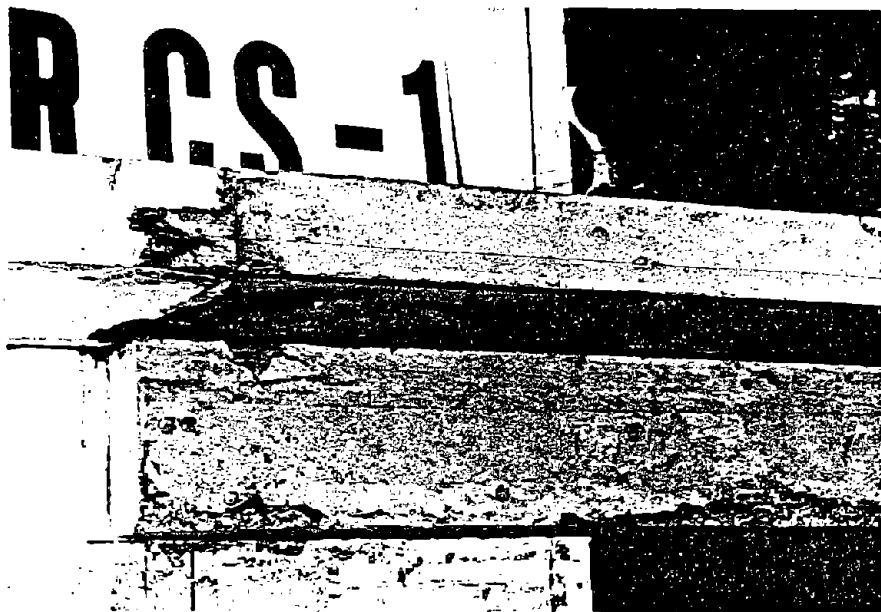
Fig. A27   Beam After Repair

APPENDIX B - EXPERIMENTAL RESULTS

In this appendix, recorded data from tests of CS-1 and RCS-1 are presented in detail. Observed behavior of both systems is described. Data on strength and deformation characteristics are discussed and compared.

Observed Behavior

Two kinds of response were observed in the tests of CS-1 and RCS-1. These were distinguished primarily by the effectiveness of coupling beams in connecting wall elements together. With different amounts of coupling, the amount of axial and shear load induced by the coupling beams on the walls varied. This changed the behavior pattern of the specimens and resulted in two different modes of failure. Observed behavior of CS-1 and RCS-1 are discussed in this section.

Wall Test CS-1

System CS-1 was subjected to six load cycles. The first three cycles corresponded to initial cracking of the specimen and yielding of flexural reinforcement in the sixth floor coupling beam. Loads applied during the last three cycles corresponded to yielding of the wall elements.

The overall crack pattern of the specimen after the first three load cycles is shown in Fig. B-1. Cracking in the beams was first observed at an applied load of 25 kips (111.2 kN). Cracks in all coupling beams were concentrated at the wall-beam interface. Scattered diagonal cracks were found in coupling beams at the top four stories. Photographs of coupling beams at
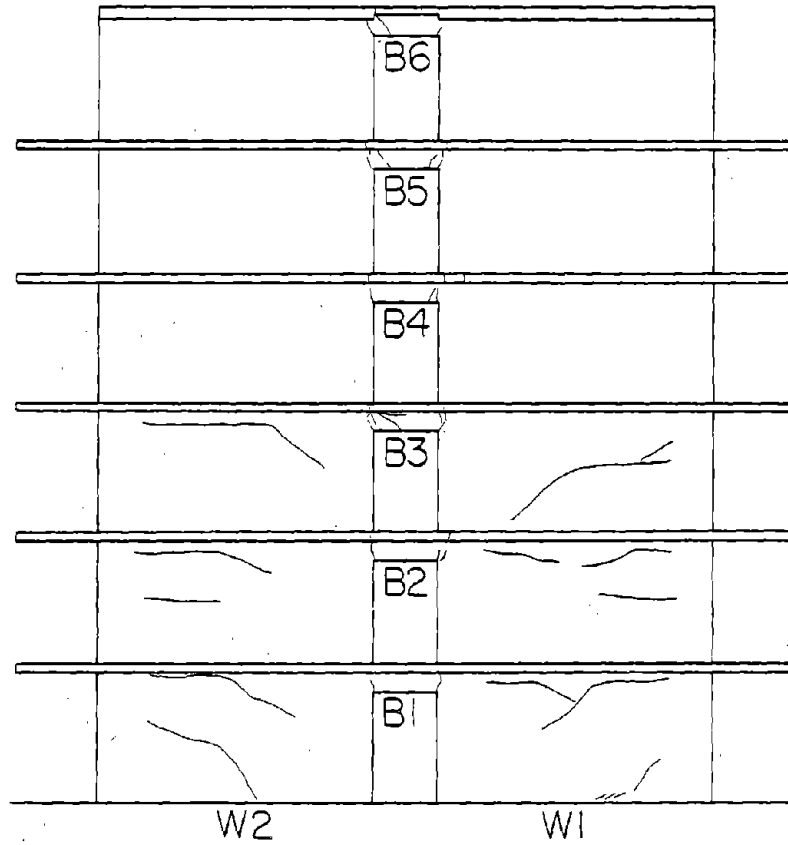
Fig. B-1   Initial Crack Pattern
           for CS-1

the fourth and fifth story are shown in Fig. B-2. These were taken during cycle 3.

Cracks in the walls started horizontally. With additional load reversals, cracks propagated diagonally to the center of the walls. No cracking was observed in the boundary elements of the walls until the third load cycle.

Initial cracking in the tension wall was recorded at an applied load of 15 kips (66.7 kN). No separation between wall elements was observed at the end of the third load cycle.

As the test continued, the compression and tension walls yielded at approximately the same load. The specimen was then cycled at the yield level of the wall system. At this point, all coupling beams were beyond yield. Deformation demands imposed on coupling beams increased as the wall specimen softened under load reversals. Deformations imposed on coupling beams at the upper stories were observed to be larger than those at lower stories.

Significant separation between walls was observed during the fourth cycle. Measured wall separation versus applied load is shown in Fig. B-3. A maximum wall separation of 0.5 in. (13 mm) was recorded. Wall separation induced axial deformations, in the coupling beams. The axial deformation in turn, reduced the deformation capacity of the beams. Therefore, with additional load cycles, the coupling mechanism between the walls deteriorated rapidly. By the end of the sixth cycle, the coupling beams acted as connecting links between walls as illustrated in Fig. B-4.
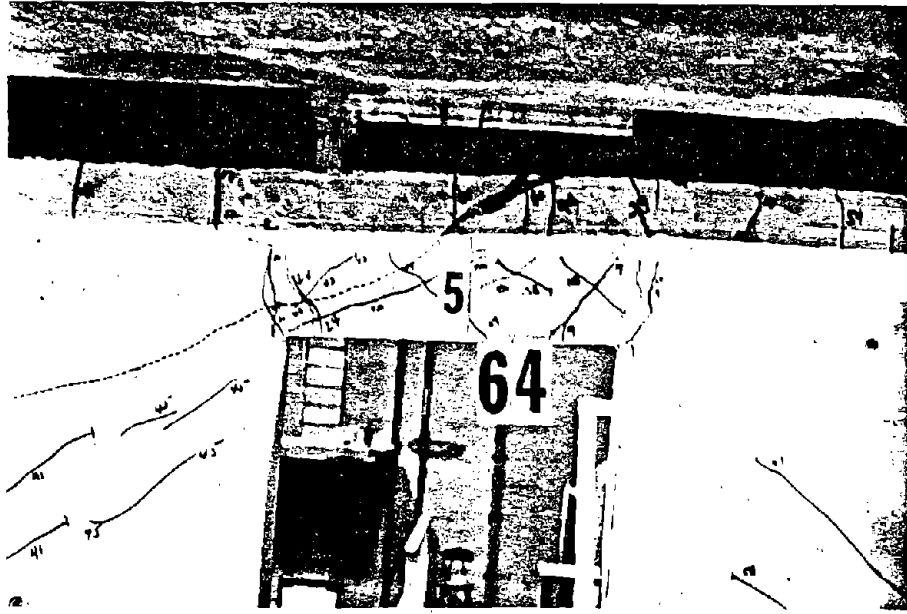
(a)   Fifth Story Beam

(b)   Fourth Story Beam

Fig. B2   Crack Patterns for Coupling Beams of System CS-1

Load, kips

200 —

100

4.0   3.0   2.0   1.0   0   1.0   2.0   3.0   4.0

Deflection, in.

100

1 in. = 25.4 mm
1 kip = 4.448 kN

200 —
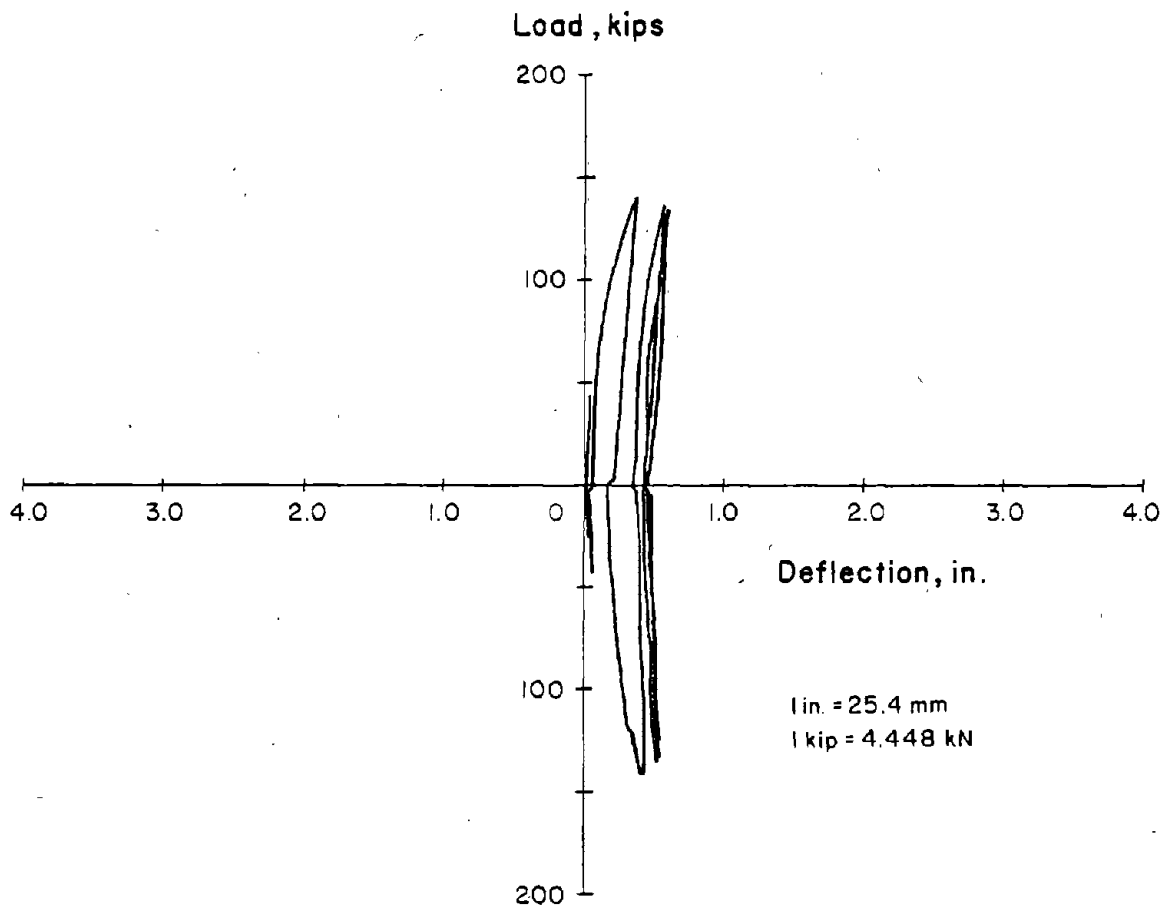
Fig. B-3   Separation Between Walls for CS-1

Connecting
Links
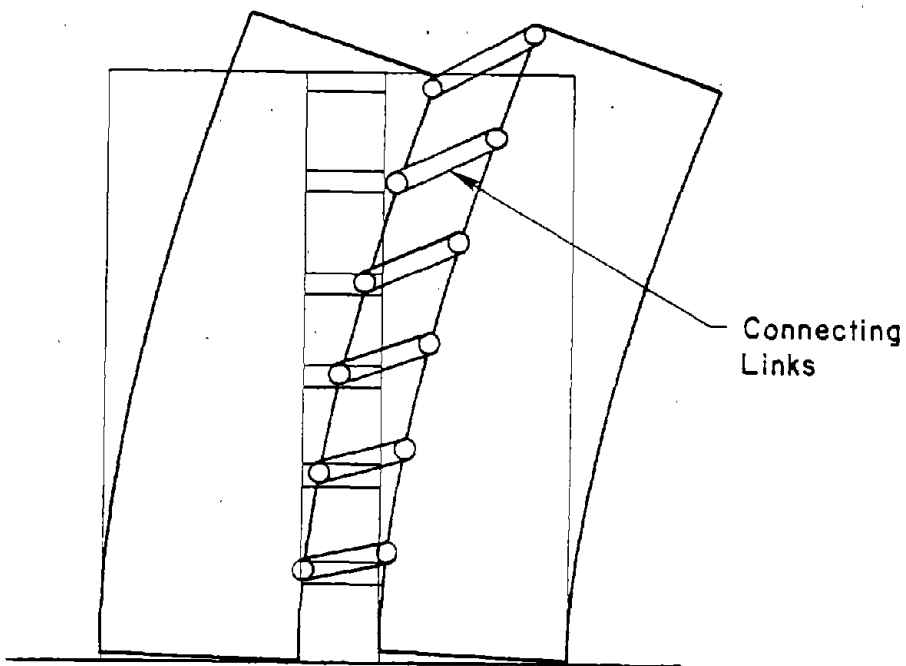
Fig. B-4   Linkage System

Applied loads were distributed equally at the top of both walls throughout the test. Before the breakdown of the coupling mechanism, horizontal forces in the tension wall were transmitted to the compression wall through the coupling beams. As hinges developed at the ends of the coupling beams, beam-wall interaction changed. Coupling action was reduced to a linkage system.

At lower story beams, concrete crushing was observed at the beam-wall interface. However, rotation measurements did not indicate flexural crushing of beams. This indicated that as the beams began to deform shear forces were transmitted from the tension wall to the compression wall. Although this kind of interaction was not of significant magnitude, it enhanced wall-separation.

Figure B-5 shows the extent of cracking at the end of the sixth load cycle. Cracks in webs of the walls widened and spread. However, cracks in the boundary elements were smaller than web cracks. The cracking pattern and observed behavior of CS-1 indicated that, in the inelastic range, this specimen acted very much like two isolated walls in parallel. Axial load induced in the walls by beams was too small to make a measurable difference in wall behavior.

A photograph of the specimen after the test was stopped is shown in Fig. B-6. Despite the heavy damage inflicted on the coupling beams, the two structural walls were in excellent condition. Cracks closed up as soon as applied load was released.
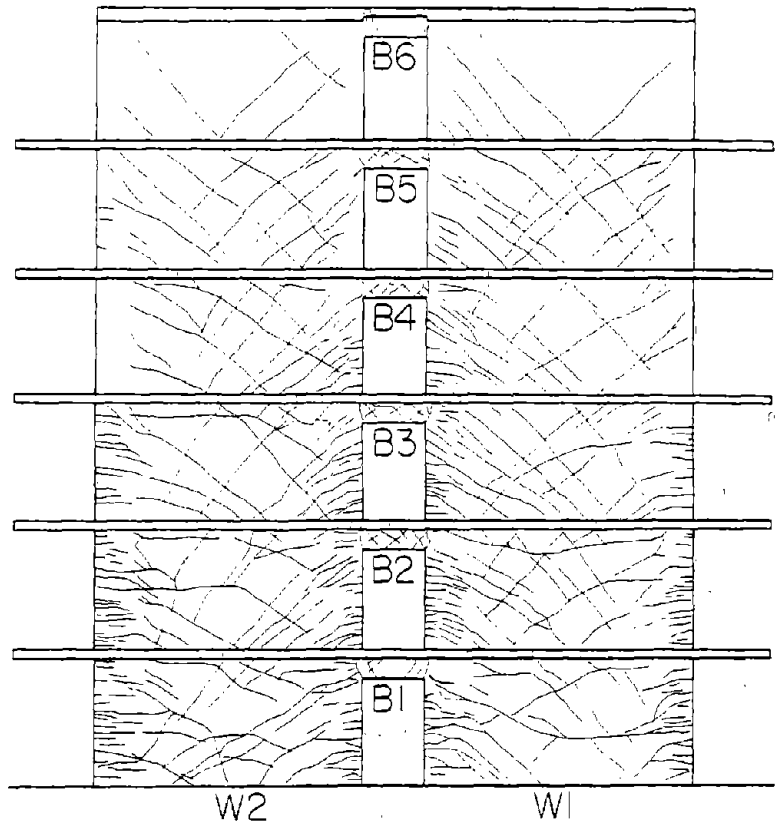
Fig. B-5   Crack Pattern for System CS-1
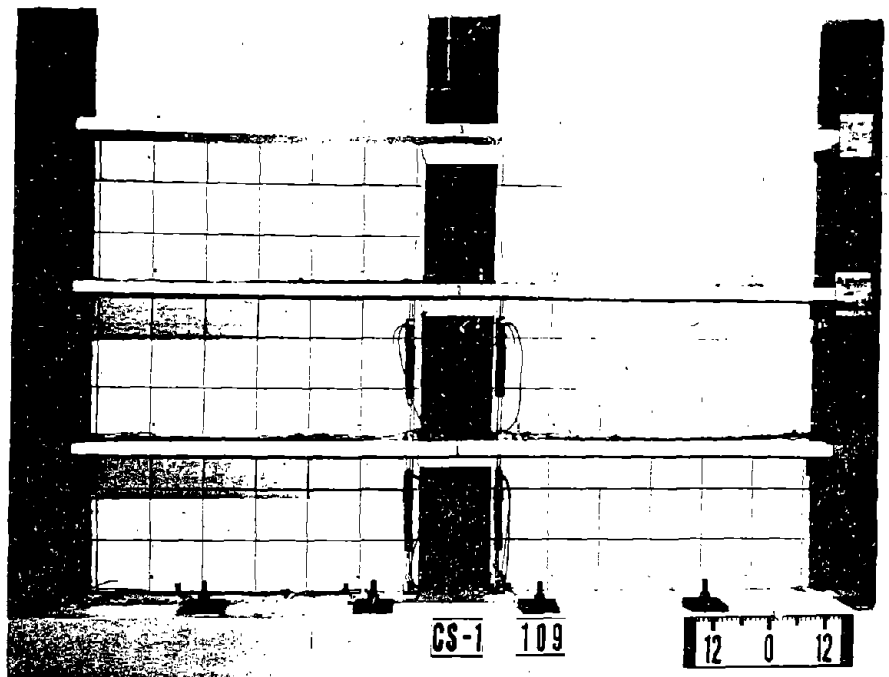
Fig. B-6   System CS-1 after Testing

Wall Test RCS-1

System RCS-1 was a heavily coupled repaired wall system that was subjected to fourteen reversing load cycles. The first six cycles were identical to the load history applied to CS-1. The eight subsequent cycles were also incremental load reversals. Loads were applied until the system lost its load carrying capacity.

As the test proceeded, crack patterns in walls and beams were found to be quite different from those in CS-1. Cracks in coupling beams were predominantly diagonal cracks as shown in Fig. B-7. No distinct hinging regions were observed. Diagonal cracks were evenly spaced throughout the beam lengths.

Diagonal cracks were scattered over both the tension and compression walls. The cracking pattern of RCS-1 after six load cycles is shown in Fig. B-8. For clarity, only cracks resulting from one direction of loading are shown. From the observed behavior and cracking patterns, the specimen behaved very much in the "overturning" mode as illustrated in Fig. B-9. Cracks initiated in the tension wall were seen propagating through the coupling beams into the compression wall.

Figure B-10 shows separation at the top level between the two outside ends of the walls. Clear distance between walls was checked and it was found that separation was not due to beam elongation. Recorded separation represented the lateral "growth" of the wall system caused by the accumulation of inelastic strains at diagonal cracks. A maximum lateral wall growth of 0.5 in. (13 mm) was observed.
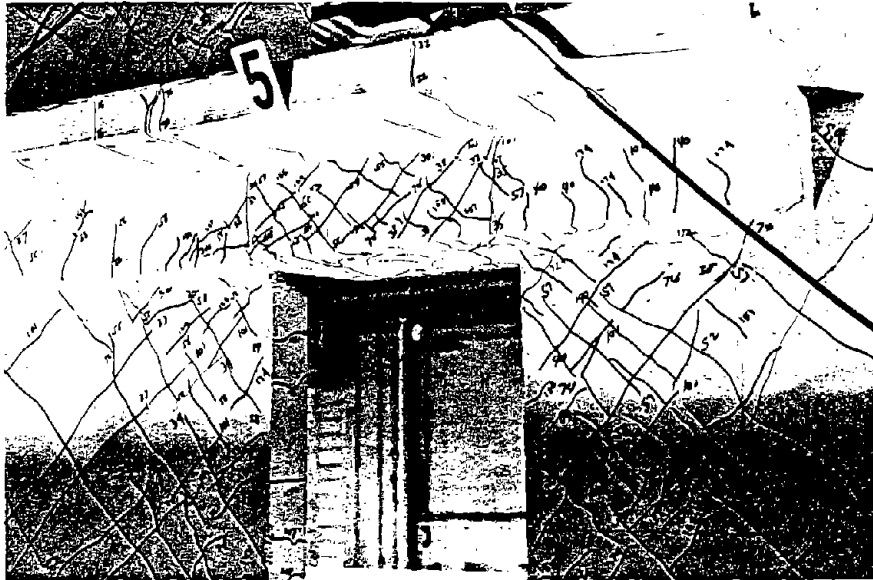
(a)   Fifty Story Beam
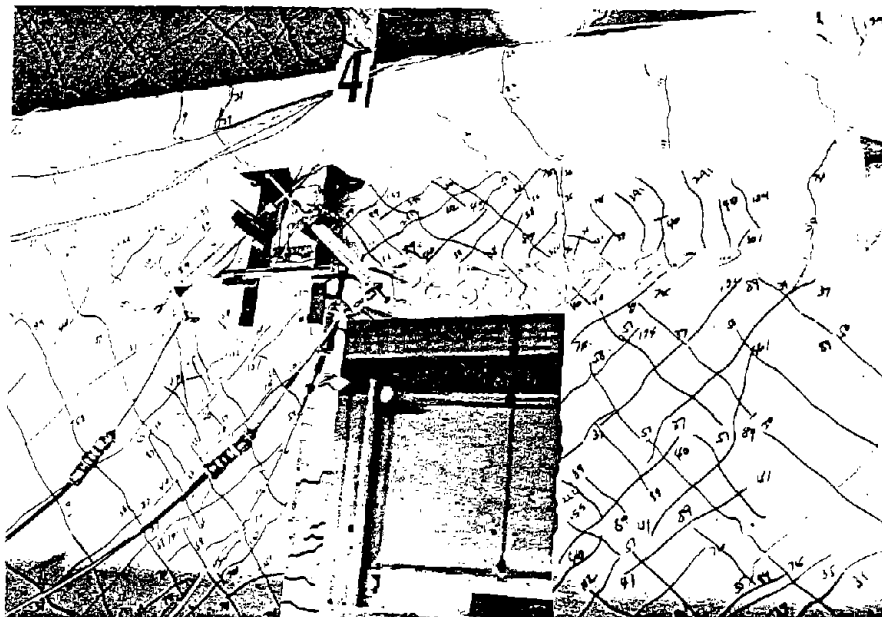
(b)   Fourth Story Beam

Fig. B-7   Cracking Patterns for Coupling Beams of RCS-1
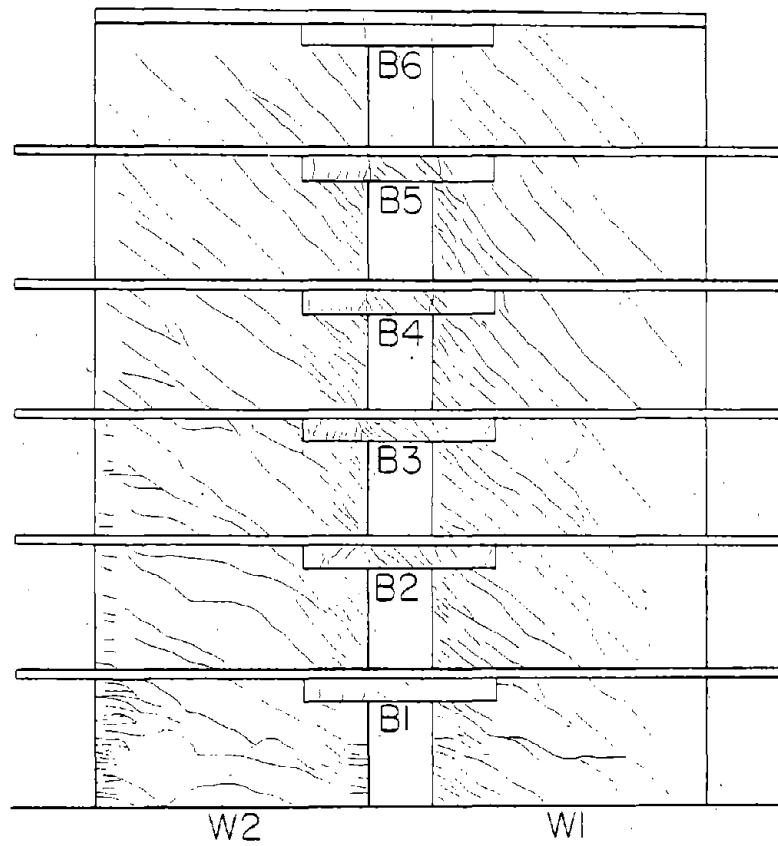
Fig. B8   Cracking Pattern of RCS-1 After Six Load Cycles

Fig. B9   Overturning Mode

Load, kips

200

100

1 in.=25.4 mm
1 kip.=4.448 kN

-4.0   -3.0   -2.0   -1.0   1.0   2.0   3.0   4.0

Deflection, in.

-100

-200
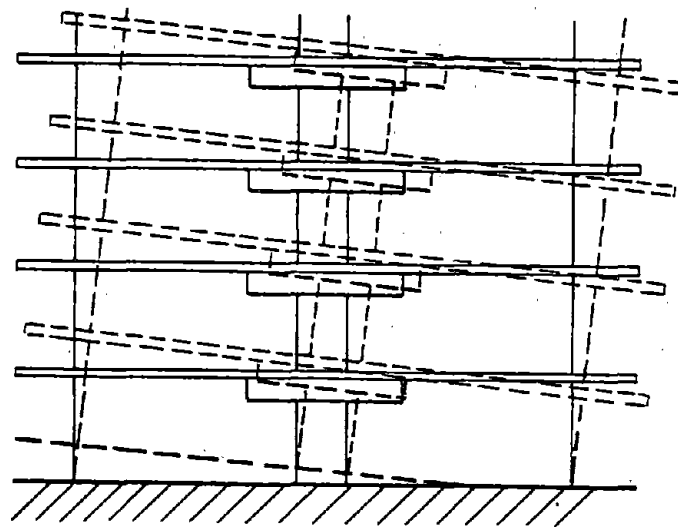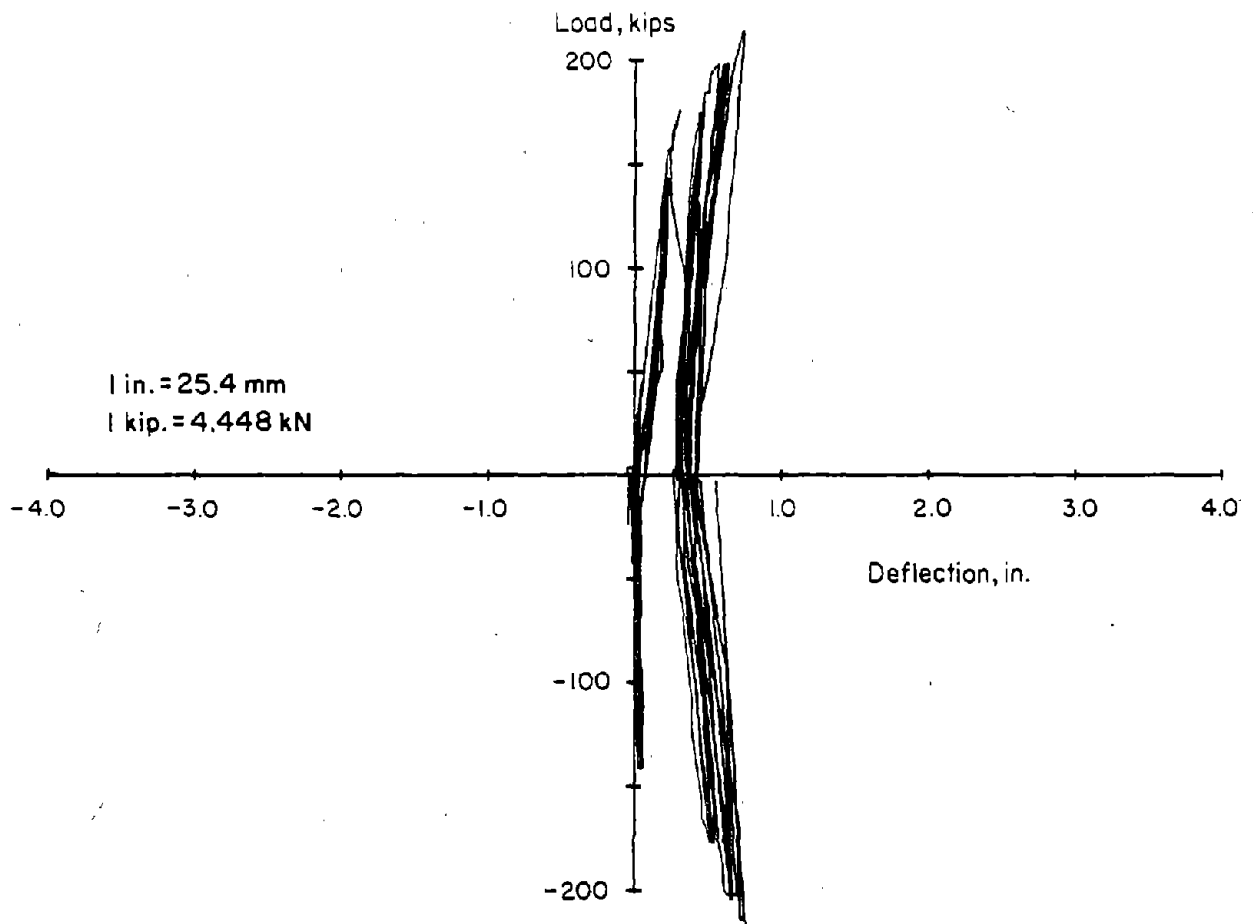
Fig. B10   Measured Separation Betwen Outside
            edges of System RCS-1
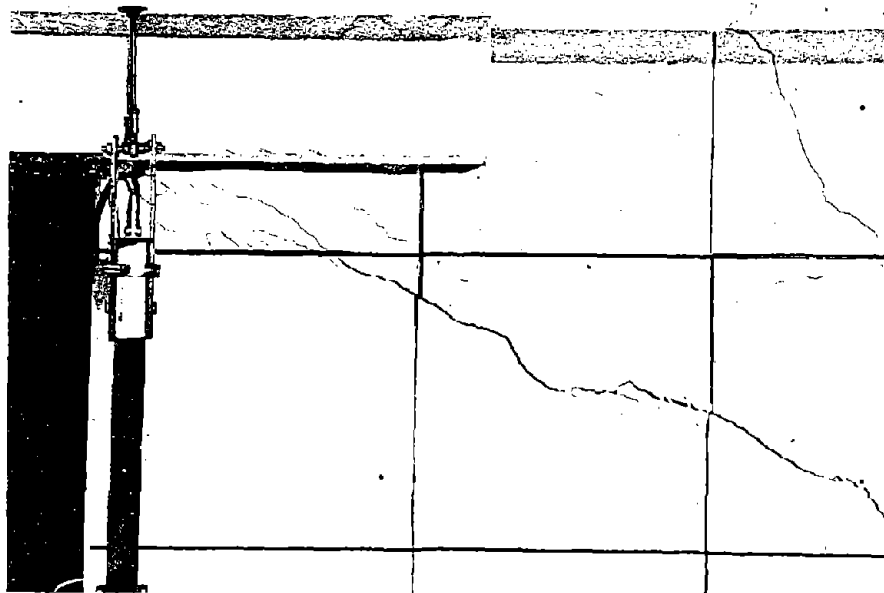
Fig. B11   Cracking Pattern at Wall-Beam
            Interface at the First Story
            After Thirteen Load Reversals

Since RCS-1 was a repair of CS-1, RCS-1 was tested with pre-existing cracks in the wall elements. With repeated load reversals, planes of weakness were formed along pre-existing horizontal cracks. Sliding shear was observed as loads were reversed. However, with increasing lateral loads, the shear resisting mechanism changed into a compression-diagonal strut system as indicated by the cracking pattern in Fig. B-8. The whole wall system then behaved as a single element in its over-turning mode. Shear forces in the tension wall were transmitted to the compression wall through the coupling beams. High axial stresses were also induced in the walls by the coupling beams.

As additional inelastic load cycles were applied, concrete crushing was observed in the compression zones of the coupling beams at the beam-wall interface. A photograph of the first-story coupling beam-wall interface after thirteen load cycles is shown in Fig. B-11. Imposed deformations on coupling beams were not sufficiently high to uncouple the wall system.

Shear stresses and axial loads induced in the walls by the coupling beams had a significant effect on the system's deforma-tion capacity and mode of failure. The combination of large axial load and shear forces in the compression wall resulted in a web-crushing mode of failure. Damage was concentrated in the first story as shown in Fig. B-12. Photographs of individual walls after test are shown in Fig. B-13.
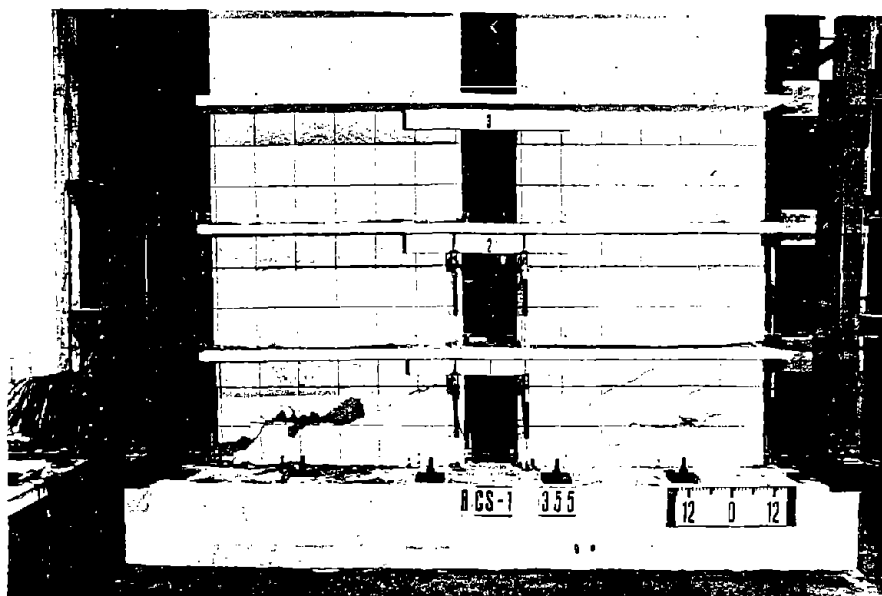
Fig. B12   System RCS-1 After Testing
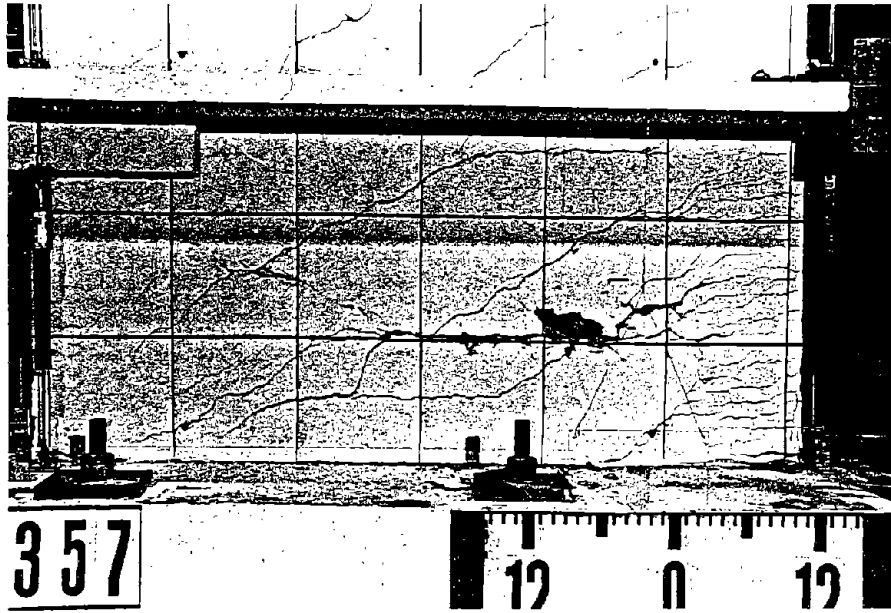
(a)   Wll Element Wl
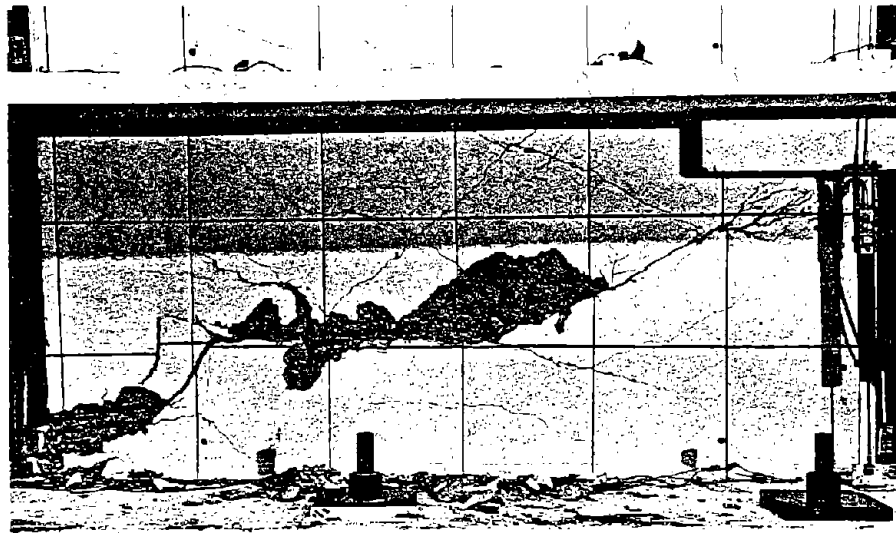
(b)   Wall Element W2

Fig. B-13   Close-up Views of Systems RCS-1 after Testing

Strength and Deformation Characteristics

Applied load versus measured deformations of CS-1 and RCS-1 are presented in this section. Lateral deflections, rotations, and shear distortions were measured.

Lateral Deflections

Top lateral deflection was measured on both sides of the specimen. Applied load versus top deflection was plotted in Figs. B-14 to B-17 for CS-1 and RCS-1. In Figures B-14 and B-16 the sequence of yielding of coupling beams for System CS-1 and RCS-1 are identified.

For Test CS-1, first yielding of a coupling beam was recorded at an applied load of 41.6 kips (185 kN) at a top deflection of 0.2 in. (5.1 mm). Wall system yielding occured at an applied load of 120k (534 kN) and a 1.3 in. (33 mm) top lateral deflection. Maximum lateral load capacity for CS-1 was 143 kips (636 kN). The test was stopped at the lateral top deflection of 2.4 in. (61.7 mm) with a corresponding lateral load of 135 kips (601 kN).

For RCS-1, first yielding of the coupling beams was measured at lateral load of 122.4 kips (544 kN) and a top deflection of 2.6 in. (66 mm). Maximum load capacity of the specimen was 217 kips (965 kN) which occurred at a deflection of 2.7 in. (69 mm). Maximum recorded deflection of the System was 4.0 in. (102 mm) at which point the system was still carrying 95% of the maximum load.

Lateral deflection profiles of three load cycles for CS-1 and RCS-1 are shown in Fig. B-18. Lateral deflections of the
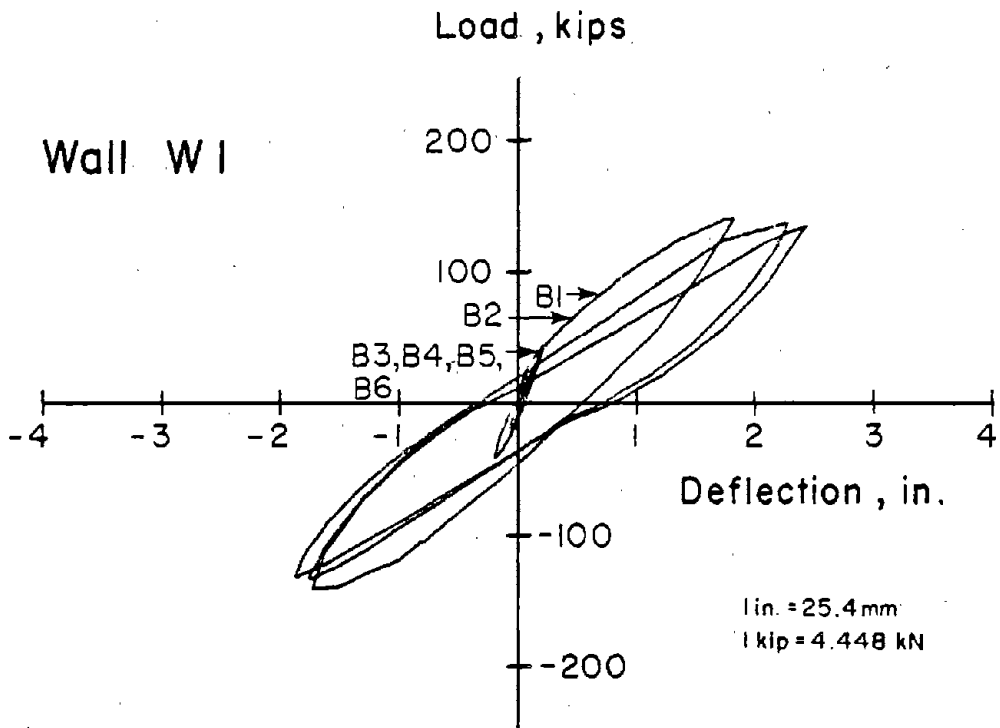
Fig. B14   Load versus Deflection Hysteresis
           for Wall Element Wl of CS-1
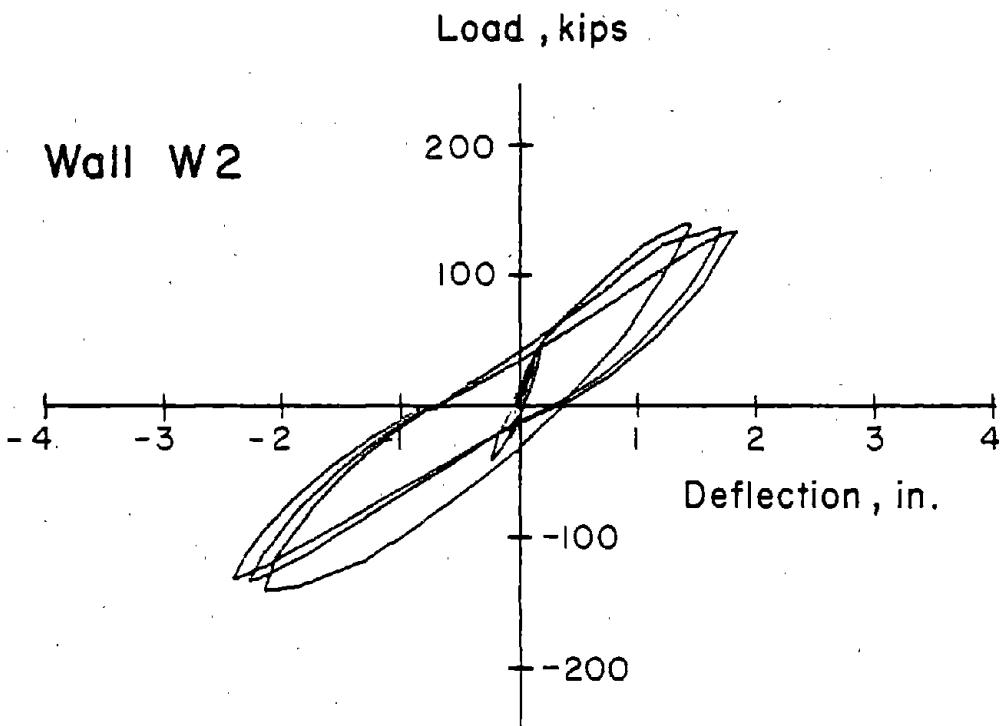
Fig. B-15   Load versus Deflection Hysteresis
            for Wall Element W2 of CS-1

Load, kips

Wall W1

200

B2 B1
B6
B3,B5
B4

100

-4   -3   -2   -1   1   2   3   4
Deflection, in.

-100

1 in. = 25.4 mm
1 kip = 4.448 kN

-200
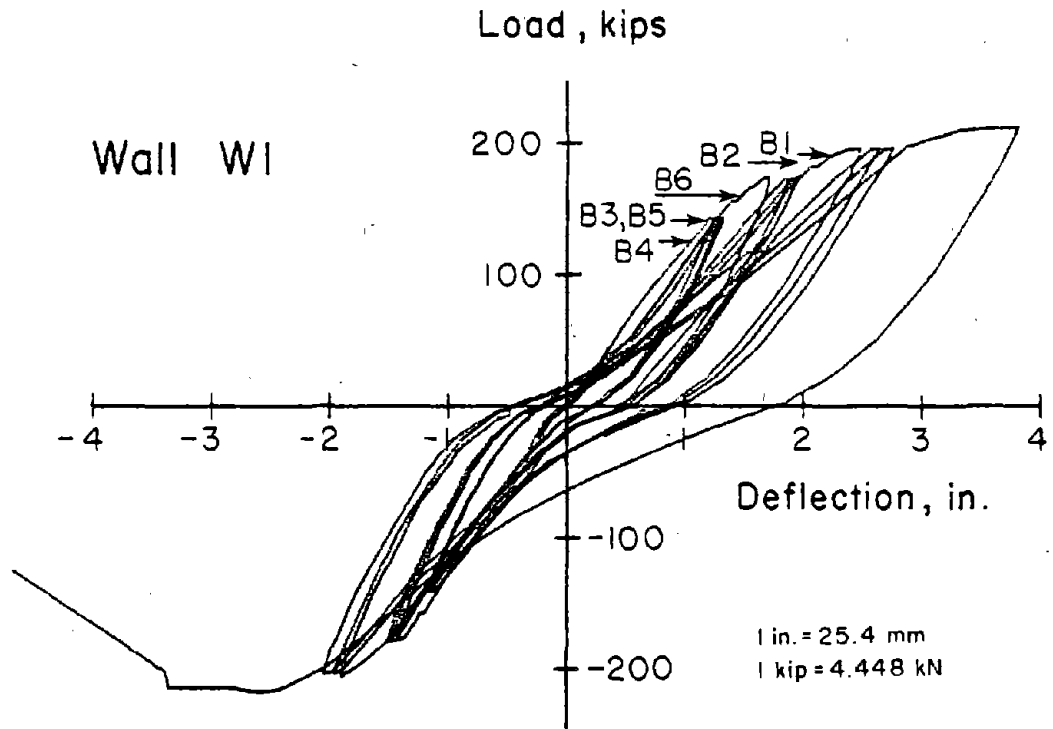
Fig. B-16   Load versus Deflection Hysteresis
for Wall Element W1 of RCS-1

Load, kips

Wall W2

200

100

-4   -3   -2   2   3   4
Deflection, in.

-100

-200
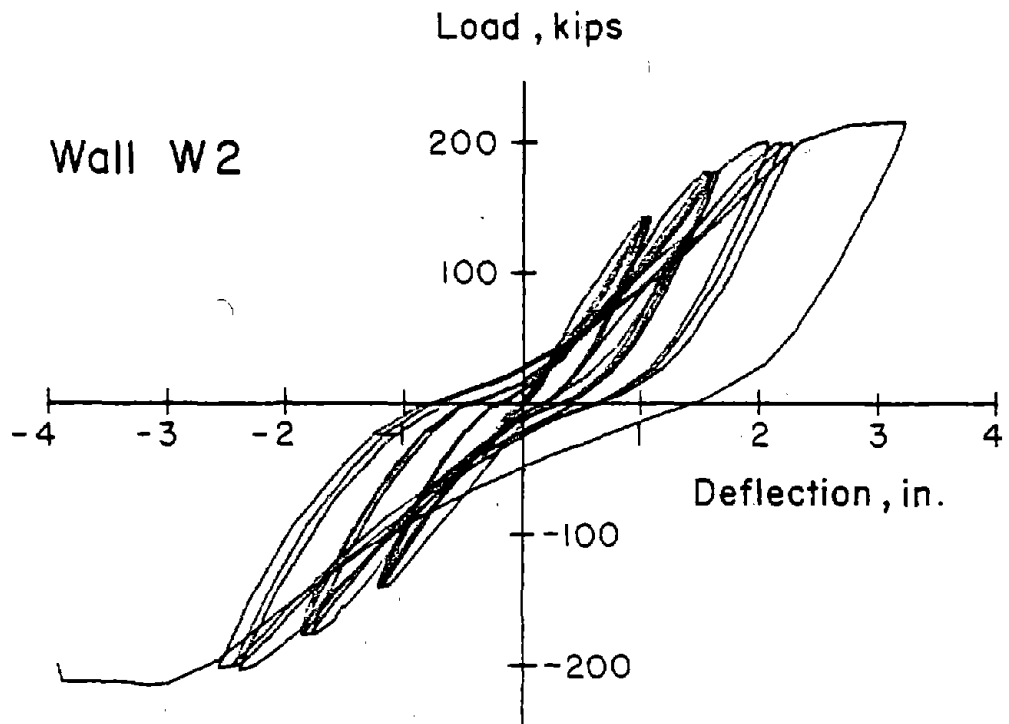
Fig. B-17   Load versus Deflection Hysteresis
for Wall Element W2 of RCS-1
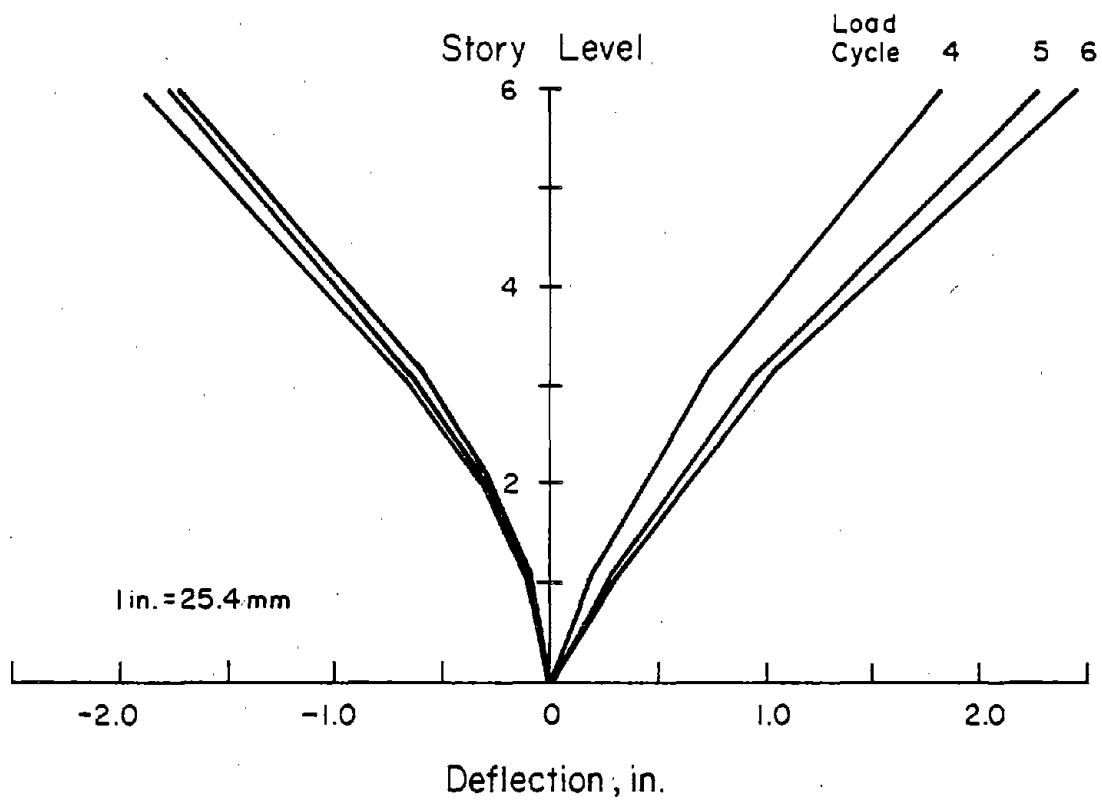
(a) Wall Element W1 of CS-1
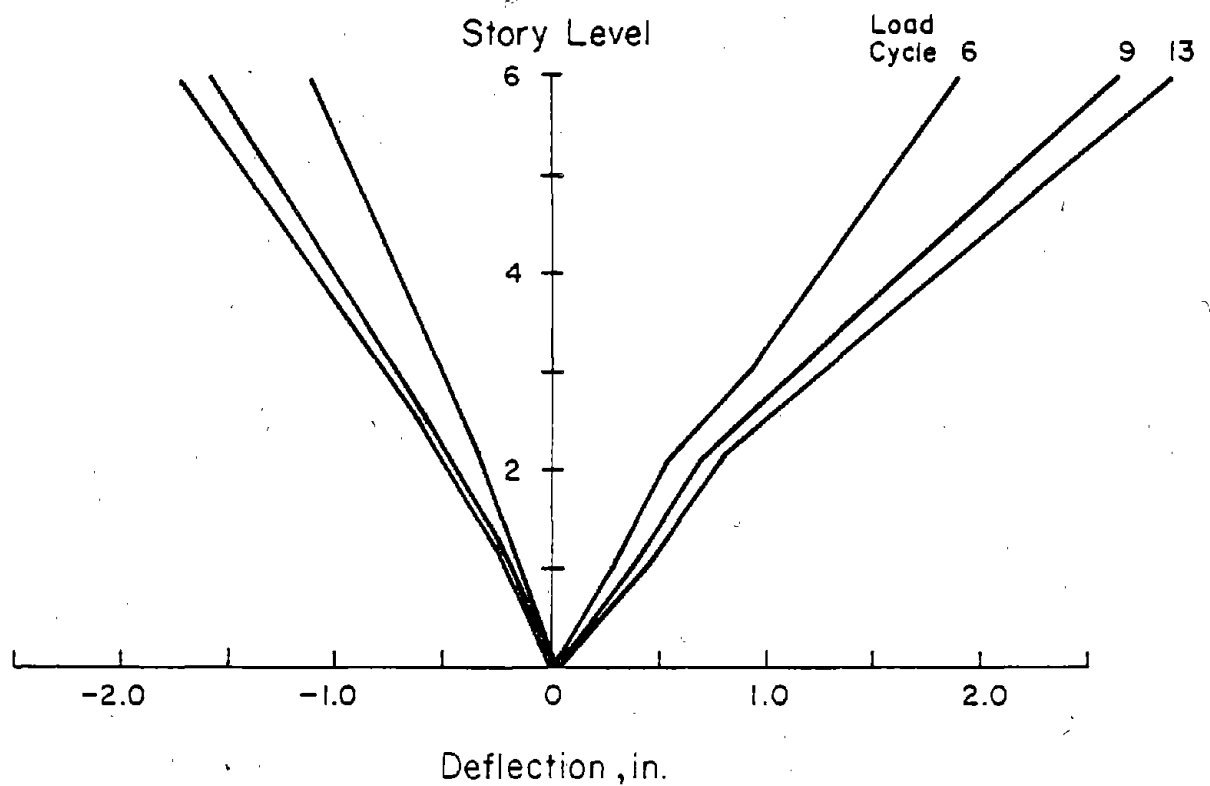
(b) Wall Element W1 of RCS-1

Fig. B-18 Lateral Deflection Profiles for CSi and RCS-1

Story Level

Load Cycle   4   5   6

1 in. = 25.4 mm

Deflection, in.

(c)   Wall Element W2 of CS-1

Story Level

Load Cycle   6   9 13
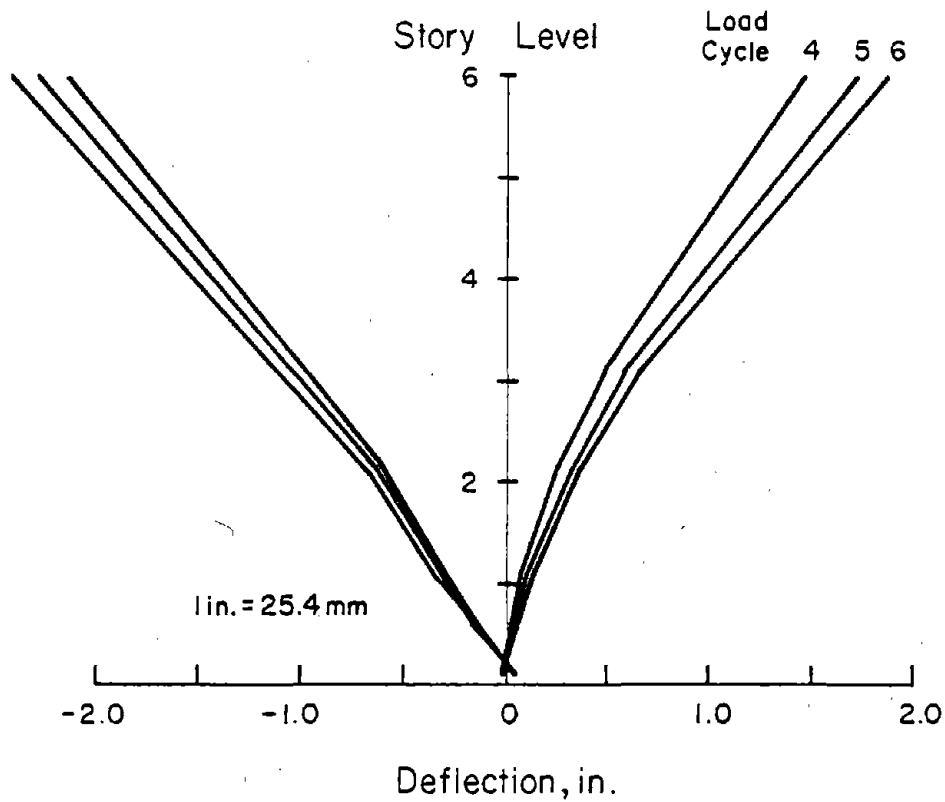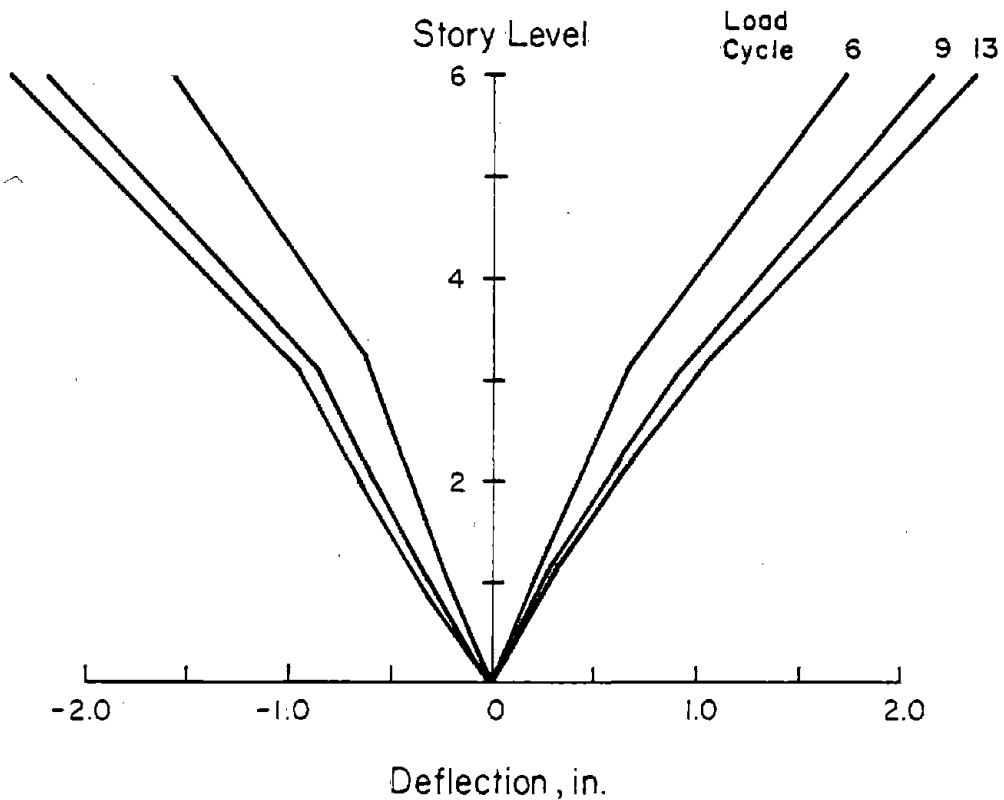
Deflection, in.

(d)   Wall Element W2 of RCS-1

Fig. B-13   Lateral Deflection Profiles for CS-1 and RCS-1 (cont.)

specimen were measured at five locations: the base, 1st floor, 2nd floor, 3rd floor, and the 6th floor. Straight lines were used to connect measured points, giving the deflection profile as shown in Fig. B-18. Curves on the positive side of the x-axis represent the deflection profile of the compression wall element while curves on the negative side of the x-axis represent deflection profiles of the tension wall.

It is apparent from Fig. B-18 that wall elements acquired different deflected shapes when subjected to either axial compression or tension. This is true for both CS-1 and RCS-1. Walls under axial compression exhibited larger displacement in the first two stories. This indicated that shear deformations were larger in the compression wall than in the tension wall. Shear was redistributed between the tension and compression walls, and this redistribution was significant.

Also noted in Fig. B-18 is that deflection profiles of the tension walls in CS-1 and RCS-1 are slightly different. The percentage of lateral displacement at 1.5 ft above the base to the top deflection for RCS-1 was slightly larger than CS-1. This, together with the observed profiles shown in Fig. B-18, indicate that deformation of the heavily coupled wall in the first two stories was larger than a lightly coupled system.

Rotations

Applied lateral load versus overall rotation of the entire wall system at the first story is given in Fig. B-19. Overall rotation was calculated assuming the wall system behaved as a single element. Though maximum rotation measured for both CS-1

1 in. = 25.4 mm
1 kip = 4.448 kN
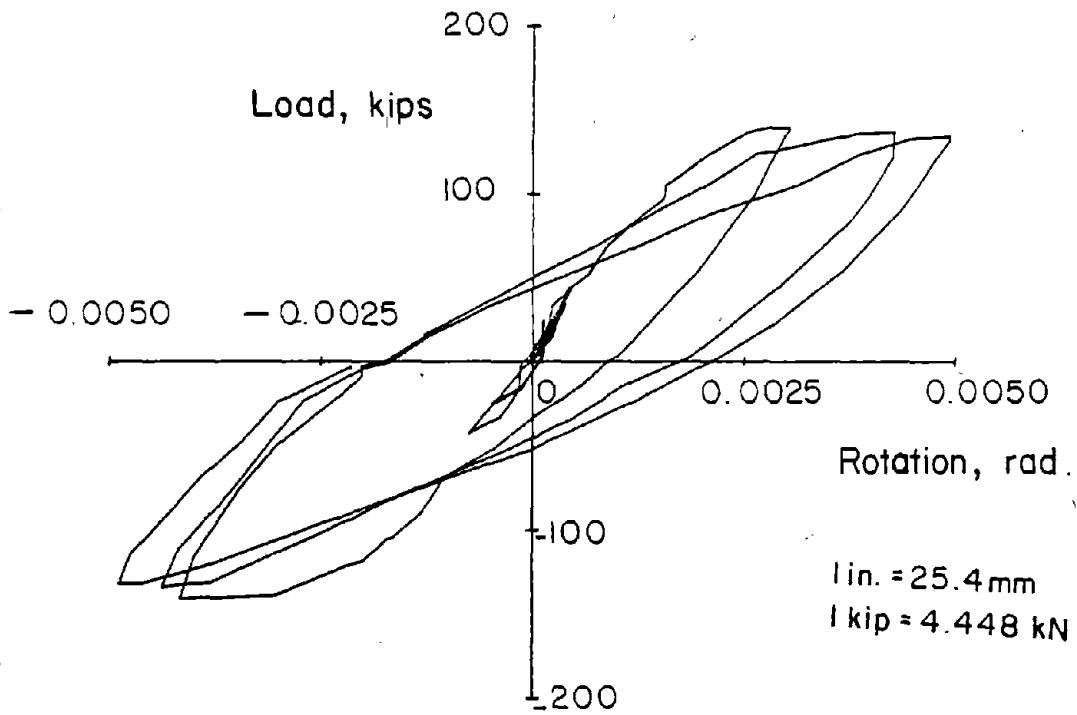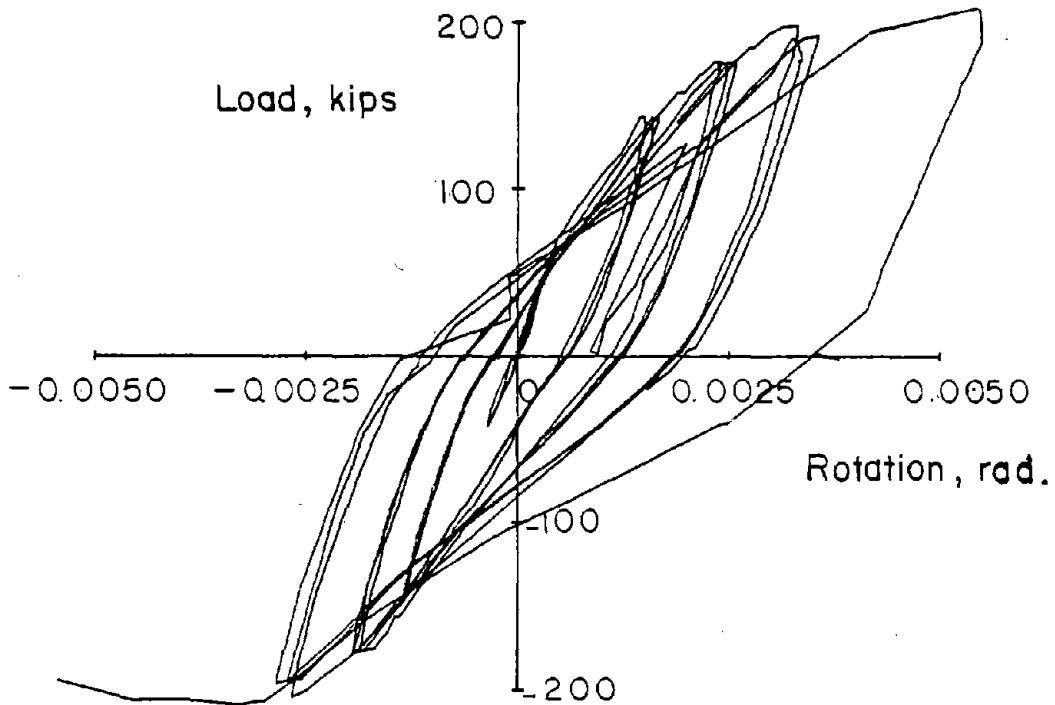
(a)   System CS-1

(b)   System RCS-1

Fig. B-19   Load versus Average First Story
Rotation of Wall System

and RCS-1 was 0.005 rad, rotational stiffnesses of the two systems were different. System RCS-1 was stiffer than system CS-1.

With the external instrumentation rotation of wall elements could be calculated at 3" (76 mm) above the base, at the first story, and at the second story. Lateral load versus rotations at the base, first story, and second story for CS-1 and RCS-1 are shown in Figs. B-20 to B-23 for each wall separately. From the figures, it is noted that the compression wall element experienced larger rotational deformation at the base than the tension wall. This can be attributed to the fact that moment was distributed from the tension wall to the compression wall through the coupling beams. It is also noted that rotation at wall base constituted a significant portion of the rotation measured at the first story level.

Rotational deformations of coupling beams at the wall-beam interface were also measured. Rotations of coupling beams at the second, fourth and sixth story for CS-1 and RCS-1 are shown in Figs. B-24 and B-25. Rotational hysteresis loops for the second story coupling beam of CS-1 were quite different from the rest. As the specimen became a "linkage system", plastic hinges formed at the end of coupling beams resulted in permanent deformations. These permanent deformations cause a shift of the rotational hysteresis loops to the right of the y-axis.

From Fig. B-24 and B-25, it was observed that measured coupling beam rotations in CS-1 were more than twice those in RCS-1. This indicated that, for a lightly coupled wall system, the coupling beams underwent larger deformations. Therefore,
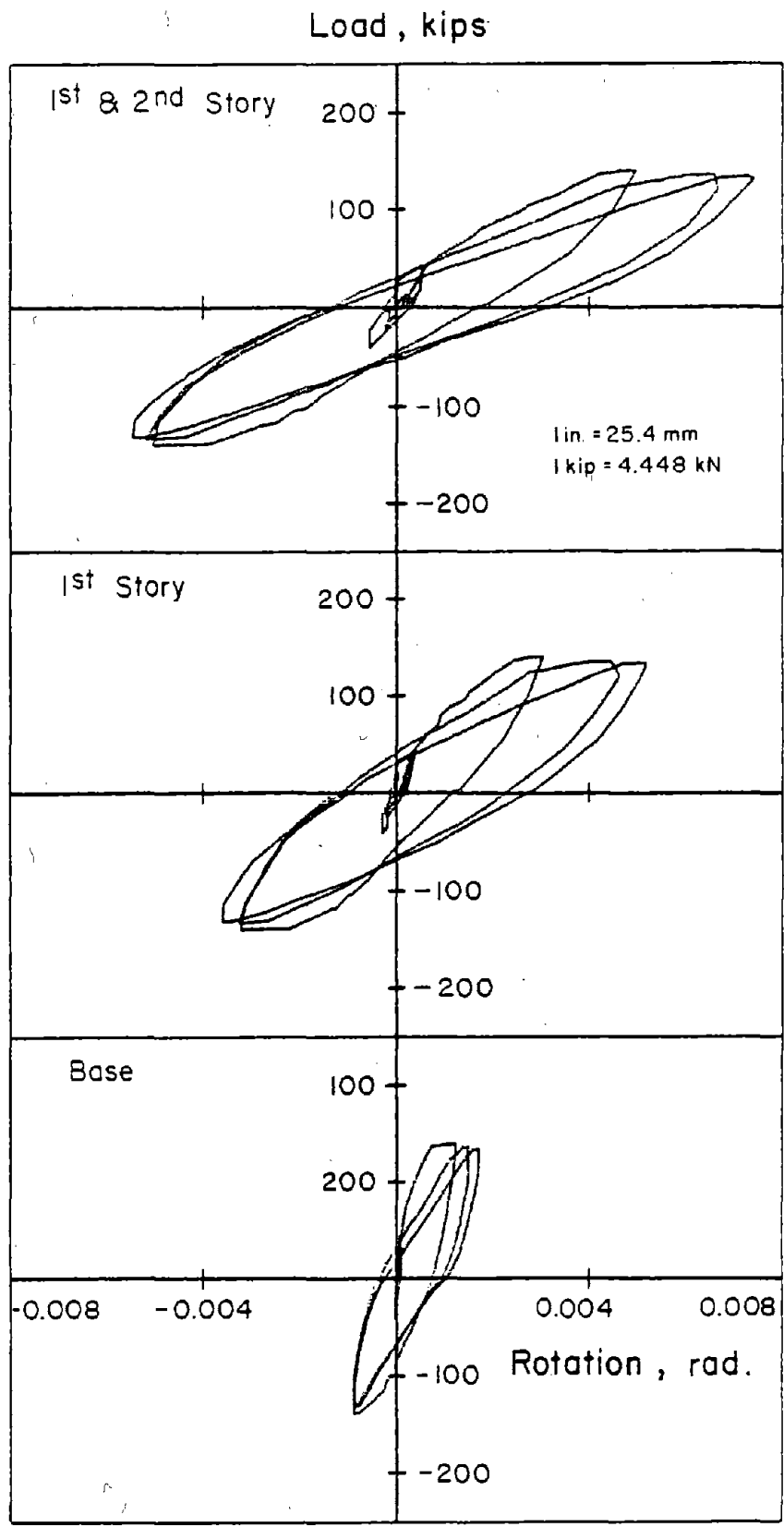
Fig. B-20   Load versus Rotation Relationships
for Wall Element W1 of CS-1
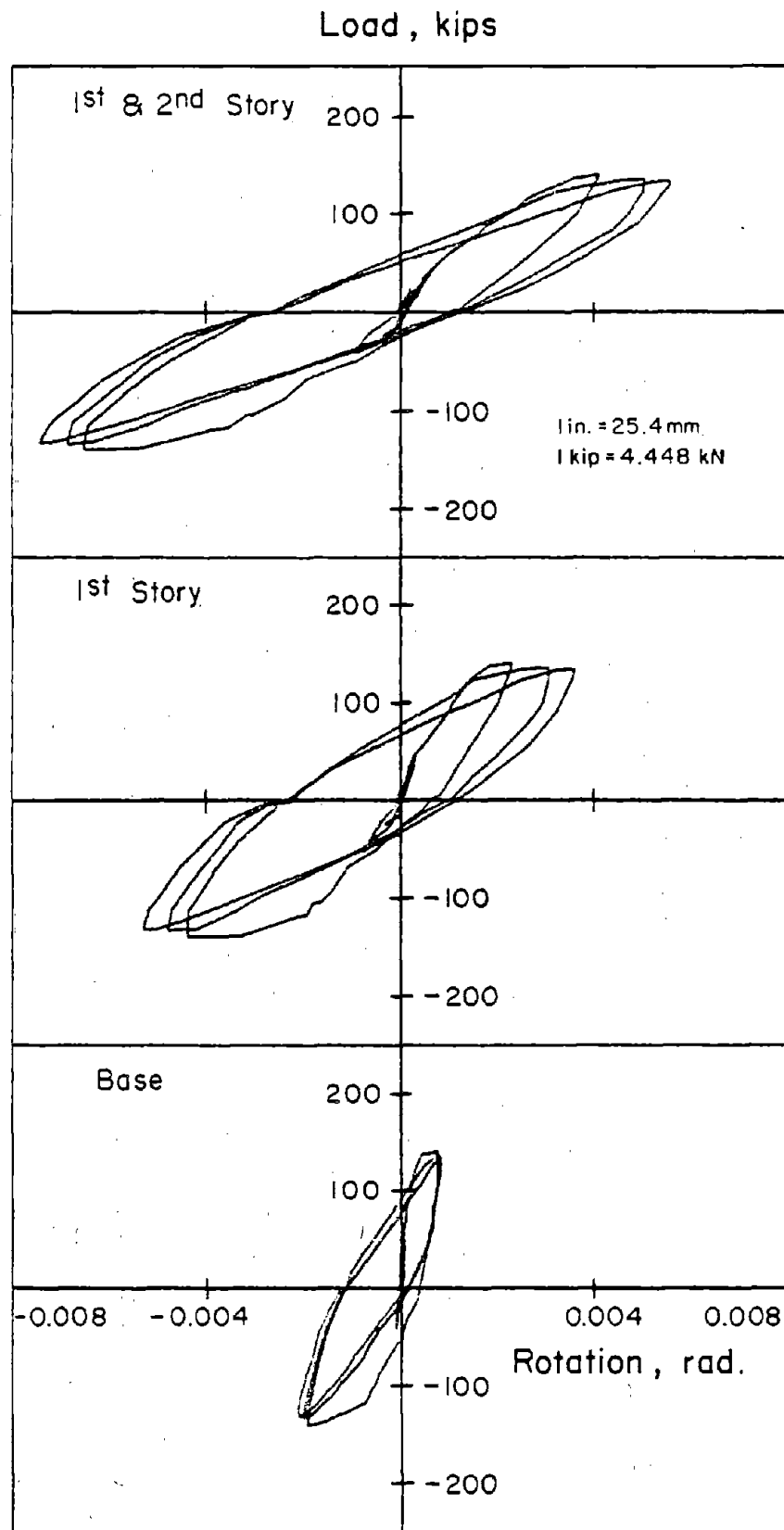
Fig. B-21   Load versus Rotation Relationships
for Wall Element W2 of CS-1

Load , kips
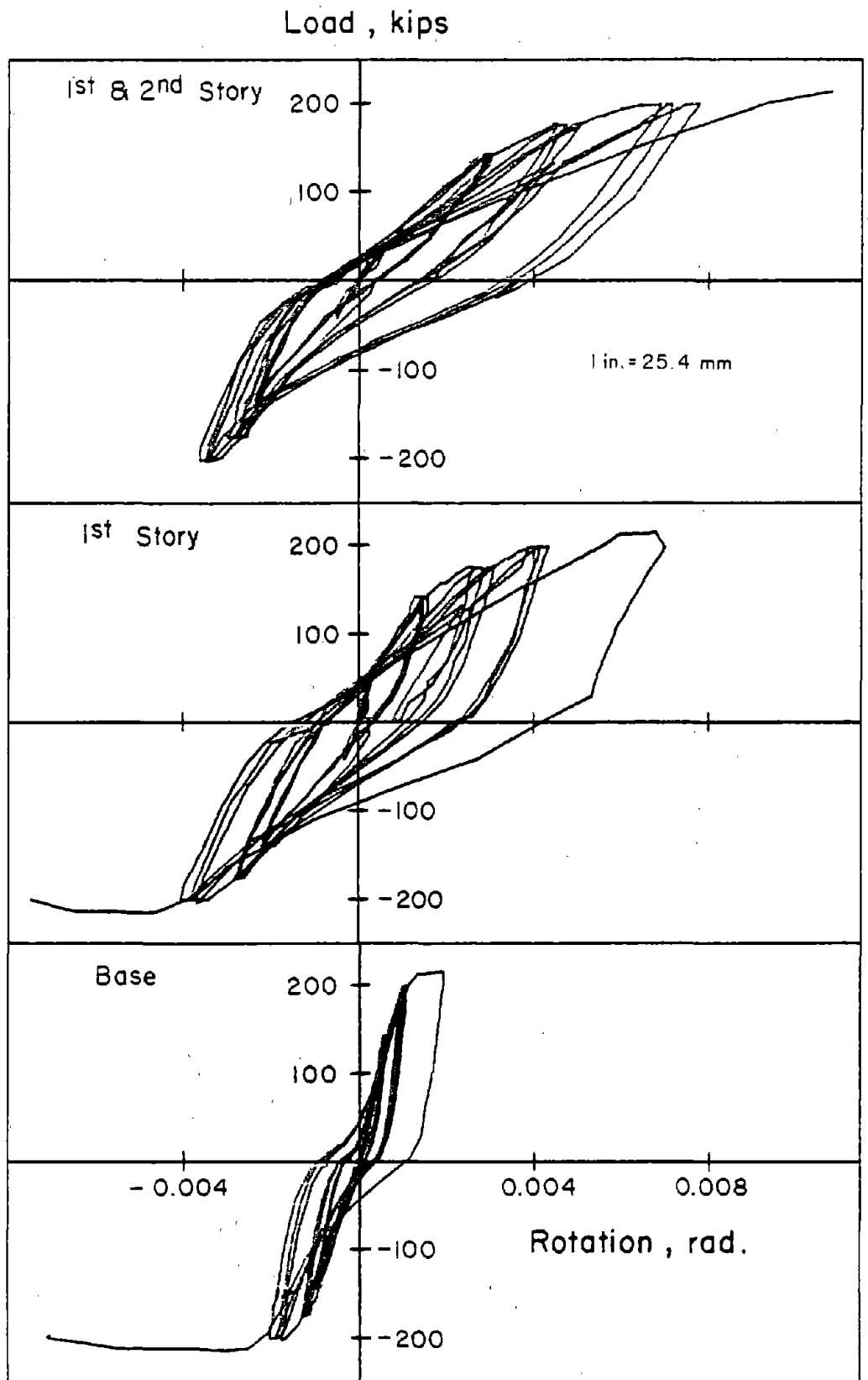
Fig. B-22   Load versus Rotation Relationships
for Wall Element W1 of RCS-1
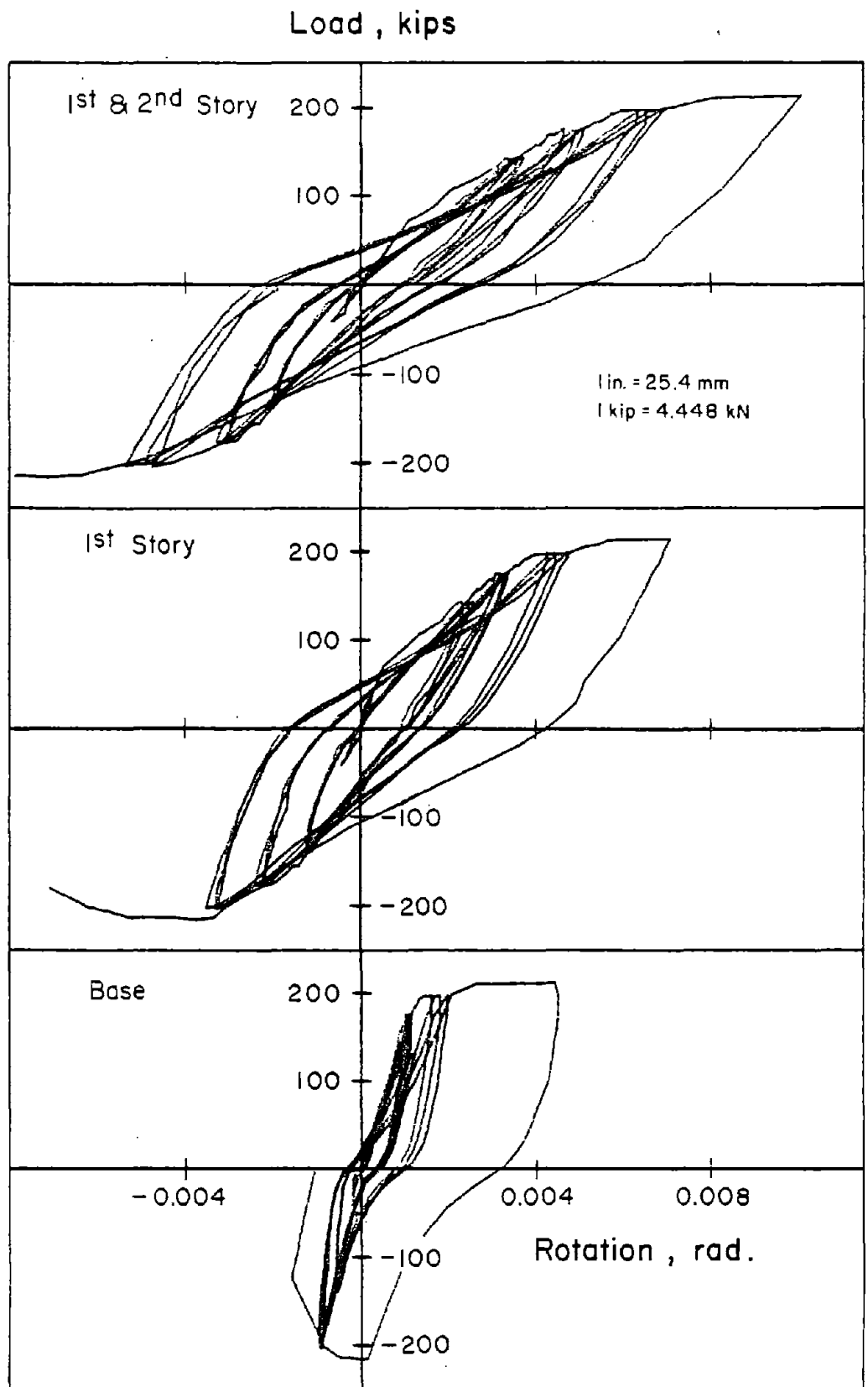
Fig. B-23   Load versus Rotation Relationships
for Wall Element W2 of RCS-1
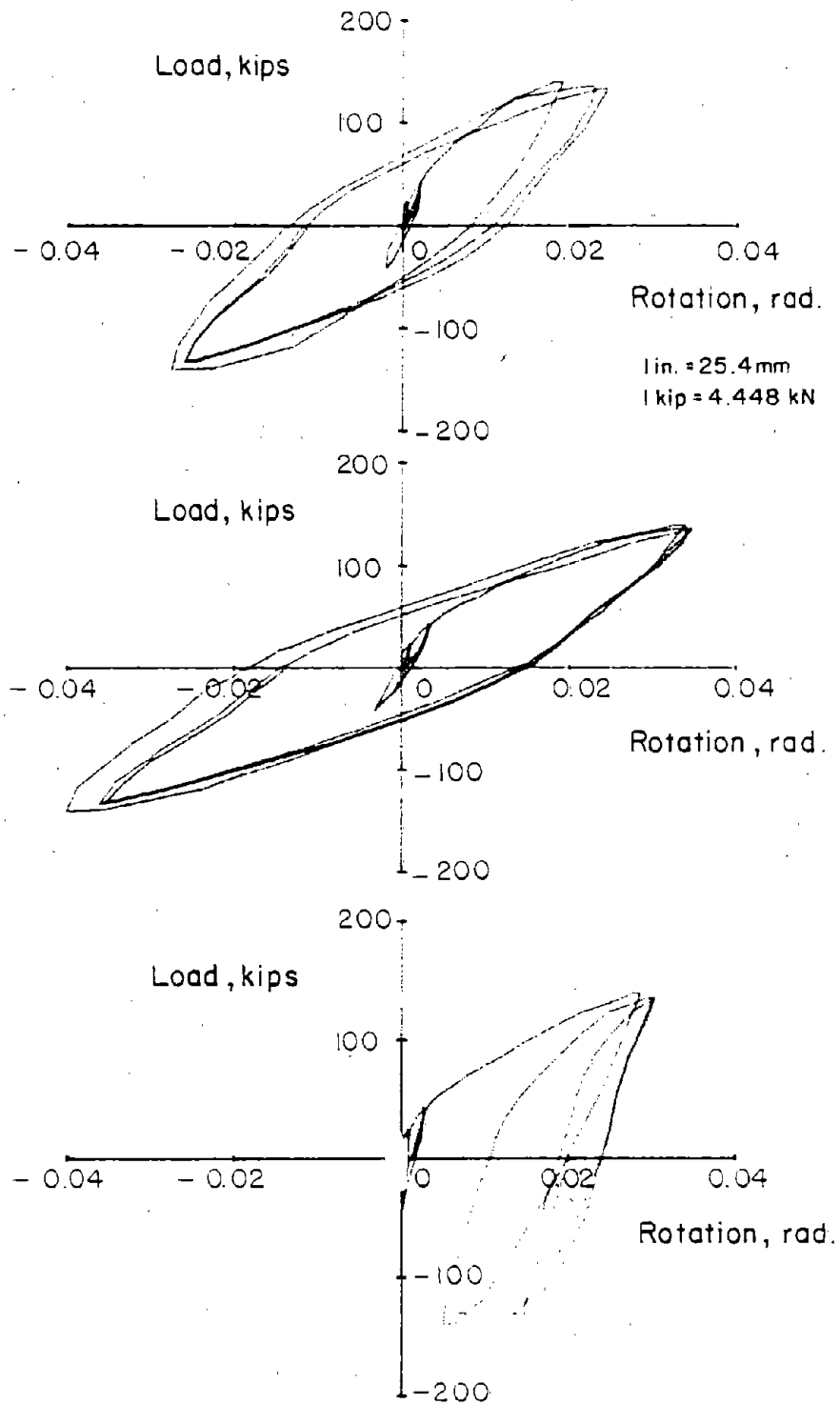
Fig. B24   Load Versus Rotation Relatiohships
Coupling Beams of System CS-1
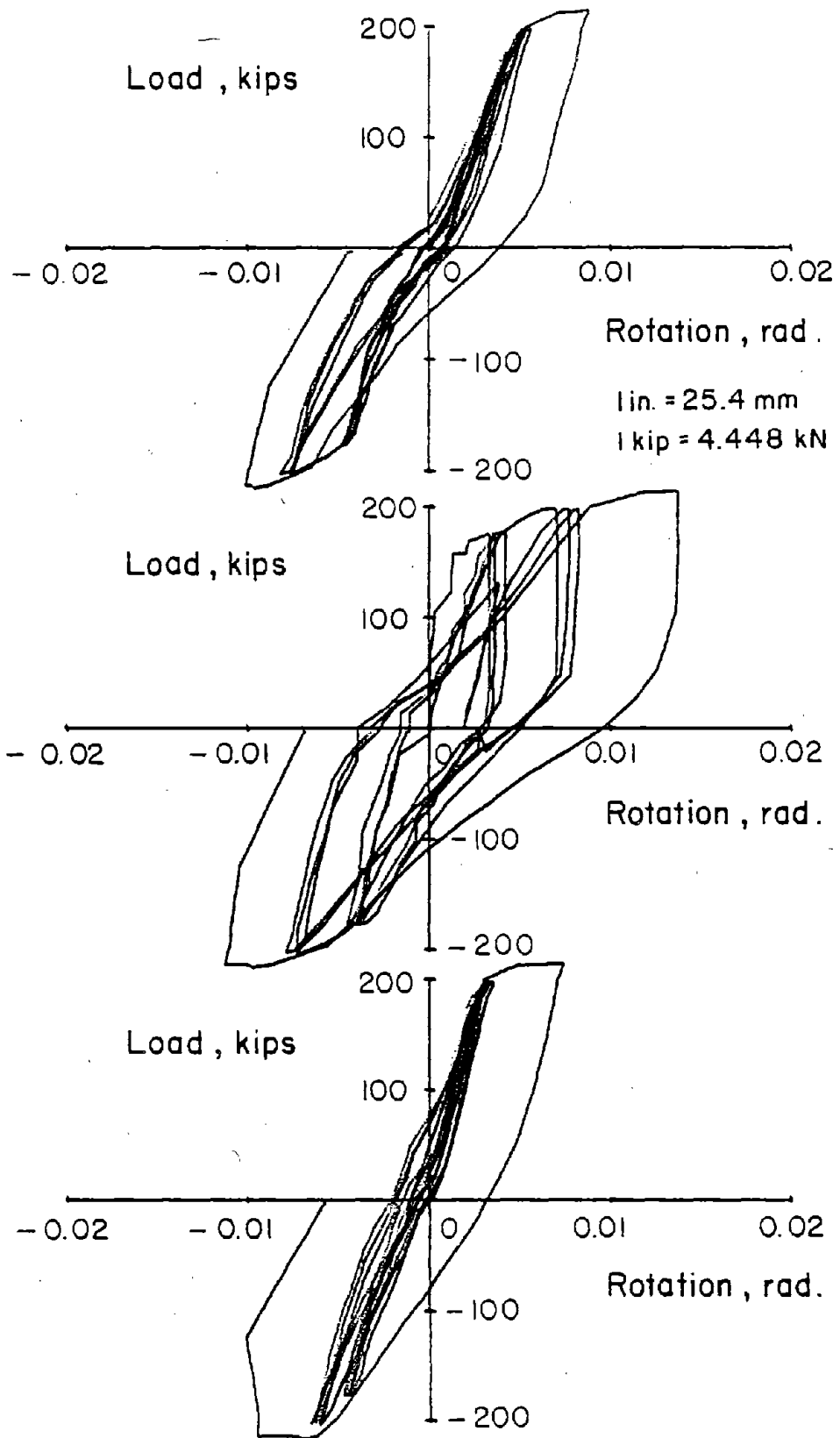
Fig. B25   Load Versus Relatiohships
Coupling Beams of System RCS-1

for lightly coupled systems, available deformation capacity of coupling beams is one of the primary design parameters. Also, coupling beams at the fourth story experienced greater deformations than other instrumented beams.

Shear Distortions

Shear distortions were measured at the first and second story of each wall element. Applied load versus shear distortions at the first and second story for CS-1 and RCS-1 are shown in Figs. B-26 to B-29. Both specimens exhibited steady degradation of the shear resisting mechanism. Shear distortions measured at the same location increased with repeated applied loads. In addition, pinching was observed in the hysteresis loops for both tests as shown in Figs. B-26 and B-29. The pinching phenomenon was especially pronounced in the test of RCS-1. Severe pinching in the load versus shear distortion hysteresis loops indicated that, as loading was reversed, initial shear resistance of the walls was quite low. This agreed with the observation that as loads were reversed, sliding occurred along horizontal wall cracks. As additional load was applied, the sliding shear resistance mechanism changed to a diagonal-strut mechanism. Also, walls under compression were found to experience larger shear distortions than wall under tension. This can be explained by the fact that shear was redistributed between the two walls through coupling beams.

Applied load versus shear distortions of coupling beams for CS-1 and RCS-1 are shown in Fig. B-30 and B-31. The maximum shear distortions of the second story coupling beam measured in
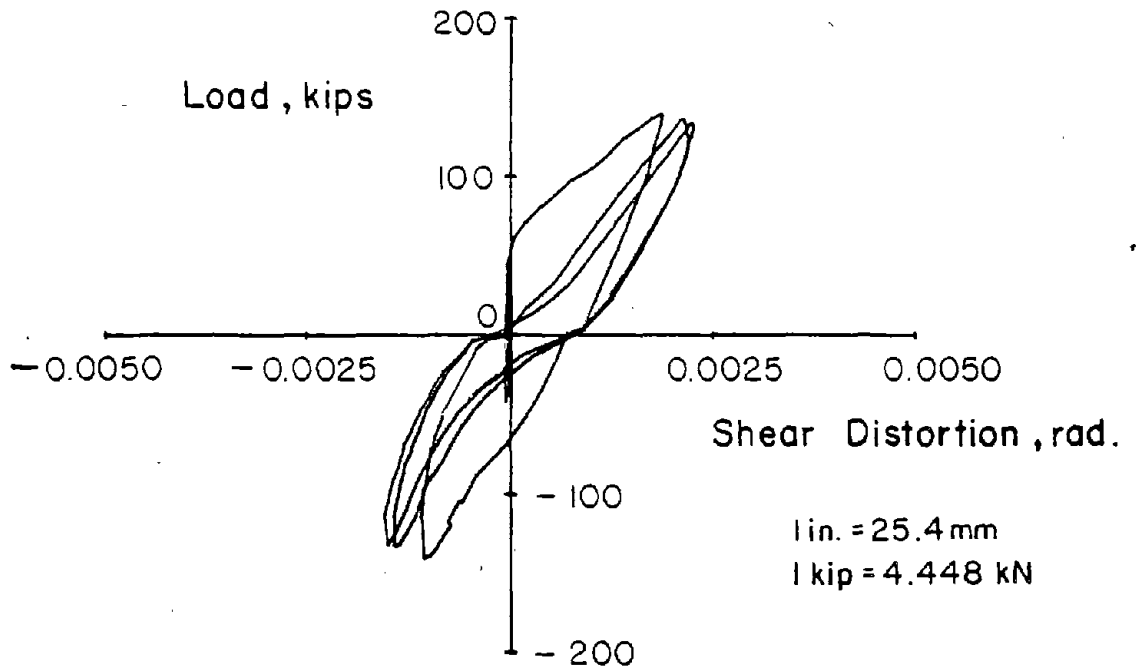
(a) At Second Story Level
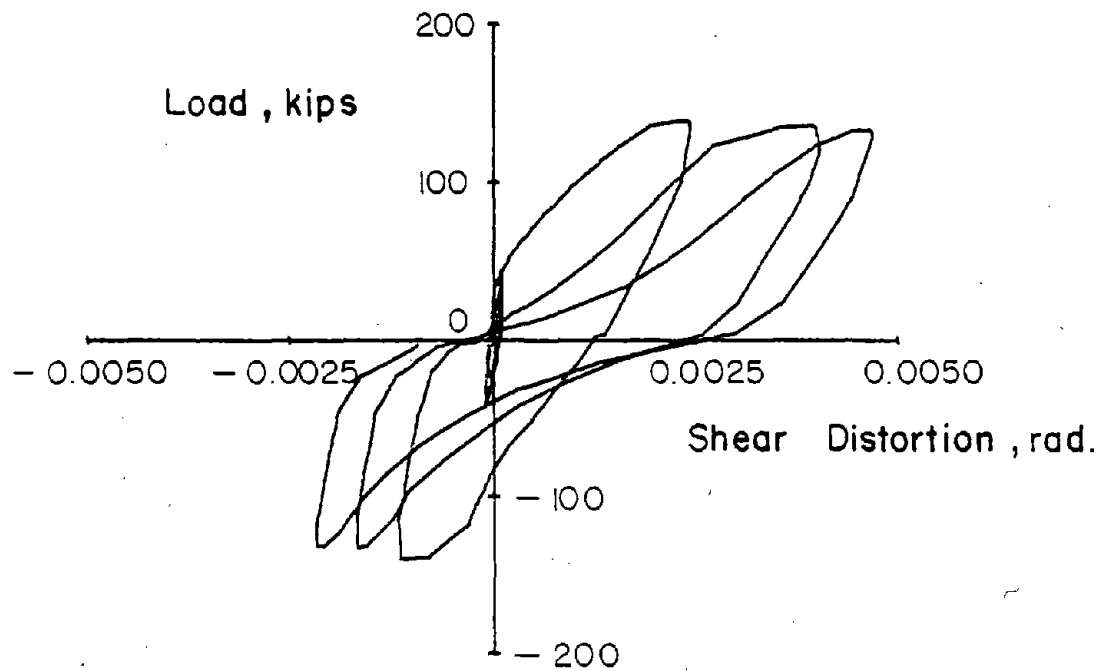
(b) At First Story Level

Fig. B-26   Load versus Shear Distortion Relationships
for Wall Element Wl of CS-1

200

Load , kips

100

−0.0050   −0.0025   0.0025   0.0050

Shear Distortion, rad.

−100

1 in. = 25.4 mm
1 kip = 4.448 kN

−200

(a)   At Second Story Level

200

Load , kips

100

−0.0050   −0.0025   0.0025   0.0050

Shear Distortion, rad.

−100

−200
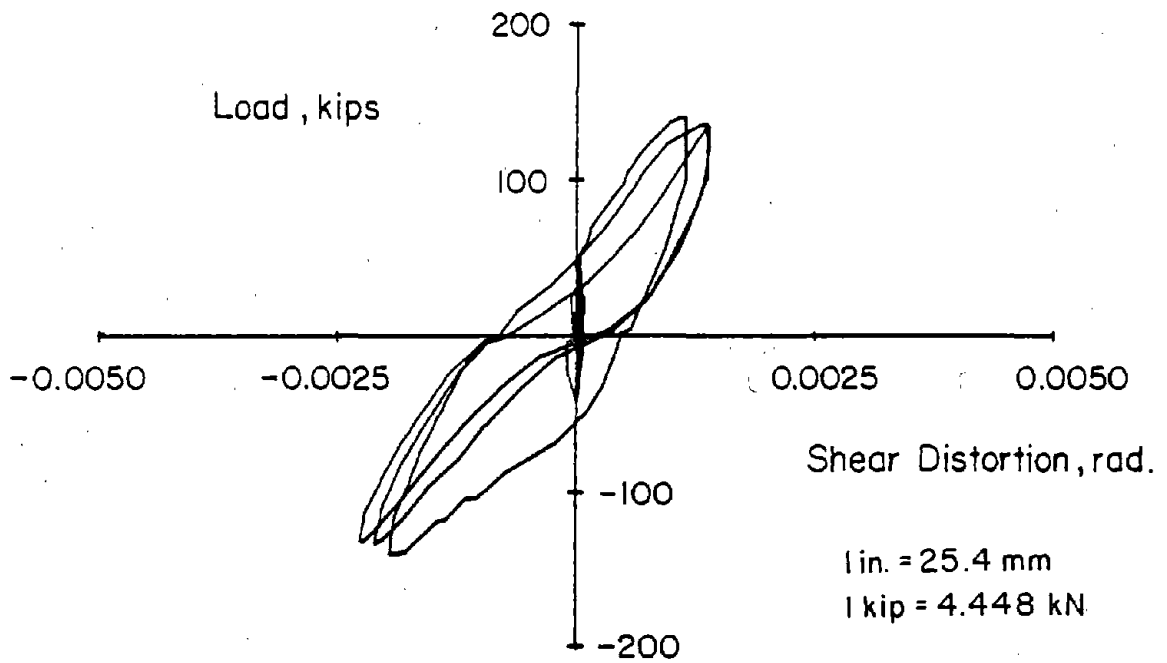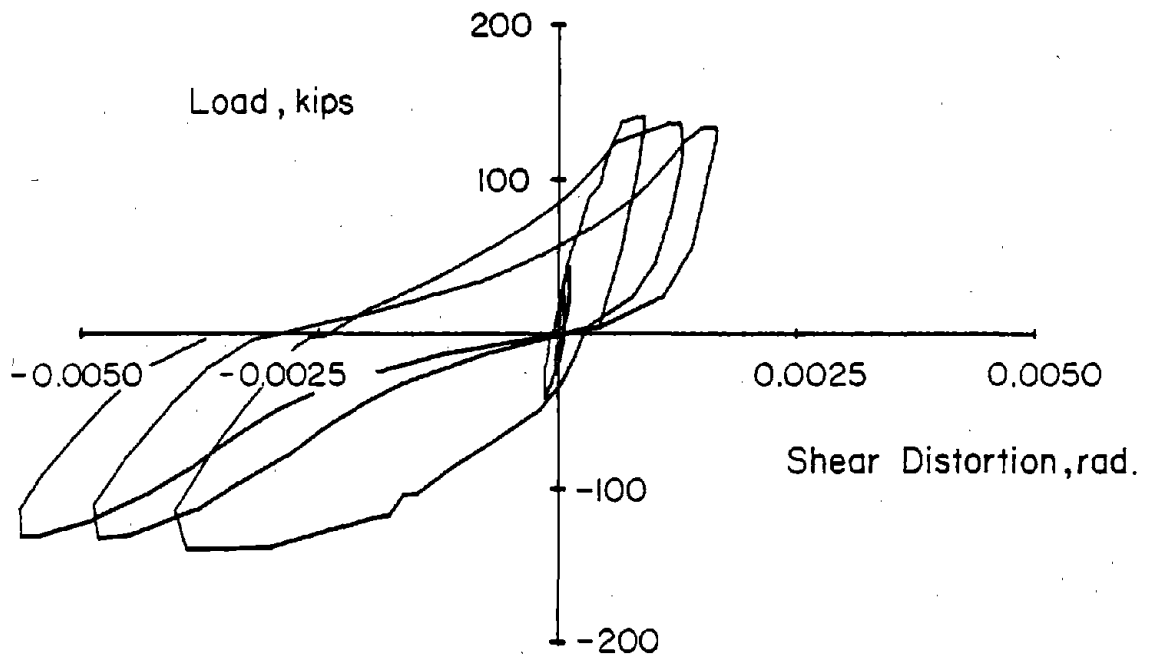
(b)   At First Story Level

Fig. B-27   Load versus Shear Distortion Relationship
for Wall Element W2 of CS-1
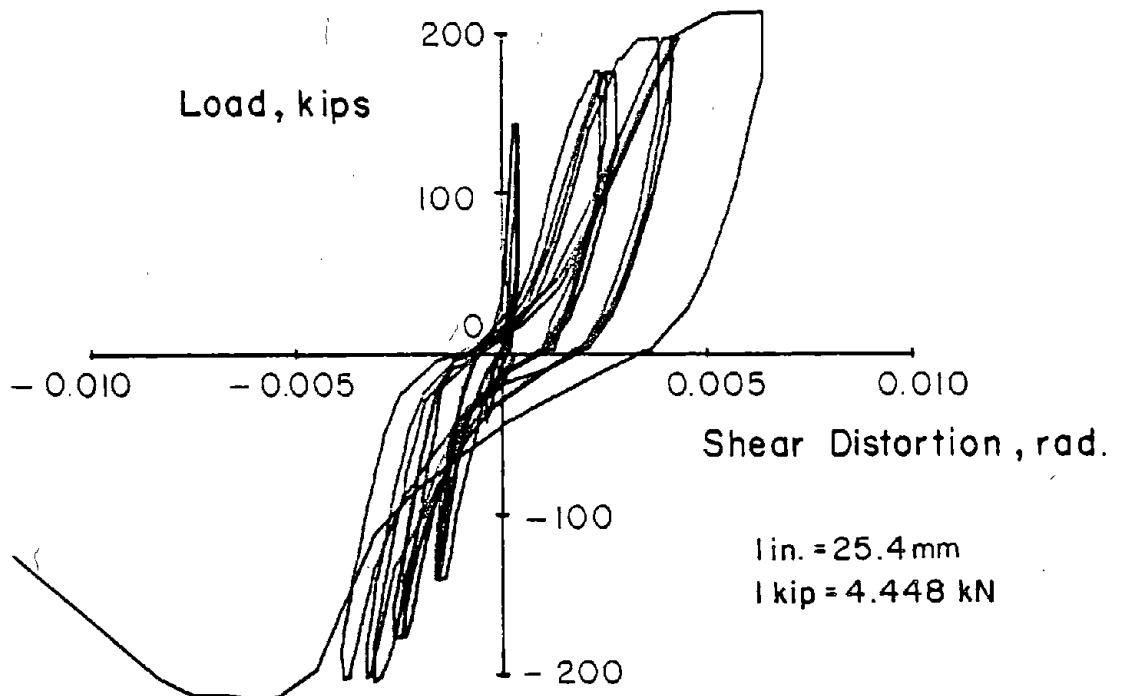
(a) At Second Story Level
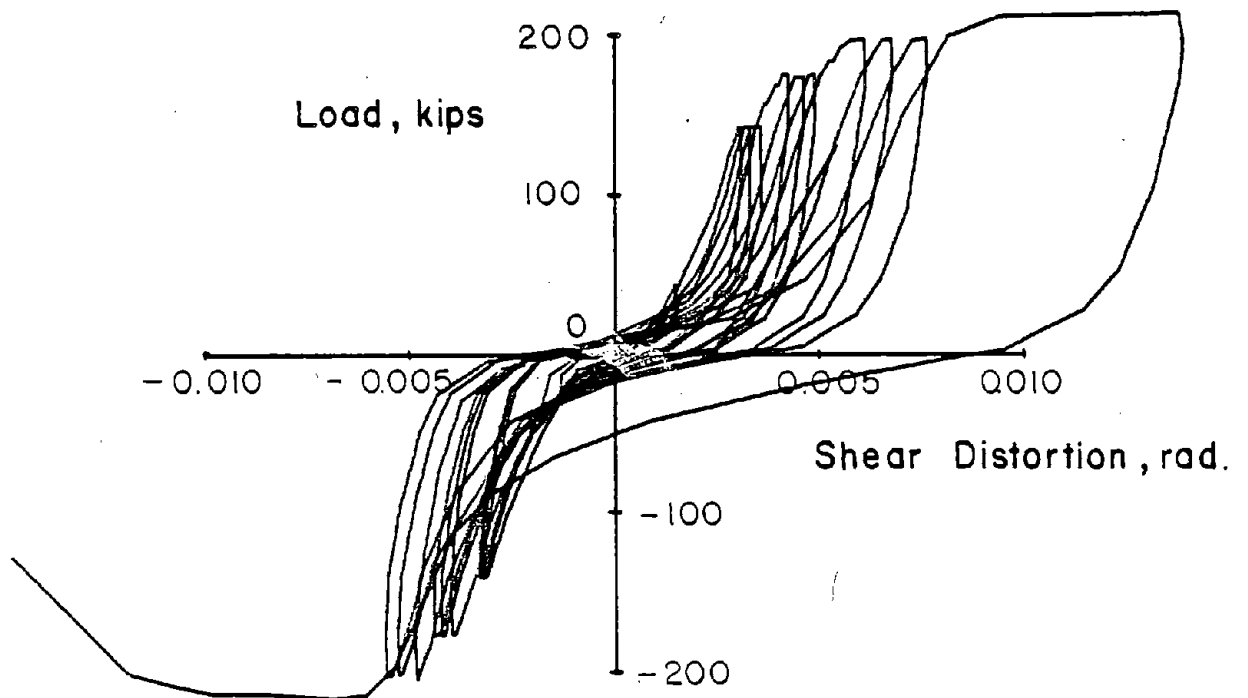
(b) At First Story Level

Fig. B-28 Load versus Shear Distortion Relationship
for Wall Element W1 of RCS-1
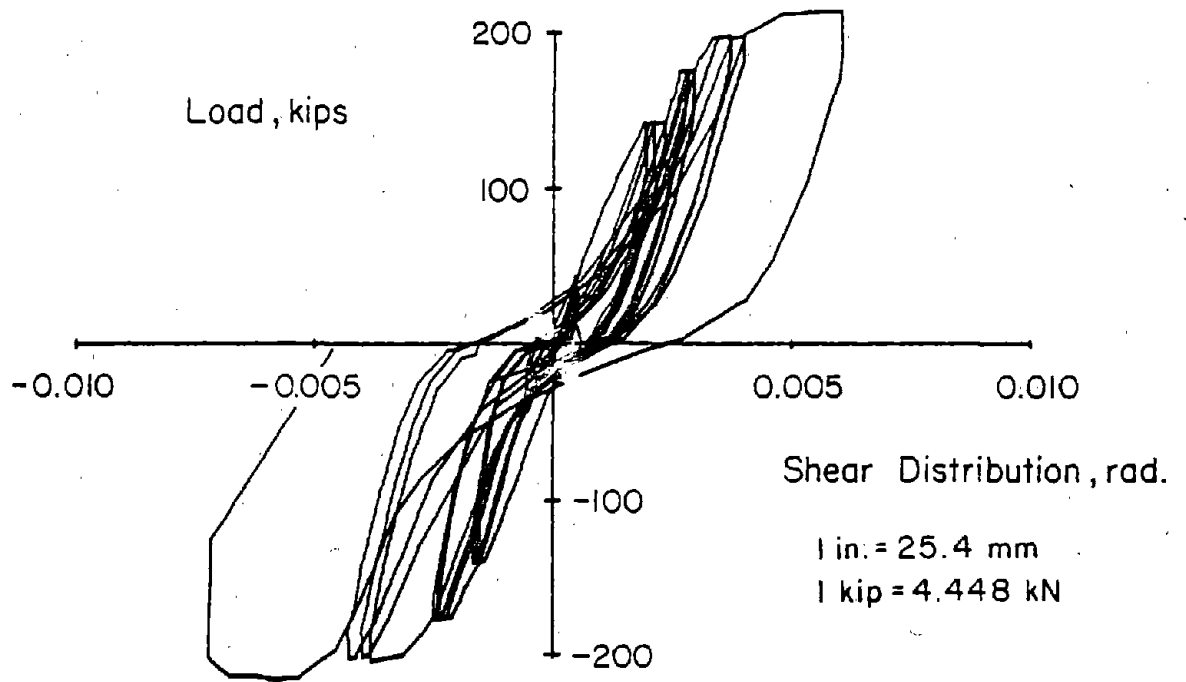
(a) At Second Story Level
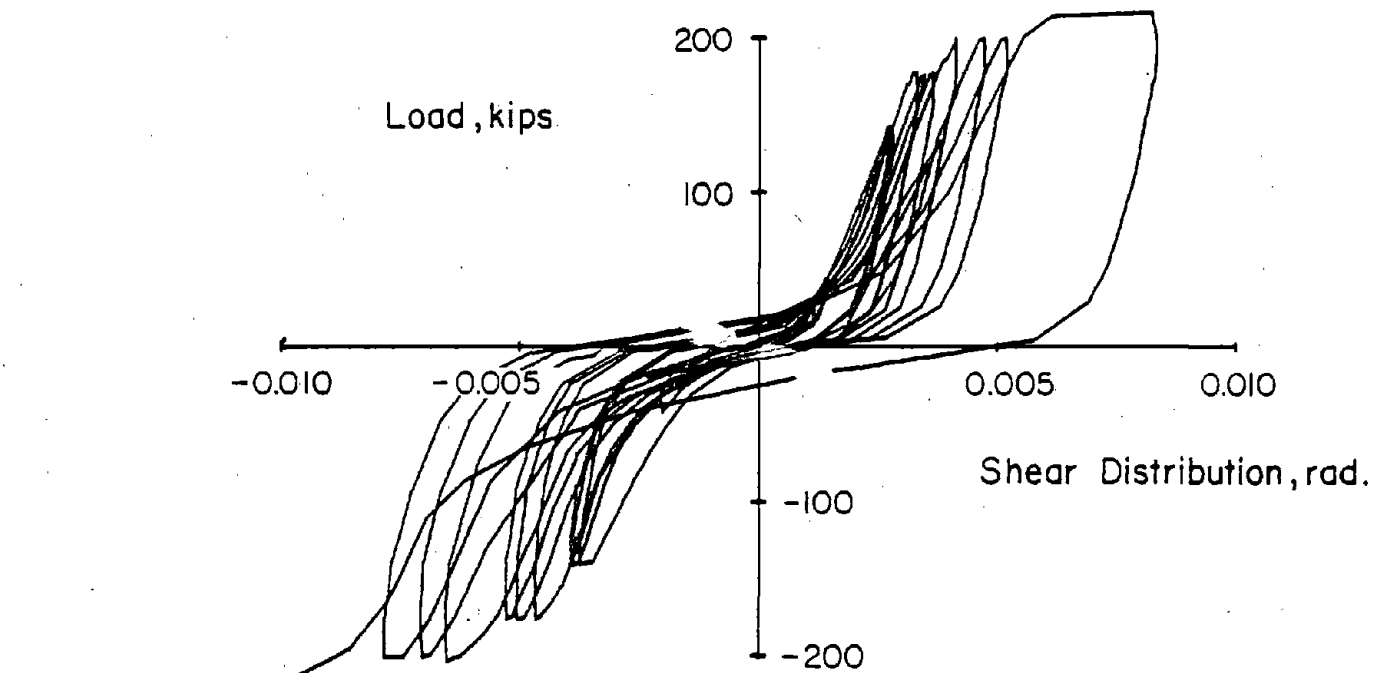
(b) At First Story Level

Fig. B-29 Load versus Shear Distortion Relationship
for Wall Element W2 of RCS-1

200

Load, kips

100

−0.40   −0.20   0.20   0.40

0   Shear Distortion, rad.

100

(a)   At Sixth Story Level

200

1 in. = 25.4 mm
1 kip = 4.448 kN

200

Load, kips

100

−0.40   −0.20   0.20   0.40

0   Shear Distortion, rad.

−100

(b)   At Fourth Story Level

−200

200

Load, kips

100

−0.40   −0.20   0.20   0.40

0   Shear Distortion, rad.

−100

(c)   At Second Story Level

−200
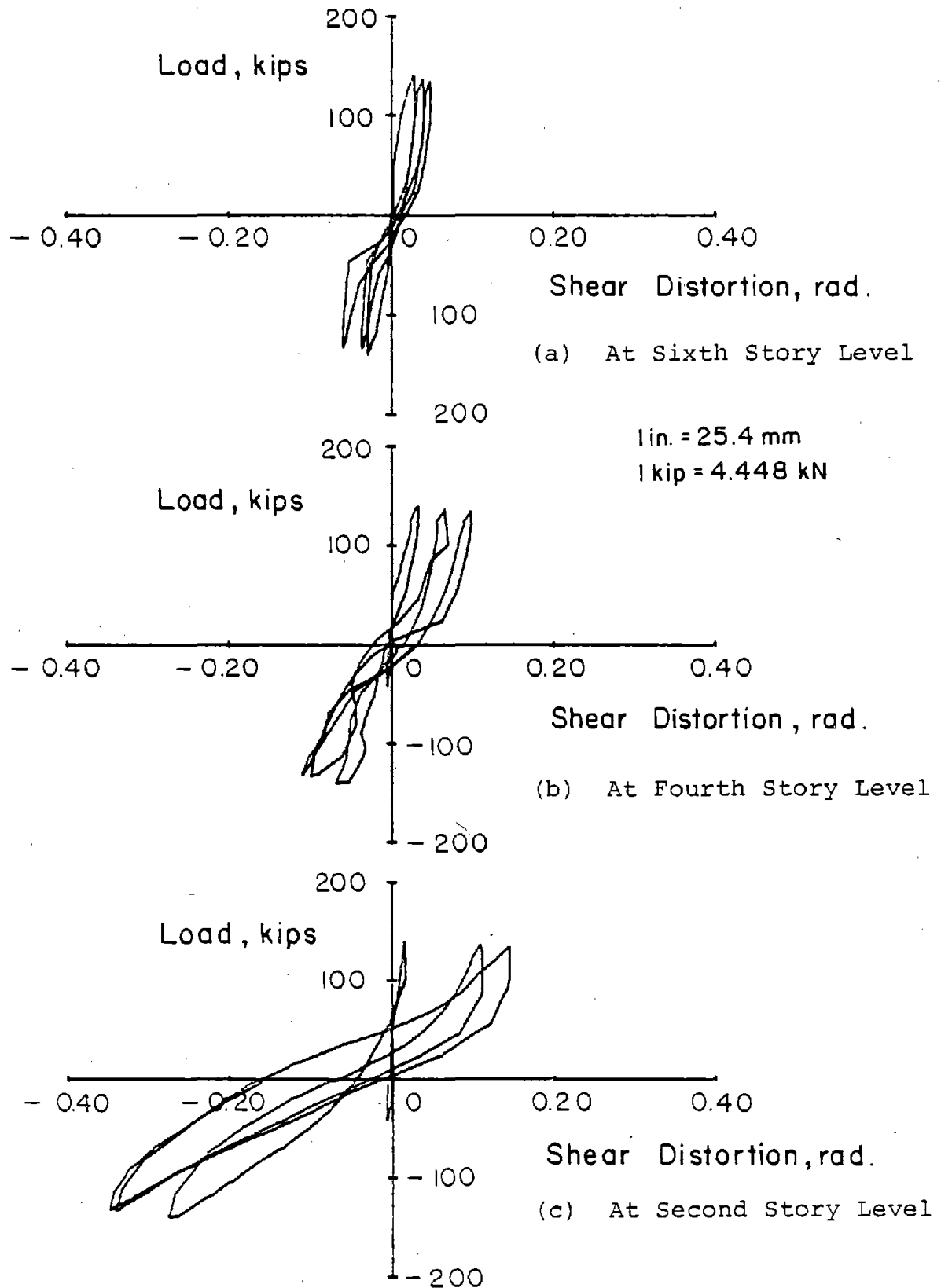
Fig. B-30   Load versus Shear Distortion Relationship
for Coupling Beams of CS-1
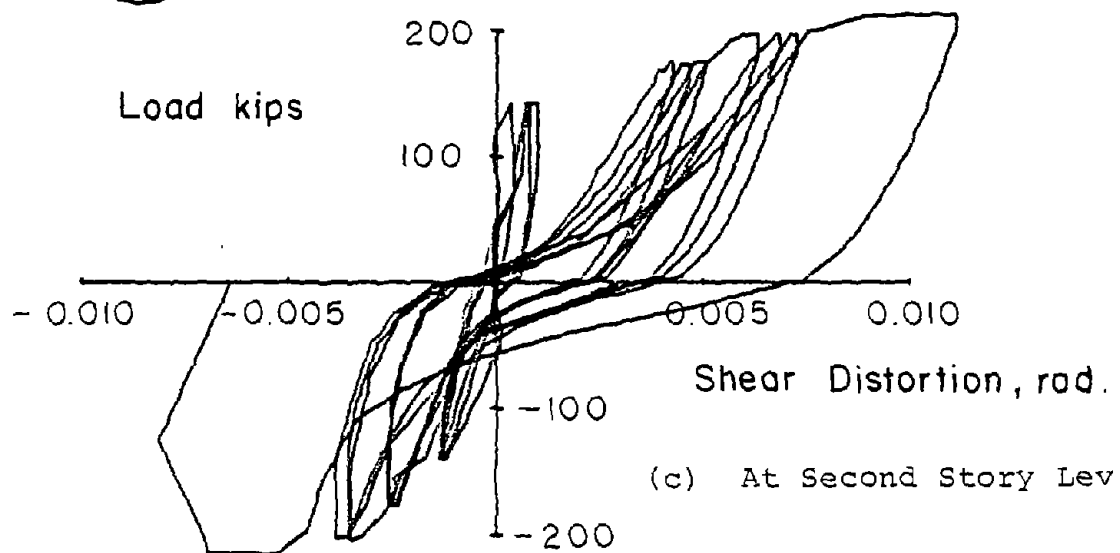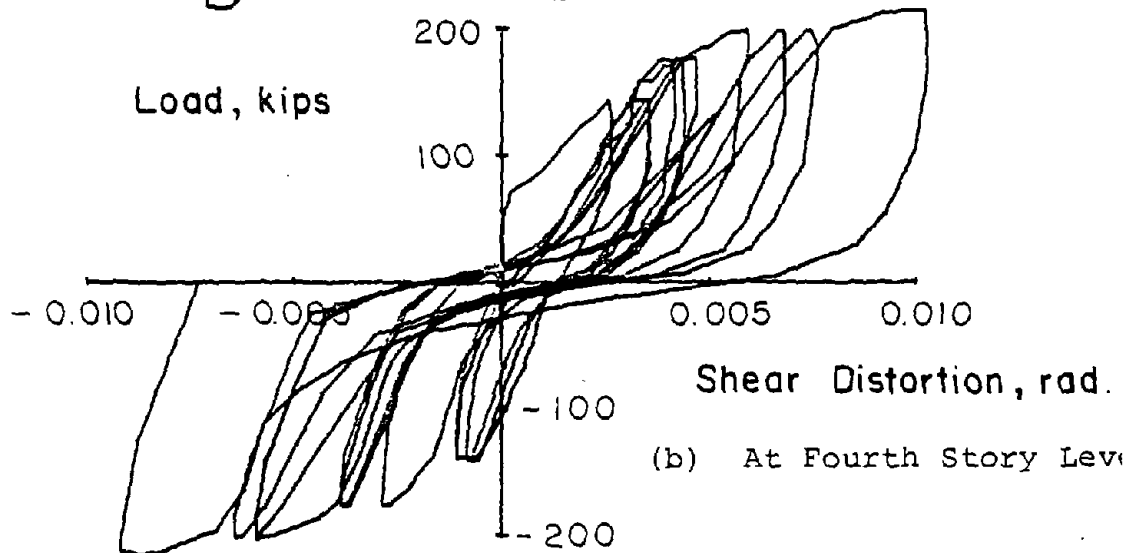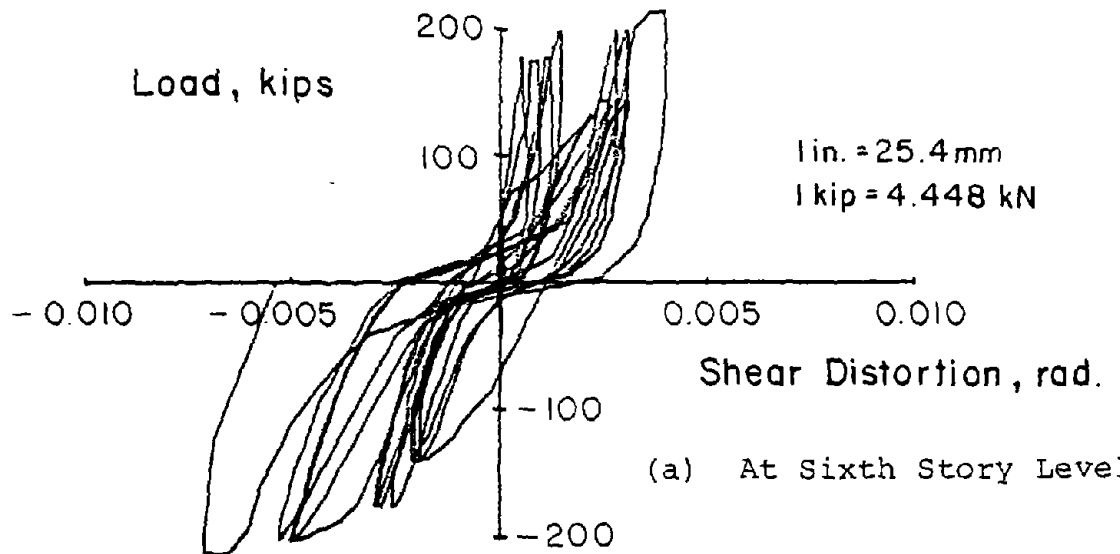
Fig. B-31   Load versus Shear Distortion Relationship
for Coupling Beams of RCS-1

CS-1 was 0.4 rad. The large shear deformation can be explained as follows. In the test of CS-1, a separation between walls resulted from elongation of the coupling beams. This reduced the coupling beam's shear resistance and resulted in larger shear distortions in the beams.

A maximum shear distortion of 0.06 rad was recorded for RCS-1. It was noted that the second and fourth story coupling beams showed larger shear deformations that those in the sixth floor beam. Significant pinching was observed in the hysteresis loops.

Strain Measurements

Strains measured on vertical wall reinforcement in the boundary element at 1.5 ft (457 mm) and 3 ft (914 mm) above the base of wall system CS-1 are shown in Figs. B-32 and B-33. It was noted that strains in both wall elements at a given location were similar. This indicated that the two walls were behaving as isolated walls in parallel with no coupling.

Strains in reinforcement at similar locations for RCS-1 is shown in Figs. B-34 and B-35. Strain hysteresis of reinforcement next to the coupling beams were smaller than those in outside boundary elements. This effect is attributed to the fact that coupling beams were effective in joining the walls together. Shear and moment were transmitted through coupling beams to wall elements. The additional induced shear and moment changed the behavior of the walls. This was reflected by the strains in boundary element reinforcement.

1 in. = 25.4 mm
1 kip = 4.448 kN
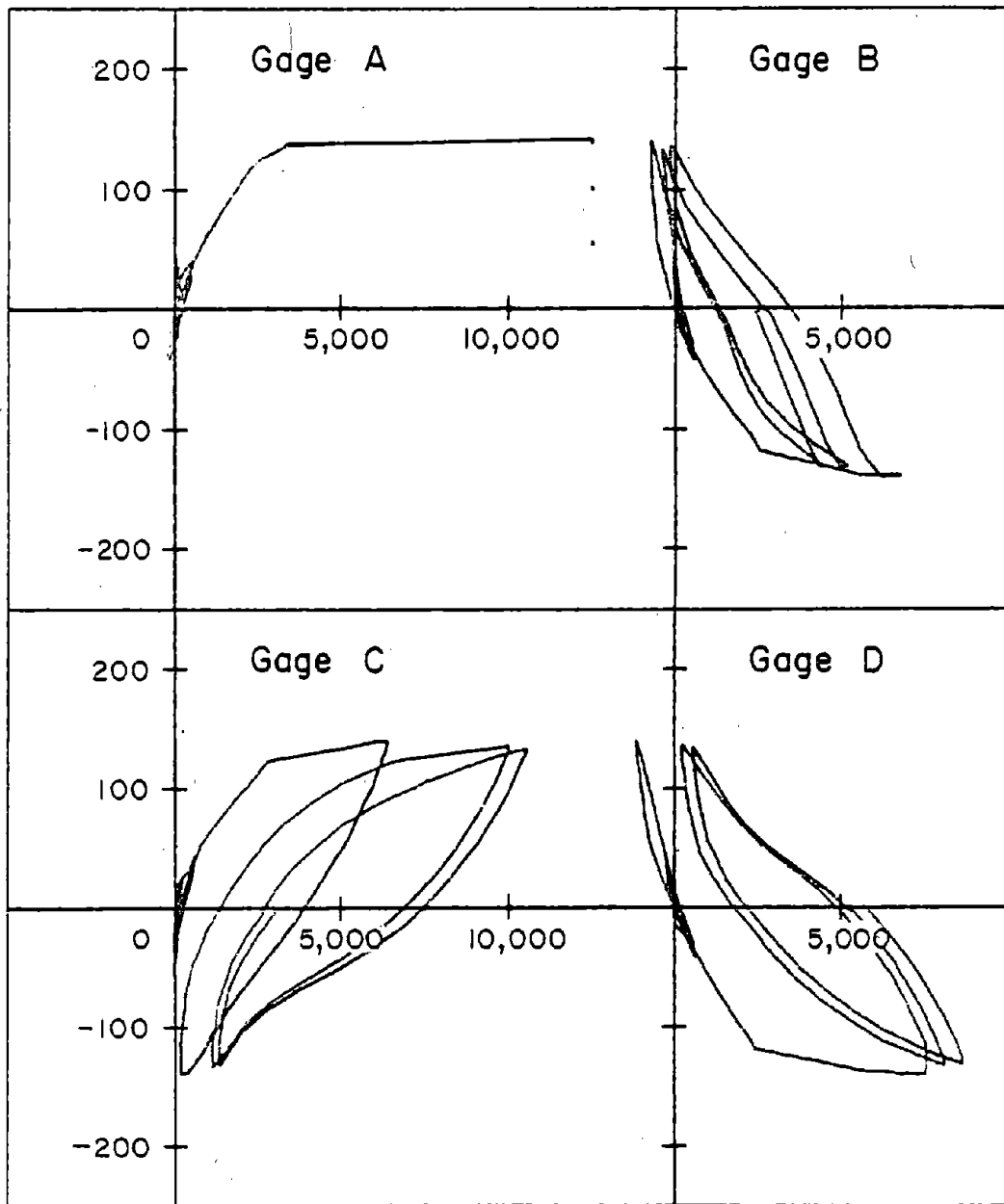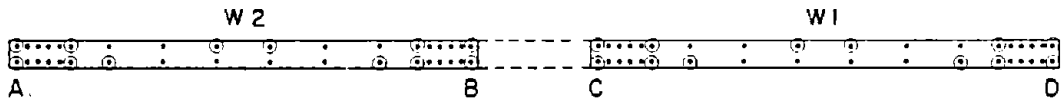
Load , kips

Strain , millionths

Fig. B-32   Load versus Vertical Steel Strains at
1.5 ft above Base for CS-1

Fig. B-33   Load versus Vertical Steel Strains at
3 ft above Base for CS-1

Fig. B-34 Load versus Vertical Steel Strains at
1.5 ft above Base for RCS-1
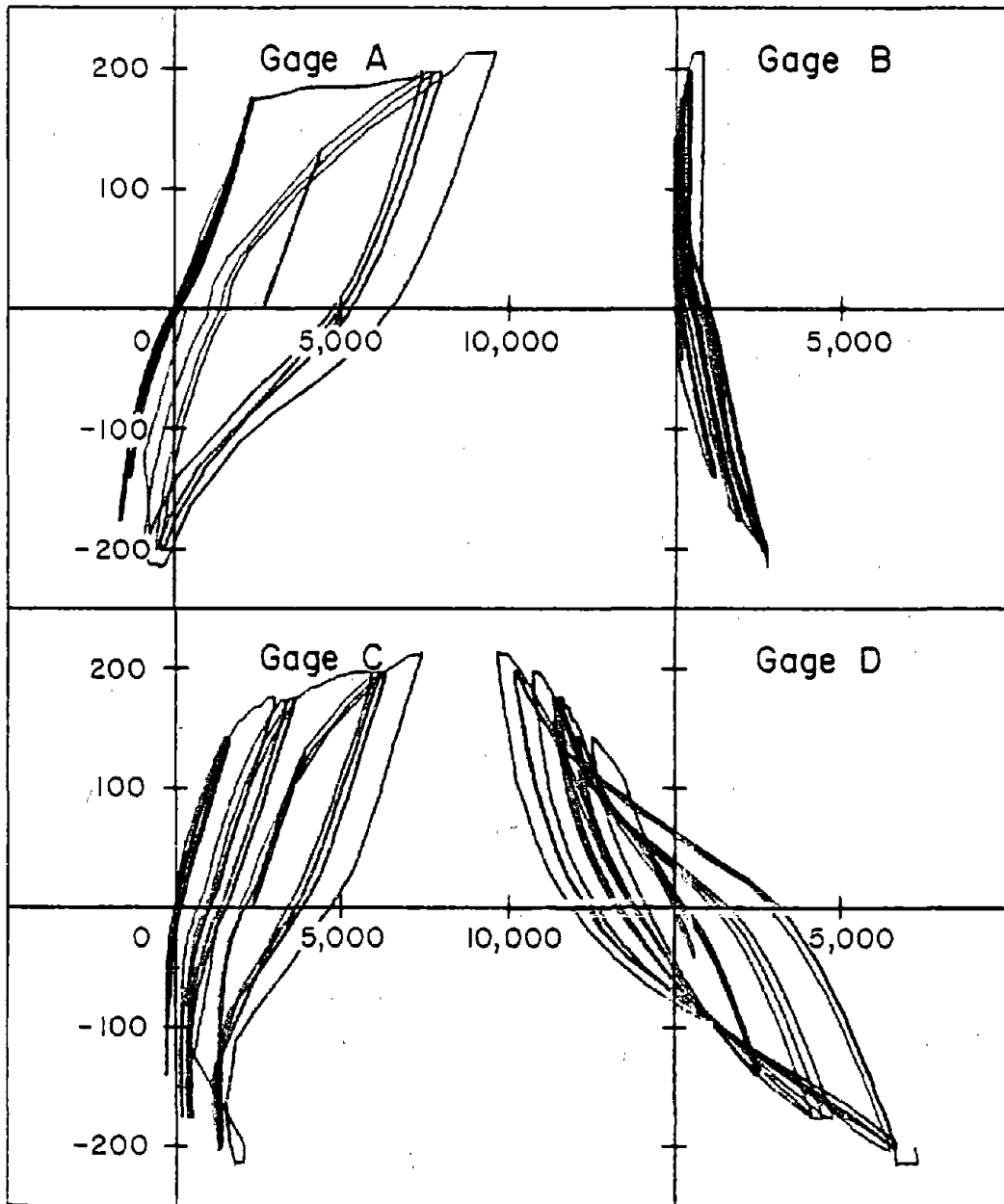
Fig. B-35   Load versus Vertical Steel Strains at
3 ft above Base for RCS-1

Applied load versus strains in flexural reinforcement of coupling beams is shown in Figs. B-36 and B-37. Comparisons of measured strains in both tests were made at every story level. It was found that beams in CS-1 yielded half way through the fourth cycle. However, measured strains for beams in RCS-1 were quite different.

Load versus hoop strains in coupling beams are shown in Fig. B-38.

Fig. B-39 gives the strain distribution in slab reinforcement at different stories. Data shown in Fig. B-39 were obtained in both tests. Similar strain data for RCS-1 are shown in Fig. B-40. From the measured strains, it is evident that the presence of slab stubs did have some effect on the behavior of the wall systems.

Variations in confining hoop strains along the height of CS-1 are shown in Fig. B-41. Hoop strains for RCS-1 are shown in the Fig. B-42. Variations in vertical reinforcement strains along the height of the specimens are shown in Figs. B-43 and B-44. Horizontal strain distributions in vertical reinforcement at 3 ft (457 mm) and 1.5 ft (914 mm) levels above the base are shown in Figs. B-45 and B-46 for CS-1 and RCS-1. Distributions of strains in horizontal wall reinforcement along the length of the walls are given in Figs. B-47 and B-48.
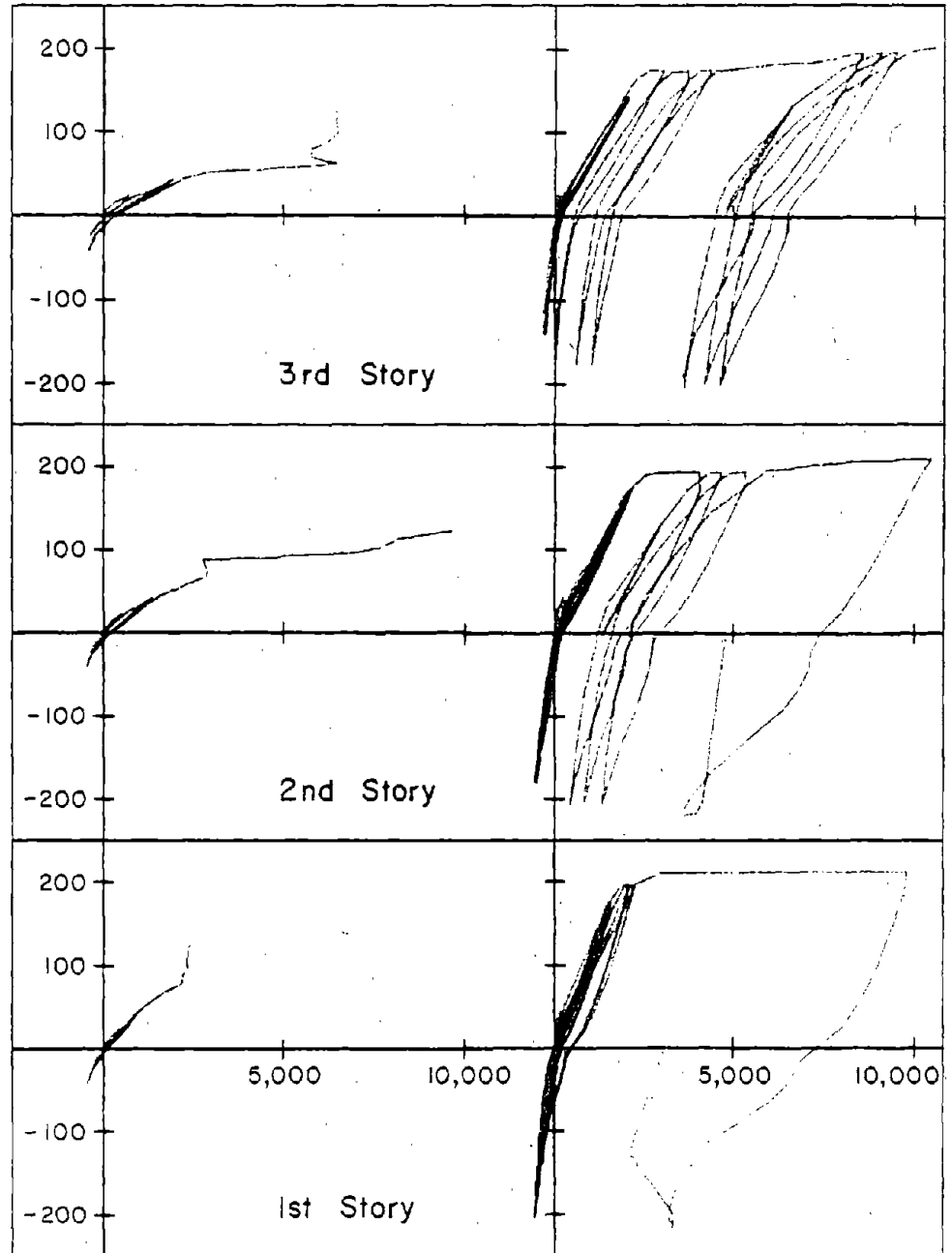
Fig. B-36   Load versus Flexural Steel Strains
for Coupling Beams
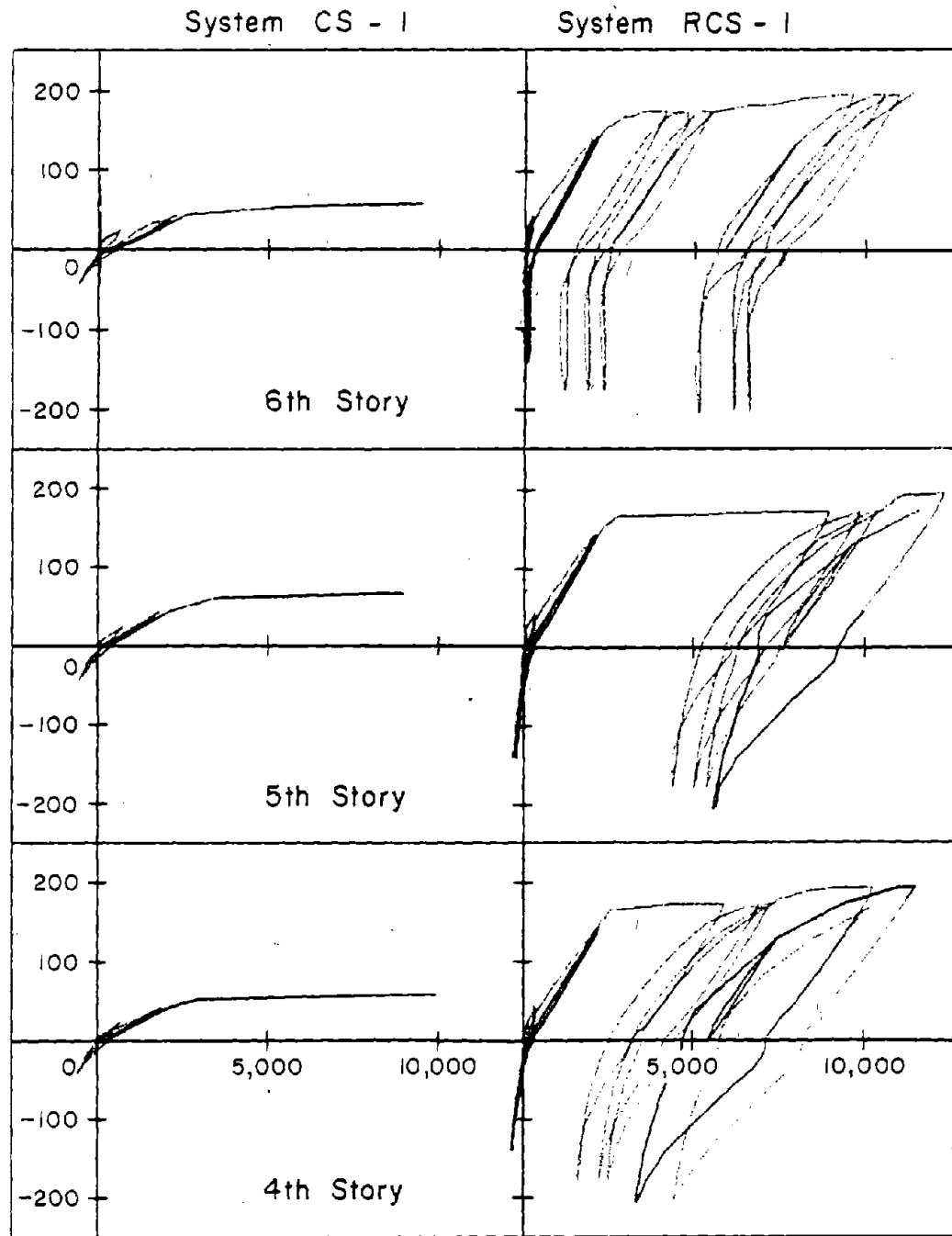
Fig. B-37   Load versus Flexural Steel Strains
for Coupling Beams
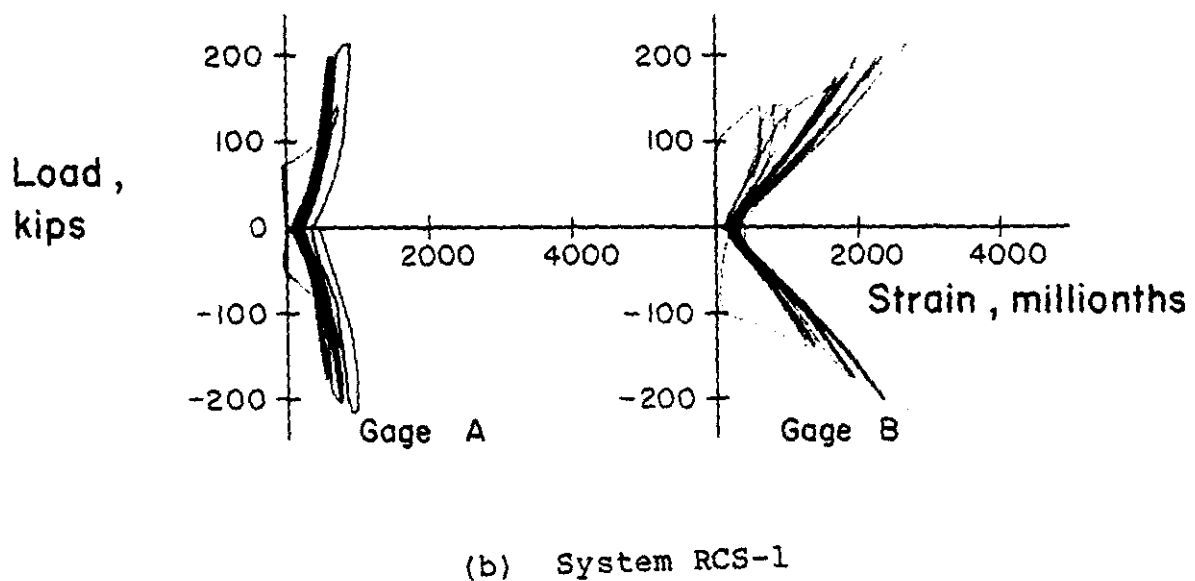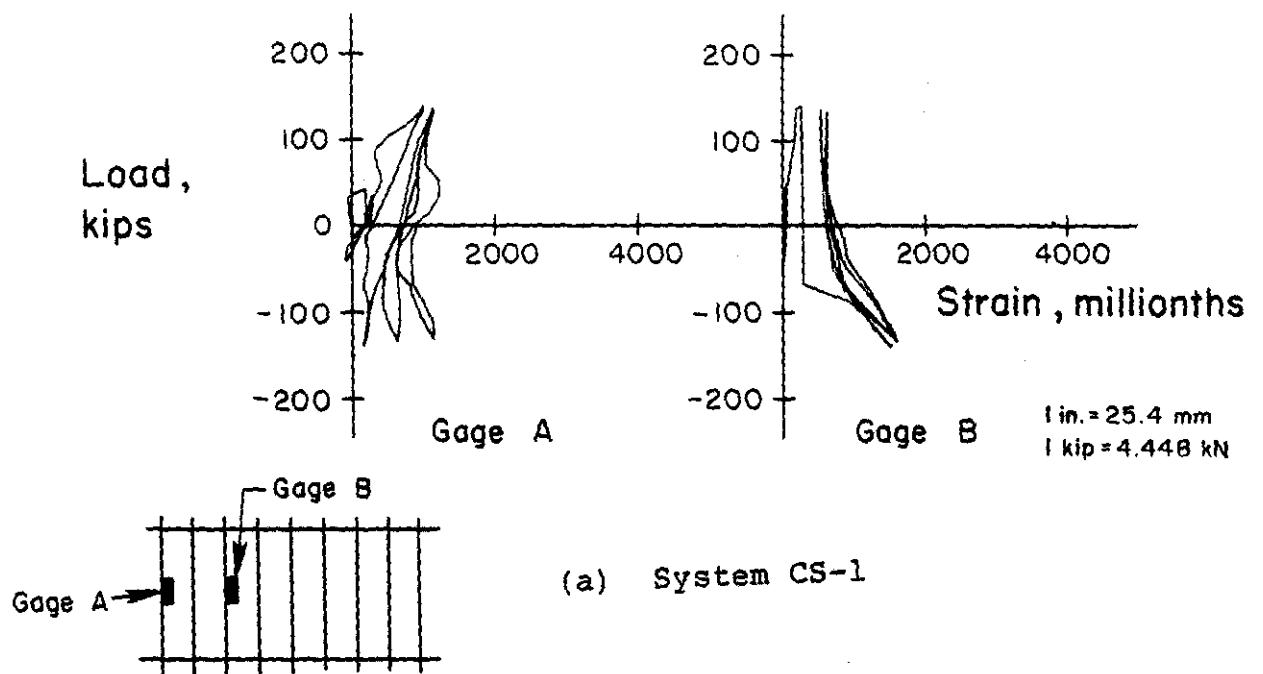
Fig. B38   Load Versus Hoop Strains in Coupling
Beams at Fourth Story Level
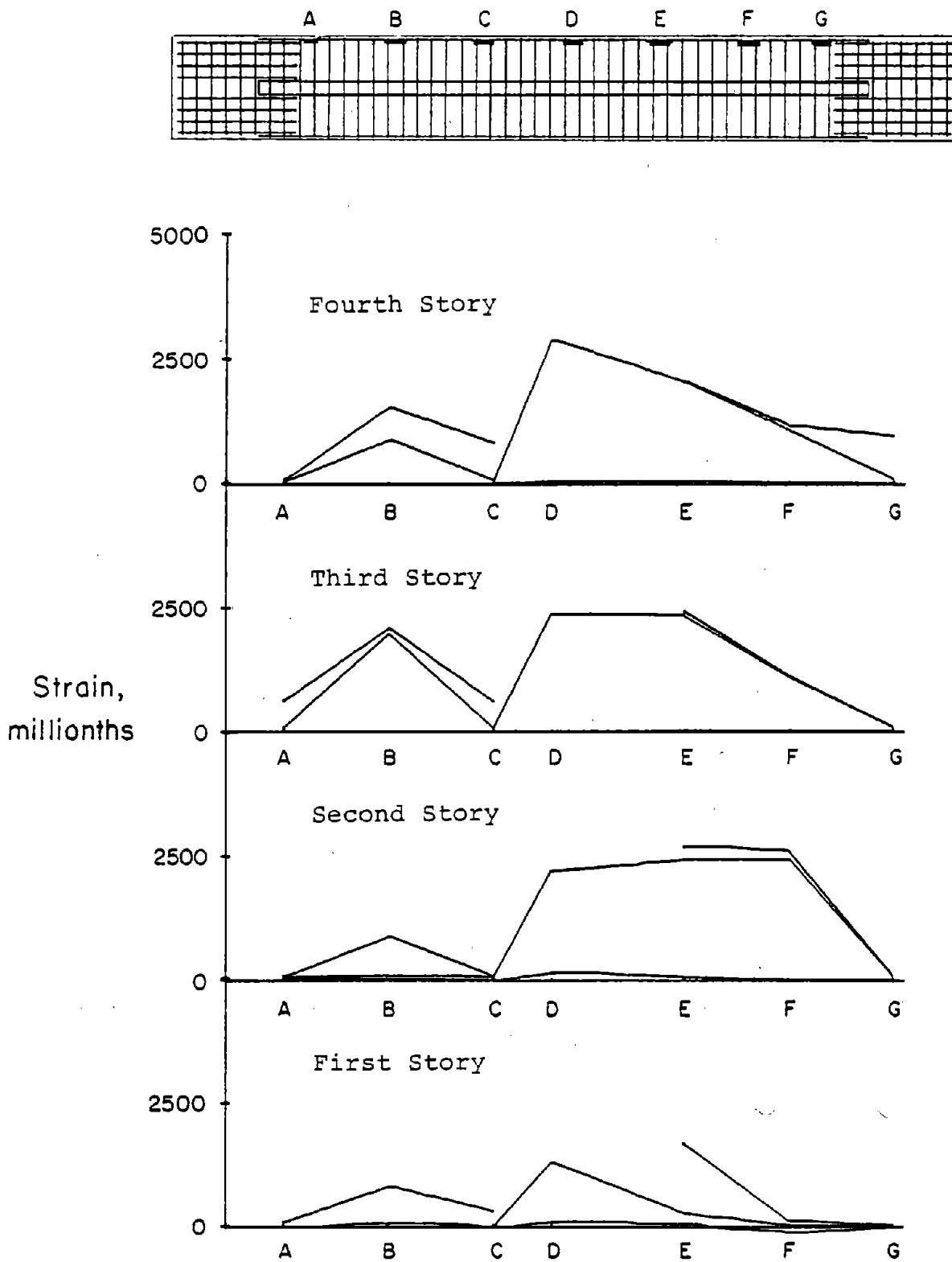
Fig. B-39   Strain Distribution of Slab Reinforcement
            for CS-1
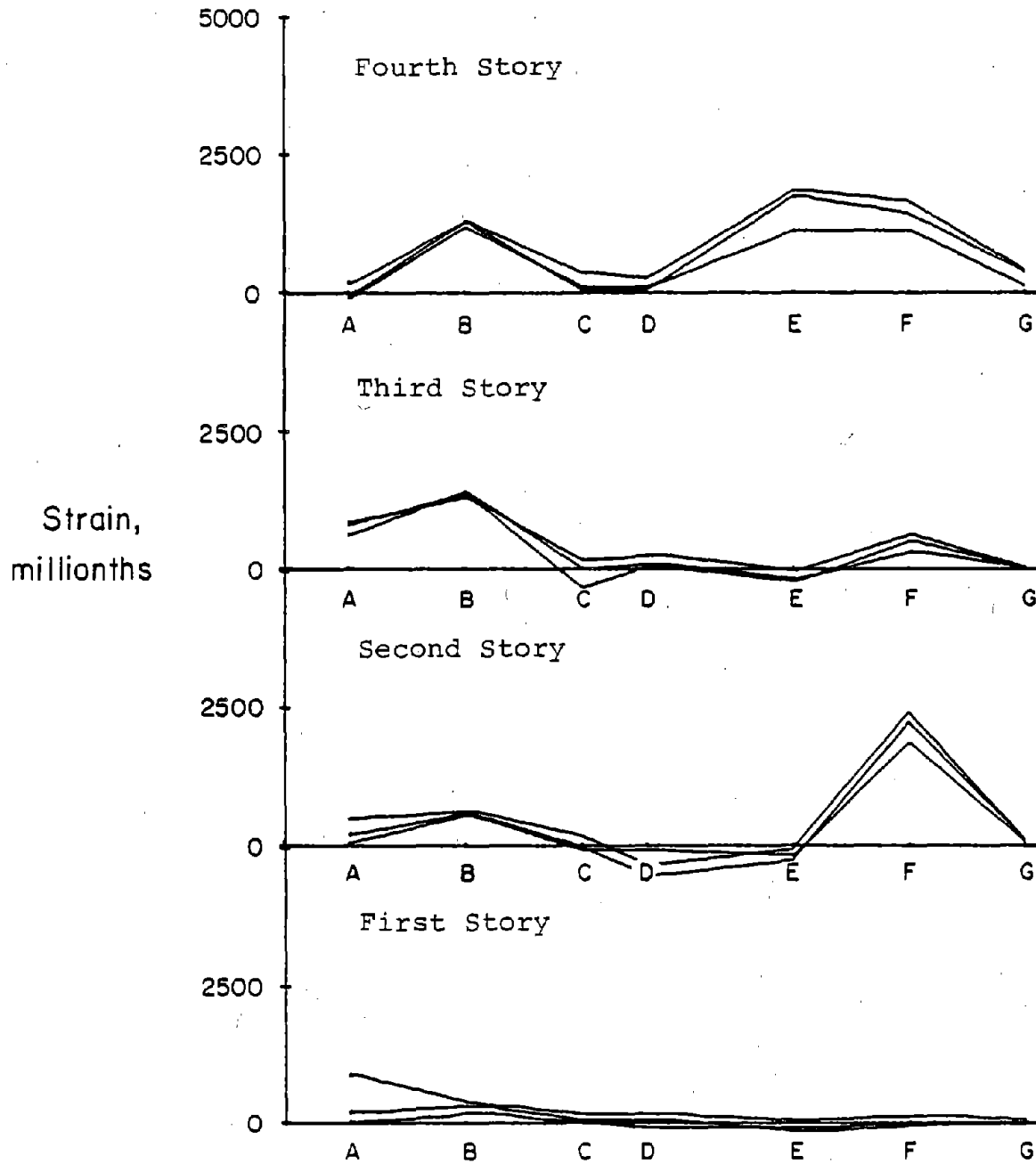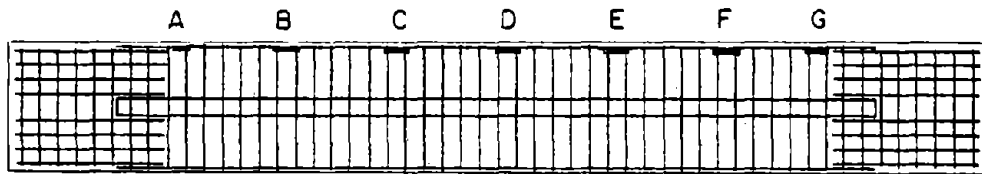
Fig. B-40   Strain Distribution of Slab Reinforcement
            for RCS-1

W2

2500   0   0   2500

W1

2500   0   0   2500
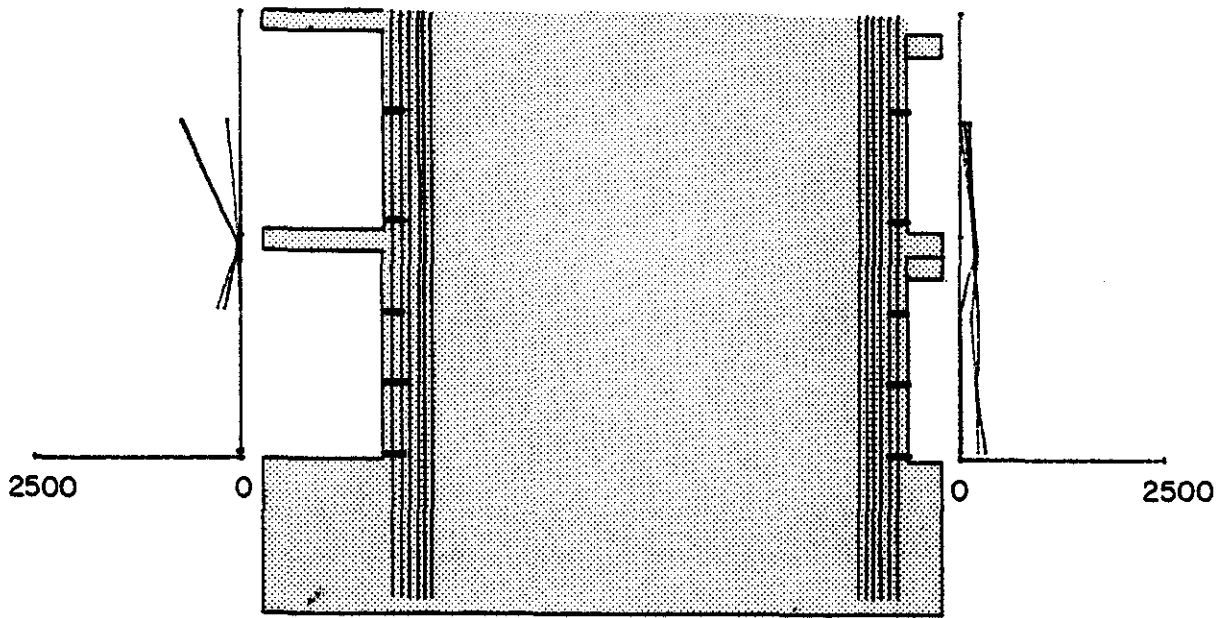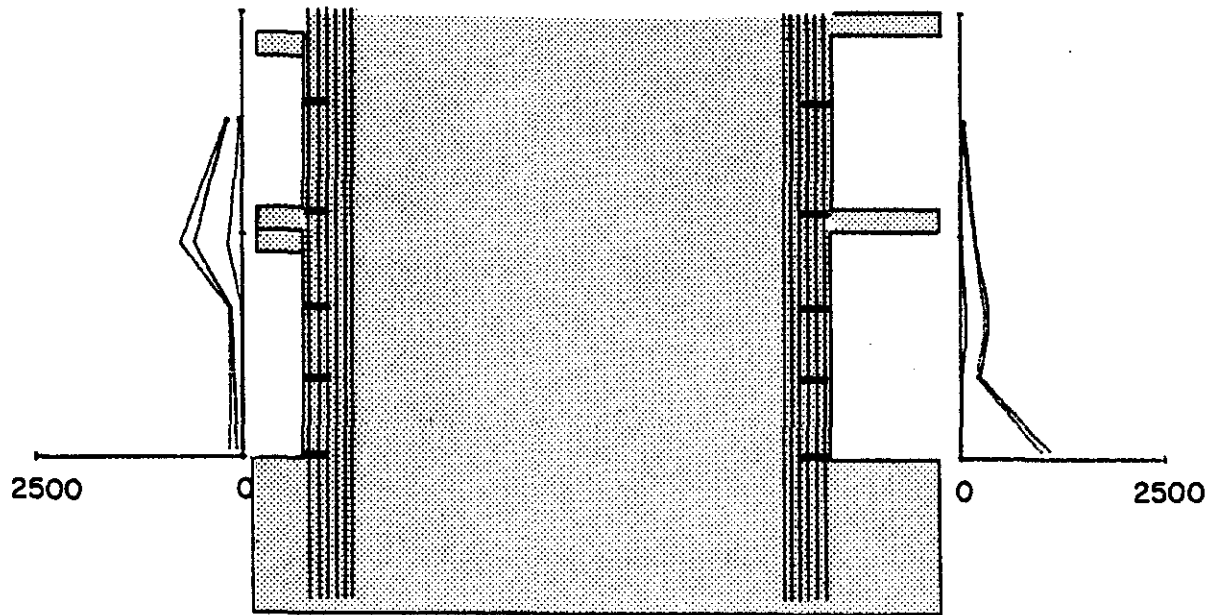
Fig. B41   Load Versus Hoop Strains in Boundary
Elements of System CS-1

W2

2500   0   0   2500

W I

2500   0   0   2500
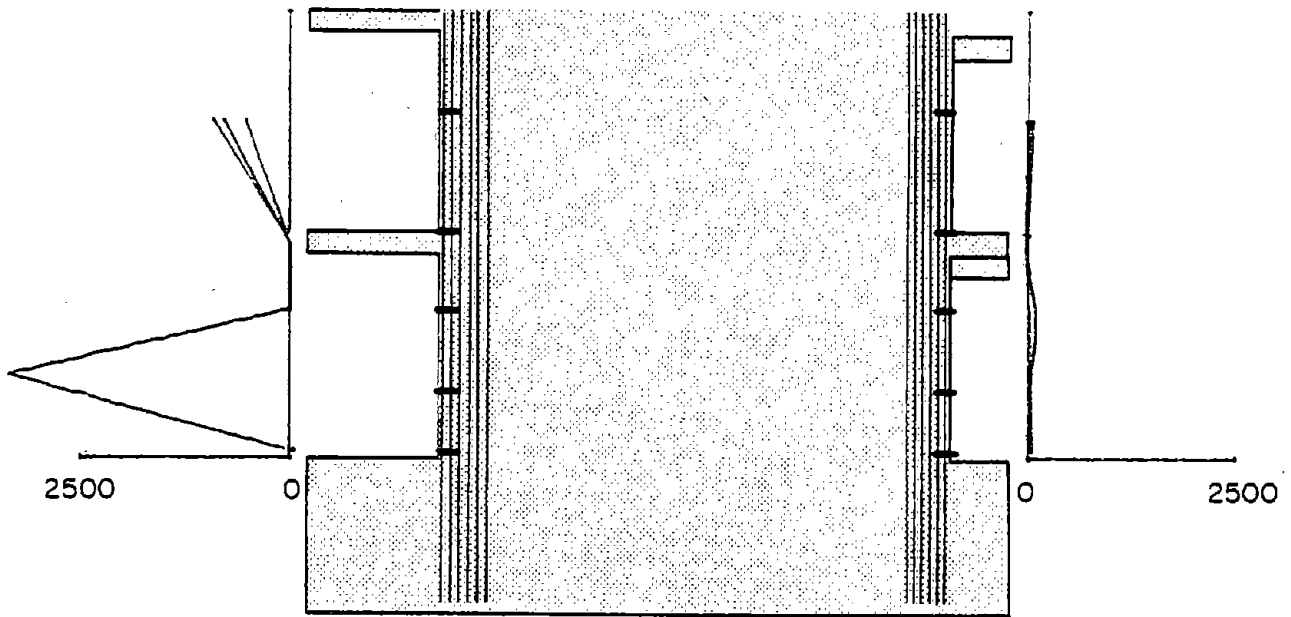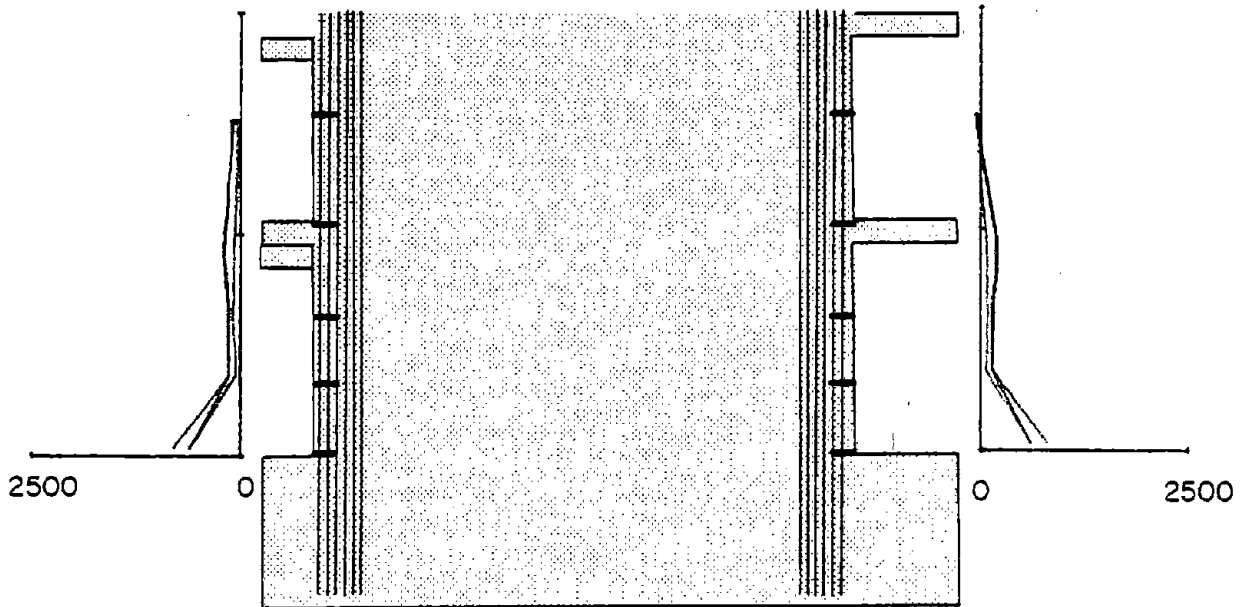
Fig. B42   Load Versus Hoop Strains in Boundary
Elements of System RCS-1
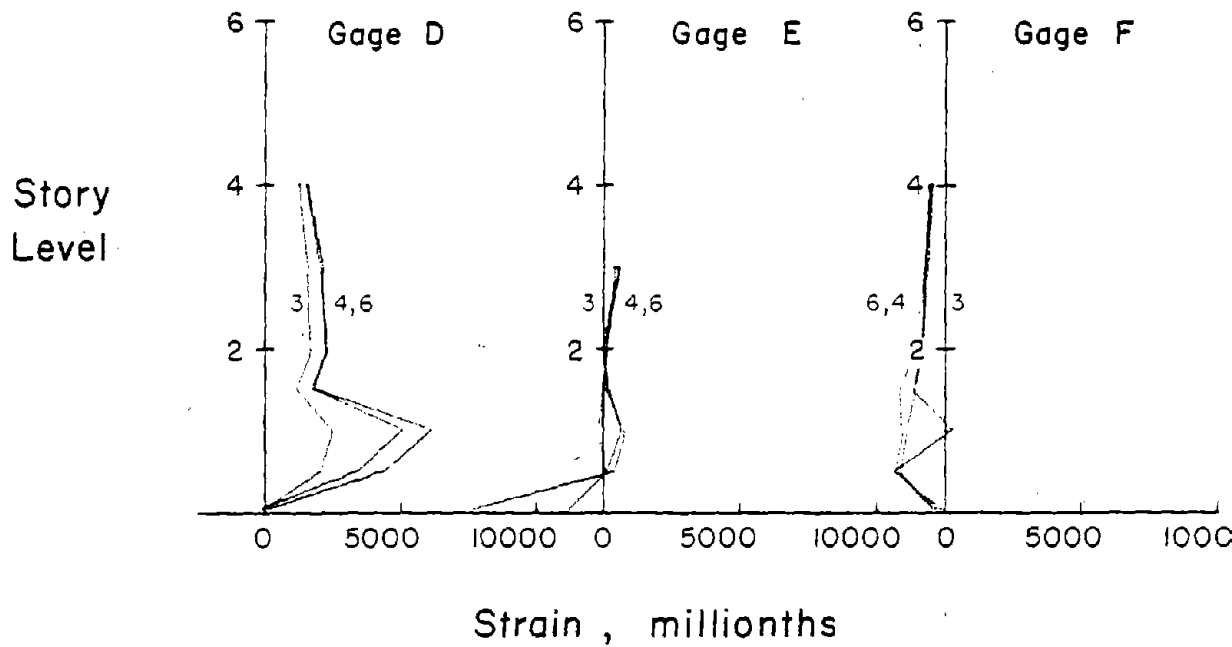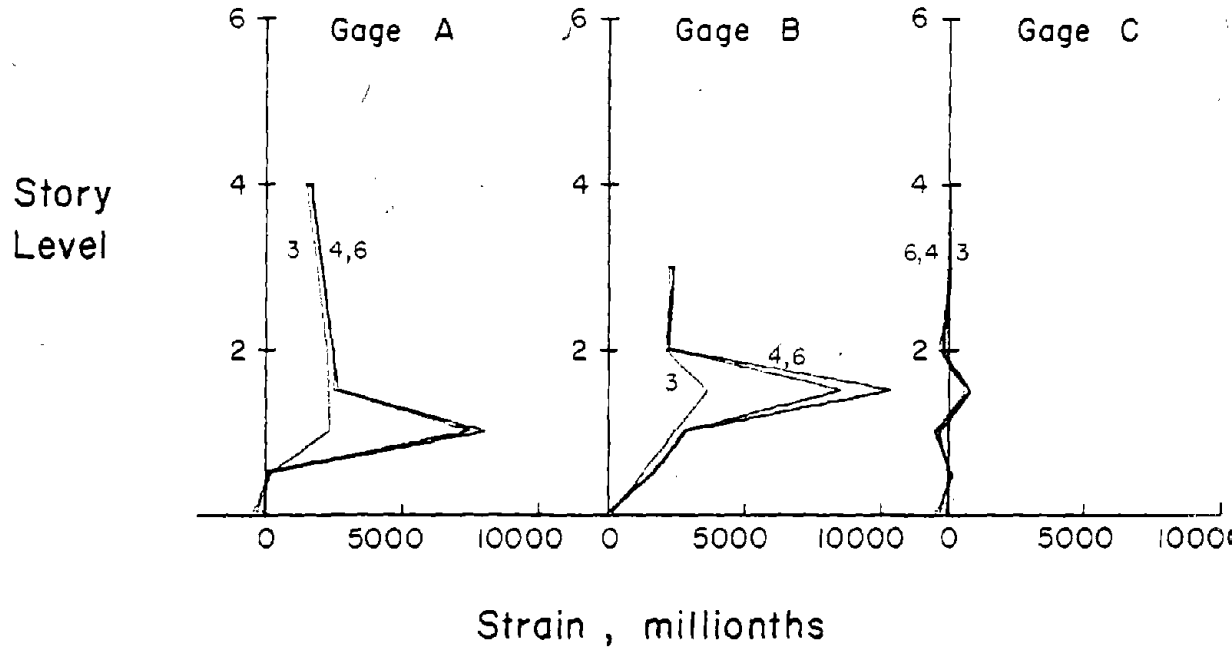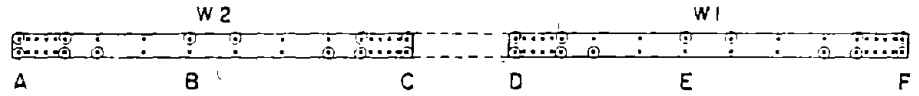
Fig. B-43   Strain Distribution in Vertical
            Reinforcement along Height of CS-1
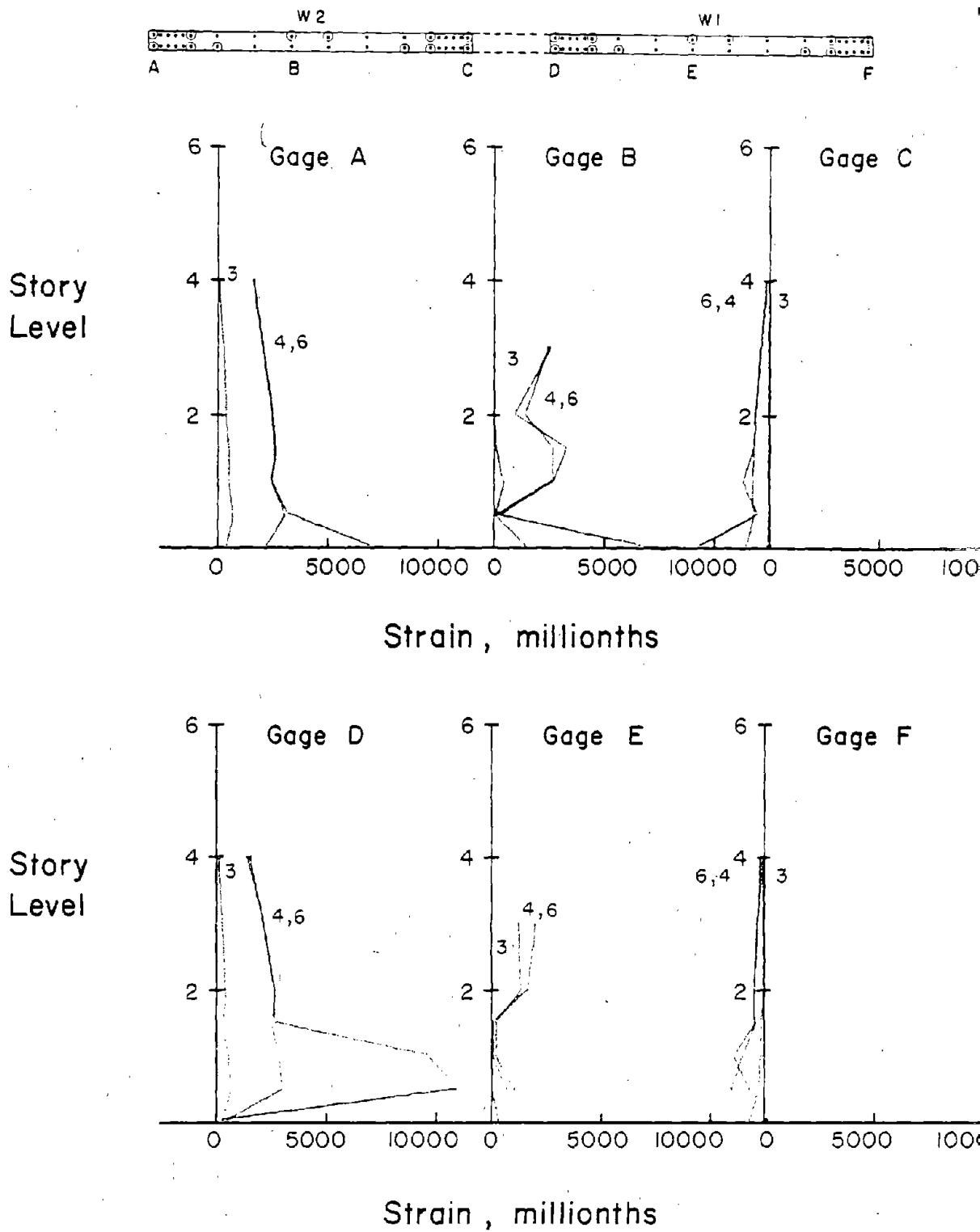
Fig. B-44   Strain Distribution in Vertical
            Reinforcement along Height of RCS-1
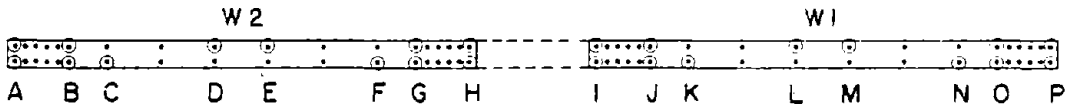
Strain, millionths
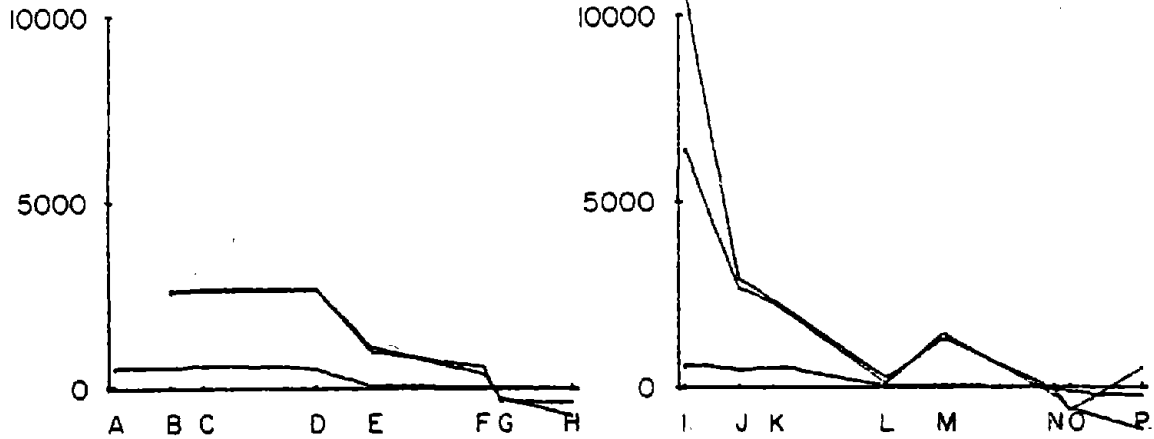
(a)   At 3 ft above Base
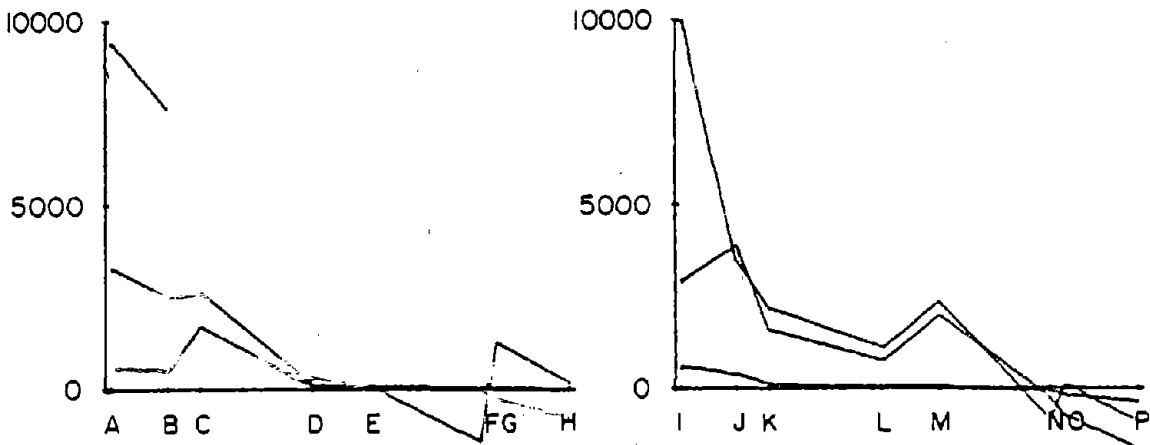
Strain, millionths

(b)   At 1.5 ft above Base

Fig. B-45   Horizontal Strain Distribution in Vertical
             Reinforcement for CS-1

Strain, millionths

W 2   W 1

A B C   D E   F G H   I J K   L M   N O P
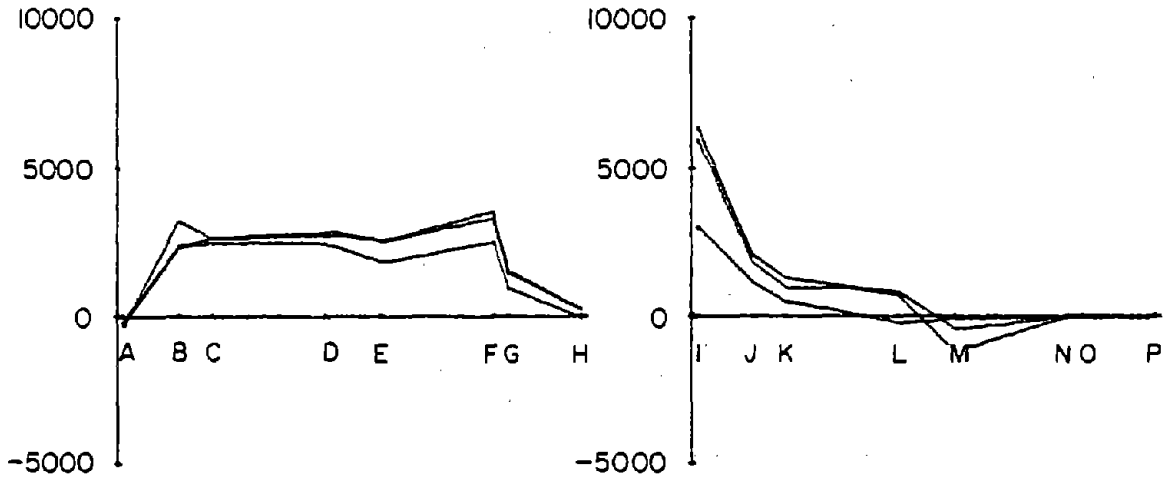
(a)   At 3 ft above Base
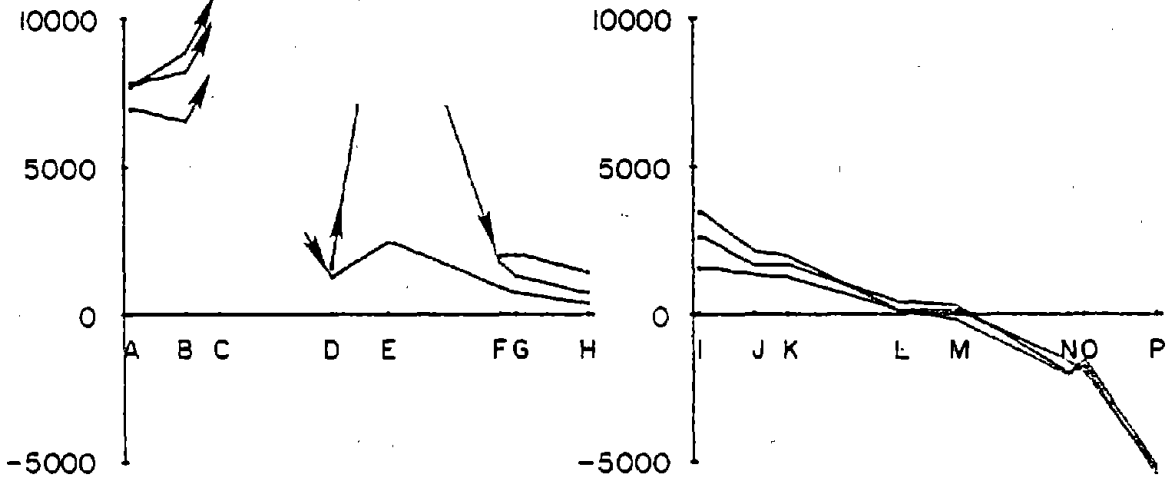
Strain, millionths

(b)   At 1.5 ft above Base

Fig. B-46   Horizontal Strain Distribution in Vertical
             Reinforcement for RCS-1
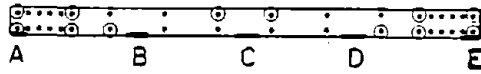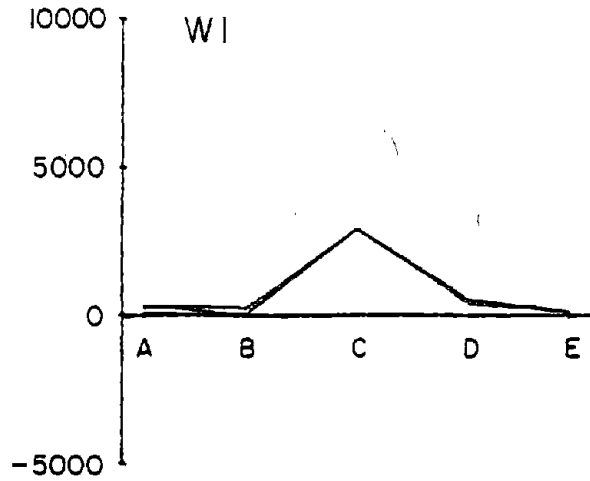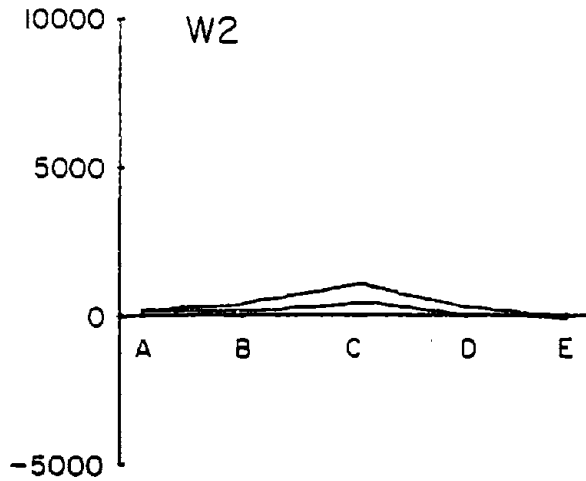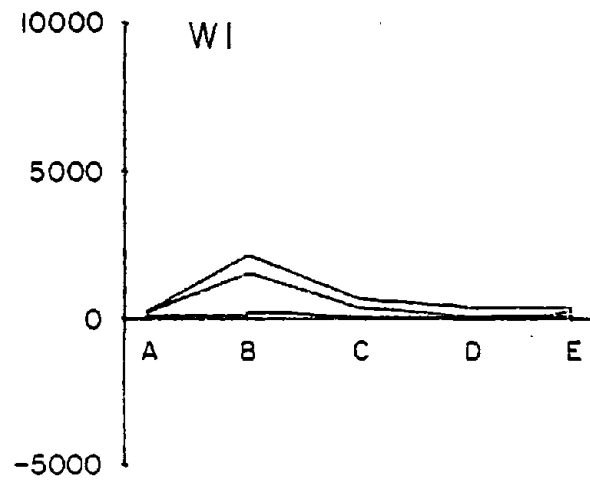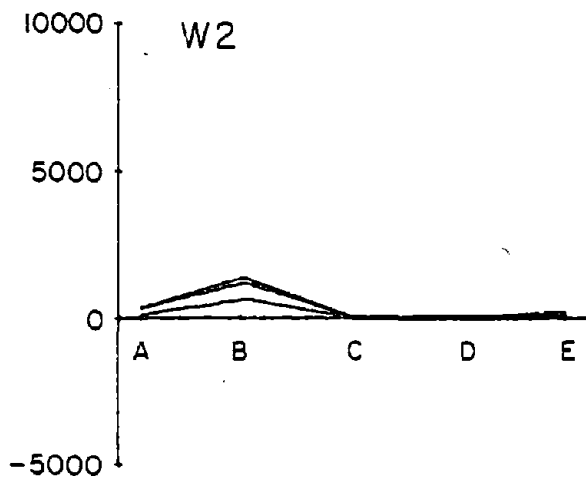
Fig. B-47   Horizontal Strain Distribution in Horizontal
Reinforcement for CS-1
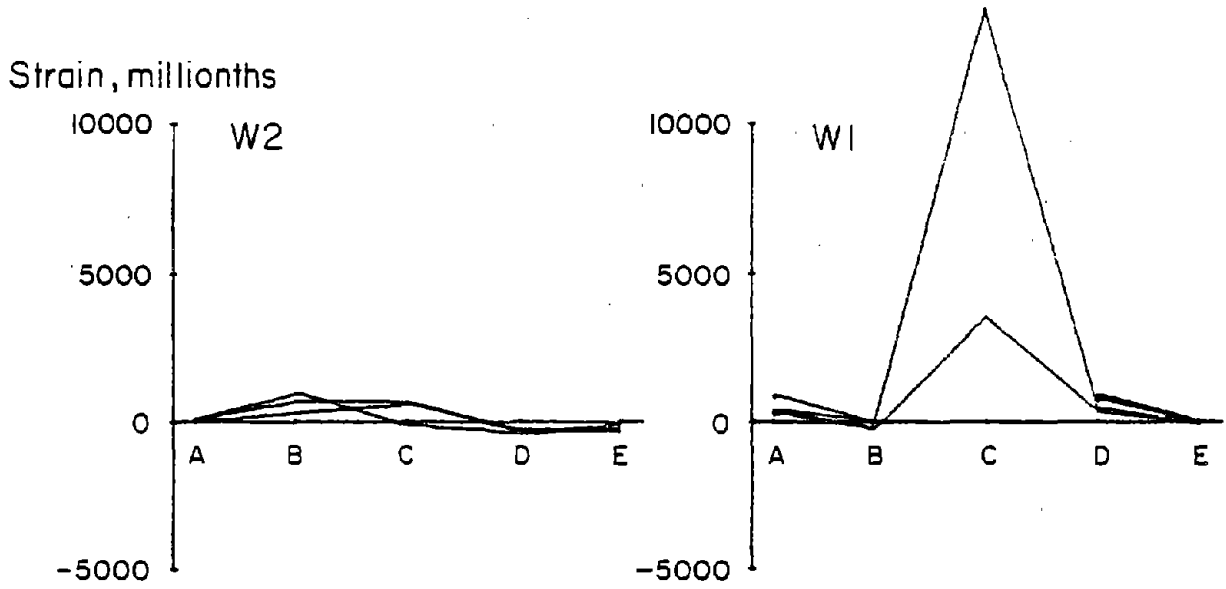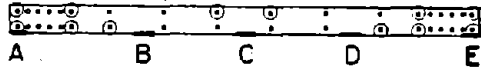
(a) At 3 ft above Base
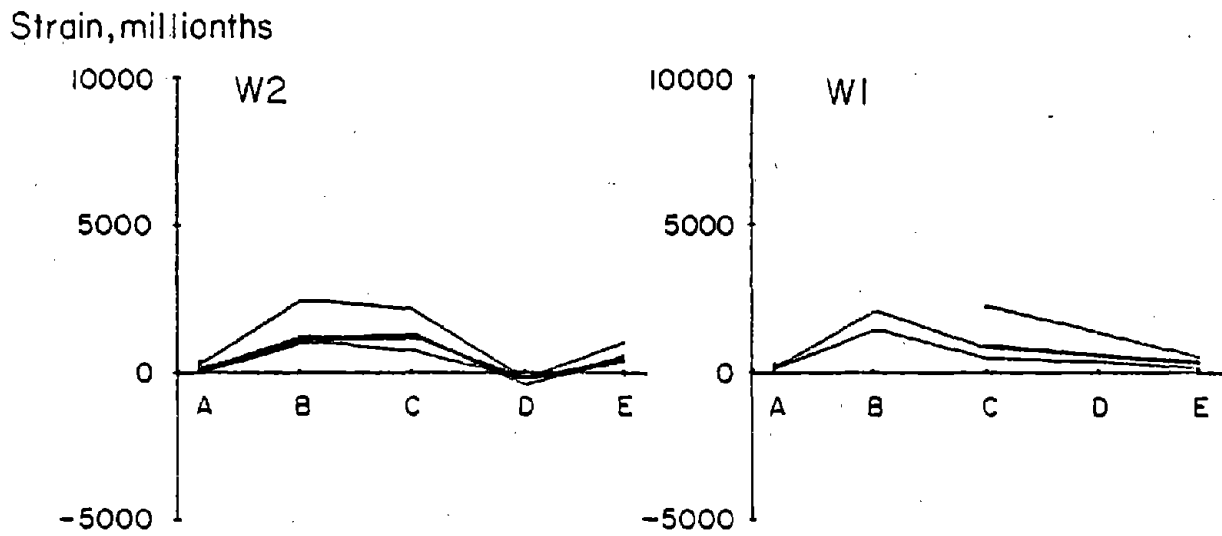
(b) At 1.5 ft above Base

Fig. B-48 Horizontal Strain Distribution in Horizontal
Reinforcement for RCS-1